ISTANBUL TECHNICAL UNIVERSITY ⋆ INSTITUTE OF SCIENCE AND TECHNOLOGY

HIGH PERFORMANCE DYNAMICAL MODELING OF COMPLEX TOPOLOGY SYSTEMS

Ph.D. Thesis by
Sıddık Murat Yeşiloğlu, M.Sc.

Department: Electrical Engineering
Programme: Control and Automation

JUNE 2007

ISTANBUL TECHNICAL UNIVERSITY ⋆ INSTITUTE OF SCIENCE AND TECHNOLOGY

HIGH PERFORMANCE DYNAMICAL MODELING OF COMPLEX TOPOLOGY SYSTEMS

Ph.D. Thesis by
Sıddık Murat Yeşiloğlu, M.Sc.

(504032102)

Date of submission: 2 March 2007
Date of defence examination: 26 June 2007

Supervisor (Chairman): Prof.Dr. Hakan Temeltaş

Members of the Examining Committee: Prof.Dr. Leyla Gören (I.T.U.)

Assoc.Prof.Dr. Ata Muğan (I.T.U.)

Assoc.Prof.Dr. Yağmur Denizhan (B.U.)

Assist.Prof.Dr. Kemalettin Erbatur (S.U.)

JUNE 2007

İSTANBUL TEKNİK ÜNİVERSİTESİ ⋆ FEN BİLİMLERİ ENSTİTÜSÜ

KOMPLEKS TOPOLOJİ SİSTEMLERİN YÜKSEK PERFORMANSLI DİNAMİK MODELLEMESİ

Doktora Tezi

Sıddık Murat Yeşiloğlu, M.Sc.

(504032102)

Tezin Enstitüye Verildiği Tarih: 2 Mart 2007
Tezin Savunulduğu Tarih: 26 Haziran 2007

Tez Danışmanı: Prof.Dr. Hakan Temeltaş

Diğer Jüri Üyeleri: Prof.Dr. Leyla Gören (İ.T.Ü.)

Doç.Dr. Ata Muğan (İ.T.Ü.)

Doç.Dr. Yağmur Denizhan (B.Ü.)

Yrd.Doç.Dr. Kemalettin Erbatur (S.Ü.)

HAZİRAN 2007

ACKNOWLEDGEMENTS

A long part of this journey, from the Winter of 1994 to the Summer of 2003 when I finally returned back home, had truly been a wild experience for me. The wilderness which was, in a way, a test of my limits offered some visdom for a great expense. I believe I need to thank God first that I survived. It would not be possible without the endless love and support of my parents and sisters.

I would like to express my sincere gratitude to Prof.Dr. Hakan Temeltaş under the supervision of whom I had a privilege to work for the last three years which were the most fruitfull because of his friendly encouragement and support. I would also like to thank Prof.Dr. Leyla Gören and other committee members for their time and valuable suggestions. I owe special thanks to my officemate and friend M. Kürşat Yalçın who kindly overtook many of my responsibilities so that I could consantrate on finishing up this dissertation.

I am also gratefull to Prof.Dr. Kurt Anderson from Rensselaer Polytechnic Institute (RPI) for his outstanding support during my tough times. Going back to RPI years, I cannot forget the great friendship of Declan Hughes, Lee Wilfinger, Padma Akella, Dan Popa, Carry Dickinson, Fernando Lizarralde and from the General Electric years, Yavuz Kadıoğlu, Rohan Kelkar, Eamon Gleeson and many others. From the Turkish community of RPI, I met my forever friends Selahattin Özçelik, Levent Ovacık, Serdar Dinçaslan, Mehmet Baran, Ertuğrul Tepe, Hikmet Yükselici, Lale Ergene, Kerem Ün, and Uğur Doğrusöz. There were times I had nothing but their friendship to keep on going.

Finally, I would like to express my greatest appreciation to my wife Nihan not only for her patience but also for her encouragement during my long hours of work for this thesis. I consider myself exceptionally lucky for being her husband.

June, 2007 **S. Murat Yeşiloğlu**

TABLE OF CONTENTS

LIST OF FIGURES

LIST OF SYMBOLS

$_3\mathbf{0}$: 3×3 zero matrix.(2.5)

$_3\mathbf{I}$: 3×3 identity matrix.(2.5)

${}^i\vec{\ell}_{k-1,k}$: link vector of link $k-1$ of arm i.(2.1)

${}^i\mathbf{L}_{k-1,k}$: lin. operator for "${}^i\vec{\ell}_{k-1,k}\times$" rep. as a skew sym. matrix.(2.1)

${}^i\vec{\ell}_{k,c}$: from the origin of the link frame k to the CM of the link.(2.18)

${}^i\vec{h}_k$: axis of rotation and/or translation vector of link k of arm i.(2.2)

${}^i\vec{\vec{H}}_k$: axis of rotation and/or translation spatial vector of the link.(2.6)

${}^i\mathbf{H}$: axis of rotation and/or translation matrix of arm i.(2.11)

$\mathbf{H}$: axis of rotation and/or translation matrix of the system.(2.28)

${}^i\dot{\theta}_k$: joint rate between link $k-1$ and link k of arm i.(2.2)

${}^i\underline{\dot{\theta}}$: stacked joint rates of arm i.(2.11)

$\underline{\dot{\theta}}$: stacked joint rates of the system.(2.28)

${}^i\ddot{\theta}_k$: joint acceleration between link $k-1$ and link k of arm i.(2.14)

${}^i\underline{\ddot{\theta}}$: stacked joint accelerations of arm i.(2.17)

$\underline{\ddot{\theta}}$: stacked joint accelerations of the system.(2.28)

$\underline{\ddot{\theta}}^f$: free accelerations.(4.15)

$\underline{\ddot{\theta}}^\delta$: correction accelerations.(4.15)

$\underline{\ddot{\theta}}_{baf}$: accelerations regarding base, actuated and free joints.(4.2)

$\underline{\ddot{\theta}}_\ell$: accelerations regarding flexible joints.(4.2)

${}^i\vec{\omega}_k$: angular velocity vector of link k of arm i.(2.2)

${}^i\vec{v}_k$: linear velocity vector of link k of arm i.(2.1)

${}^i\vec{\vec{V}}_k$: spatial velocity vector of link k of arm i.(2.3)

${}^i\vec{\vec{V}}_b$: base spatial velocity vector of arm i.(2.8)

${}^i\vec{\vec{V}}_t$: tip spatial velocity vector of arm i.(2.12)

${}^i\underline{V}$: stacked link spatial velocities of arm i.(2.11)

$\underline{V}$: stacked link spatial velocity of the system.(2.28)

${}^i\mathbf{\Phi}_{k,k-1}$: propagation operator from link $k-1$ to link k of arm i.(2.5)

${}^{i}\mathbf{\Phi}_{b}$	:	prop. operator from the first joint of arm i to the base.(2.17)
${}^{i}\mathbf{\Phi}_{t}$	:	prop. operator from the last joint to the tip point of arm i.(2.12)
${}^{i}\mathbf{\Phi}_{t,b}$	:	propagation operator from base to the tip point of arm i.(2.13)
${}^{i}\mathbf{\Phi}$	:	propagation operator of arm i.(2.11)
$\mathbf{\Phi}_{t}$	:	${}^{i}\mathbf{\Phi}_{t}$s for all arms stacked.(2.30)
$\mathbf{\Phi}$	:	propagation operator of the system.(2.28)
${}^{i}\mathcal{E}_{\phi}$	:	adjacent-link propagation operator of arm i..(3.9)
$\mathcal{E}_{\phi}$	:	adjacent-link propagation operator of the system.(3.8)
${}^{i}\mathbf{\Psi}_{k,k-1}$	:	quasi prop. operator from link $k-1$ to link k of arm i.(3.2)
$\mathbf{\Psi}$	:	quasi propagation operator of the system.(3.21)
${}^{i}\vec{a}_{k}$	:	bias spatial acceleration of link k of arm i.(2.16)
${}^{i}\underline{a}$	:	stacked bias spatial accelerations of arm i.(2.17)
$\underline{a}$	:	stacked bias spatial accelerations of the system.(2.28)
$\vec{g}$	:	gravitational acceleration vector.(2.29)
${}^{i}\vec{b}_{k}$	:	bias spatial forces of link k of arm i.(2.20)
${}^{i}\underline{b}$	:	stacked bias spatial forces of arm i.(2.21)
$\underline{b}$	:	stacked bias spatial forces of the system.(2.30)
$\vec{b}_{b}$	:	base bias spatial force.(2.25)
${}^{i}\mathcal{I}_{k}$	:	inertia matrix of link k of arm i.(2.18)
${}^{i}m_{k}$	:	mass of link k of arm i.(2.18)
${}^{i}\mathbf{M}_{k}$	:	link mass matrix of link k of arm i.(2.20)
${}^{i}\mathbf{M}$	:	mass matrix of arm i.(2.21)
$\mathbf{M}$	:	mass matrix of the system.(2.30)
$\mathbf{M}_{b}$	:	mass matrix of the base.(2.27)
$\mathbf{M}_{c}$	:	mass matrix of the common load.(4.25)
$\mathbf{M}_{1}$	:	portion of $\mathcal{M}$ regarding $\underline{\ddot{\theta}}_{baf}$ caused by $\underline{\mathcal{T}}_{baf}$.(4.2)
$\mathbf{M}_{2}$	:	portion of $\mathcal{M}$ regarding $\underline{\ddot{\theta}}_{baf}$ caused by $\underline{\mathcal{T}}_{\ell}$.(4.2)
$\mathbf{M}_{3}$	:	portion of $\mathcal{M}$ regarding $\underline{\ddot{\theta}}_{\ell}$ caused by $\underline{\mathcal{T}}_{baf}$.(4.2)
$\mathbf{M}_{4}$	:	portion of $\mathcal{M}$ regarding $\underline{\ddot{\theta}}_{\ell}$ caused by $\underline{\mathcal{T}}_{\ell}$.(4.2)
${}^{i}\mathcal{M}$	:	generalized mass matrix of arm i.(2.24)
$\mathcal{M}$	:	generalized mass matrix of the system.(2.32)
$\mathbf{M}_{\star}$	:	spring and damper embedded mass matrix of the system.(4.7)

$\mathbf{M}_s$: augmented mass matrix of the system w/ spring and damper.(4.12)

${}^i\vec{\mathcal{T}}_k$: torque vector of link k of arm i.(2.18)

$\underline{\mathcal{T}}$: applied torques/forces stacked.(2.31)

$\underline{\mathcal{T}}_{baf}$: applied torques/forces regarding $\underline{\ddot{\theta}}_{baf}$.(4.2)

$\underline{\mathcal{T}}_{\ell}$: applied torques/forces regarding $\underline{\ddot{\theta}}_{\ell}$.(4.2)

$\underline{\mathcal{T}}_s$: loads including Coriolis for the system regarding $\underline{\ddot{\theta}}_{baf}$.(4.13)

${}^i\vec{f}_k$: force vector of link k of arm i.(2.19)

${}^i\vec{\mathcal{F}}_k$: spatial force of link k of arm i.(2.20)

${}^i\underline{F}$: stacked spatial forces of arm i.(2.21)

$\underline{F}$: stacked spatial forces of the system.(2.30)

${}^i\vec{\mathcal{F}}_t$: spatial tip force of arm i.(2.21)

$\underline{F}_t$: stacked spatial tip forces of the system.(2.30)

$\vec{\mathcal{F}}_b$: base spatial force.(2.26)

${}^i\underline{C}$: bias terms including Coriolis and the gravity for arm i.(2.24)

$\underline{C}$: bias terms including Coriolis and the gravity of the system.(2.32)

$\underline{C}_{baf}$: $\underline{C}$ of the system regarding $\underline{\ddot{\theta}}_{baf}$.(4.2)

$\underline{C}_{\ell}$: $\underline{C}$ of the system regarding $\underline{\ddot{\theta}}_{\ell}$.(4.2)

$\underline{C}_{\star}$: spring and damper embedded $\underline{C}$.(4.7)

$\underline{C}_s$: augmented $\underline{C}_{\star}$.(4.12)

${}^i\mathcal{J}$: Jacobian of arm i.(2.32)

$\mathcal{J}$: Jacobian of the system.(2.32)

$\mathcal{J}_{baf}$: Jacobian of the system regarding $\underline{\ddot{\theta}}_{baf}$.(4.2)

$\mathcal{J}_{\ell}$: Jacobian of the system regarding $\underline{\ddot{\theta}}_{\ell}$.(4.2)

$\mathcal{J}_{\star}$: spring and damper embedded Jacobian.(4.7)

$\mathcal{J}_s$: augmented $\mathcal{J}_{\star}$.(4.12)

$\mathbf{S}$: sorting matrix.(4.1)

$\mathbf{D}$: Diagonal matrix of the LDU type mass matrix factorization.(**??**)

$\mathbf{K}$: Contributing term in the LDU type mass matrix factorization.(3.16)

$\mathbf{L}_s$: constant diagonal matrix for spring parameters.(4.3)

$\mathbf{L}_d$: constant diagonal matrix for damper parameters.(4.3)

$\mathbf{L}_{sd}$: matrix of spring and damper parameters.(4.12)

$\mathbf{B}$: applied loads' weight matrix.(4.7)

$\mathbf{B}_s$: augmented $\mathbf{B}$.(4.12)

$\underline{W}$: flexible joint angles and their rates stacked(4.12)

$\underline{W}^f$: unforced $\underline{W}$.(4.16)

$\mathbf{\Omega}$: arm cooperation matrix enforcing kinematic loop closure.(4.29)

HIGH PERFORMANCE DYNAMICAL MODELING OF COMPLEX TOPOLOGY SYSTEMS

SUMMARY

A mechanical system is said to be in a complex topology when it includes multiple subgroups, which may include one or more of the serial topology, tree topology and closed topology systems. These subgroups can be further classified according to their actuation (under-actuated or fully-actuated), according to their manipulability (kinematically deficient, full DOF or redundant) and according to their constraints (holonomic or nonholonomic). Out of all possible configurations, we identified the issues and provided the solutions. For example, in the pseudo-joint method we first augment the system with additional joints called pseudo joints and then remove them from the system by constraints called pseudo-torques. These constraints actually correspond to stress along the pseudo-joints. Therefore, for the price of stress computation, we obtain full propagation of forces and torques including the constrained ones throughout the system. Our goal from the forward dynamics problem, on the other hand, is to solve for the complete force/torque and acceleration distribution of the system including those at the constraints. The methodology presented is modular so as to apply no matter how complicated the systems is. Mass matrix factorization and inversion is also an issue for large order systems. A modified order-n algorithm is embedded to enhance the performance. We believe that the application of our algorithm to complex topology systems with nonholonomic constraints is the domain where it fits best.

KOMPLEKS TOPOLOJİ SİSTEMLERİN YÜKSEK PERFORMANSLI DİNAMİK MODELLEMESİ

ÖZET

Kompleks topoloji sistemler çoklu rijid cisim dinamiğinin en üst kümesini oluşturur. Bu küme içerisinde seri topoloji, ağaç topolojisi ve kapalı çevrim topoloji bulunur. Ayrıca tahrik düzenine göre eksik-tahrikli ya da tam-tahrikli sistemler, serbestlik derecelerine göre de kinematik-yeterli ya da kinematik-yetersiz, kısıtlarına göre holonomik-olan ya da holonomik-olmayan olarak sınıflandırılabilirler. Bütün bunların kombinasyonları değerlendirildiğinde ortaya çıkan problemler anlatılmış ve bunlar için yöntemler geliştirilmiştir. Örnek olarak kinematik yetersiz manipulatörler, çalışma uzaylarında geçerli bütün konfigürasyonlara ulaşmak için gereken serbestlik derecelerinden (SD) daha azına sahip olan manipülatörlerdir. Üç boyutlu çalışma uzayı için bu durum, bir manipülatörün serbestlik derecesinin (SD) altıdan daha küçük olmasına karşı düşer. Çünkü üç boyutlu çalışma uzayına sahip kinematik yeterliliği olan bir manipülatörün uç noktası, üç boyutta dönme ve üç boyutta öteleme olmak üzere toplam altı boyutlu bir manifold tanımlar. Birlikte çalışan manipülatörlerden oluşan bir sistem üzerindeki kuvvet ve moment dağılımlarını hesaplayabilmek için sistemin Jakobiyen matrisinin sütunlarının bütün kombinasyonları bu manifoldu tamamıyla tarayabilmelidir. Bundan dolayı literatürde genellikle manipülatörlerin kinematik yeterliliği ve tekil durumda olmamaları bu problemin çözümüne ön koşul olarak getirilmektedir. Birlikte çalışan manipülatörlerin dinamik analizinde kinematik yeterlilik ön koşulunun kaldırılması amacıyla manipülatörlerin taşıdığı yükü bir mobil platform olarak modellemek ve gerektiğinde sisteme “sözde eklem” eklemek olarak özetlenebilecek bir yöntem tanıtılmıştır.

1. INTRODUCTION

A manipulator is a mechanical device generally built as a chain of structurally rigid links articulated by rotary or sliding joints which contribute as a degree of freedom (DOF). Multiple manipulators that work together to perform a common task are called *cooperating manipulators.* In this regard, a multibody system forming a closed-kinematic chain, from the modeling perspective, is equivalent to cooperating manipulators. In real life, there is a good likelyhood that a mechanical system has multiple open and/or closed-kinematic chains. We call such system a *complex topology system.*

Most mechanical systems are subject to certain auxiliary conditions called constraints. Keen understanding of the motion and the interaction of subsystems some of which may be constrained is the essence of multibody dynamics. This can only be achieved by through analysis using particular methodology which provides great insight into the structure in a concise manner. The most concise way of examining physical phenomena can be carried out through the use of vector analysis. Since the formulation of *Newton-Euler*, when compared to that of *Lagrange-Euler*, provides greater insight into the structure of the rigid multibody dynamics, the core of the methodology presented in this dissertation is *Newton-Euler* based dynamic modeling methodology using vectorial representation.

1.1 Problem Statement and Motivation

For the forward dynamics problem, inverse of the mass matrix is needed. In generalized coordinates, mass matrix is $n \times n$ matrix where n is the number of links. Generally speaking, n^3 operations are required to invert a nonsparce $n \times n$ matrix. Therefore, its complexity is said to be $\mathcal{O}(n^3)$. If n is a large number, this becomes a major issue regarding the overall performace of the computation. On the other hand, utilizing the properties of the mass matrix, one can reduce the complexity of this process to

$\mathcal{O}(n)$. In this thesis, the factorization and inversion technique is adopted from [1] and modified to broaden its applicability.

Manipulators can be classified into a few categories. If the number of actuators to drive individual joints is equal to or less than the number of DOF of that manipulator than it is called a *fully actuated* or an *underactuated* manipulator, respectively. Depending upon having more, same, or less DOF to achieve any admissible configuration in its workspace, a manipulator is called a *redundant*, *full DOF*, or *kinematically deficient*, in the order given. Full DOF and redundant manipulators temporarily may become kinematically deficient when they are at singularity.

Generally speaking, the load at the end effector of a manipulator is known when dealing with the dynamics of a serial manipulator. If the end effector of a manipulator is in contact either with that of another manipulator or with the environment, the computation of induced forces and torques at the contact is not a straight forward task. Obviously, dynamical modeling of complex topology systems is a major challenge.

Often times, forward dynamics problem of a complex topology system means to solve for the acceleration of its center of mass when the applied torques or forces are given. These are usually over simplified models that lack inner dynamics of the system. Our goal from the forward dynamics problem, on the other hand, is to solve for the complete force/torque and acceleration distribution of the system including those at the constraints. The algorithms known in the literature deal with this problem only when the manipulators are fully actuated and are not kinematically deficient. Our challenge is to remove these limitations.

A manipulator does not need to be in the form of a robotic arm. In fact a bicycle, for example, can very well be considered as a cooperating manipulator if each wheel is regarded as a manipulator subject to nonholonomic constraint. To be able to compute the traction forces between the wheel and the terrain and even perform a stress analysis on the spokes of the wheel motivates us. One should note that the constraint at the contact point of a pure rolling wheel is a *nonholonomic* constraint where the generalized velocity satisfies an auxiliary condition that is not expressible as a function of its generalized position. We believe that the application of our algorithm to complex topology systems with nonholonomic constraints is the domain where it comes to fruition.

1.2 Historical Review of Related Studies

To understand what had been available in the literature by the time the ideas in this dissertation were defended is very important to assess the contributions listed in the next section. Therefore, this section is dedicated for literature review which is divided, for clarity purposes, to five subsections; $\mathcal{O}(n)$ algorithms, spatial operators in multibody dynamics, underactuated systems, kinematically deficient systems, nonholonomic systems.

1.2.1 $\mathcal{O}(n)$ algorithms

Armstrong [2] presented one of the first results in $\mathcal{O}(n)$ formulation of multi-body dynamics. The method was based on a Newton-Euler formulation, and it could model chain systems with spherical joints for the forward dynamics problem. Shortly after that, Walker and Orin [3] presented their $\mathcal{O}(n)$ algorithm also based on a Newton-Euler formulation.

Several studies yielding $\mathcal{O}(n)$ formulations for rigid body dynamics rooted in Kane's method [4, 5]. One of these works was done by Rosenthal [6] who presented an algorithm that performs about 200 multiplication and 200 addition per degree of freedom in an open loop system. Another researcher needed to be mentioned here is Anderson whose work is explained next.

Based on Kane's method, Anderson [7] presented an algorithm which accommodates closed loop topologies in $\mathcal{O}(n)$. The algorithm consist of three recursive steps: calculation of velocities from base through tip, calculation of forces through base, and finally, calculation of accelerations through tip. The proposed method first deems some of the joints to be cut by removing the constraints so that closed loops become open loops. After performing the velocity, force and acceleration propagations, constraint forces are considered. In finding these forces, proposed method introduces an advantageous approach over penalty formulation [8], constraint stabilization [9], and stabilized penalty procedures [10] based on Lagrange multipliers. The challenge with finding the multipliers, or constrained forces in Anderson's case, is to avoid drift resulting from the roundoff error characteristic of digital computer floating point operations which may cause numerical instability. The proposed alternative approach adds a PD-type

control law to the constrained forces to limit the constraint violation. More precisely, proportional and derivative terms include kinematic constraint and its time derivative, respectively.

An Order-N formulation of multi-body tethered systems has recently been studied [11]. Although this is not a rigid body dynamics, once the equation of motion is driven the rest of the algorithm is analogous to that of rigid body dynamics. The proposed method for solving the equation of motion for accelerations in $\mathcal{O}(n)$ is to factor generalized mass matrix in a way similar to the one proposed in spatial operator algebra [1] with certain differences still yielding to same results. As an example to such differences it can be shown that after coordinate and velocity transformations to inertial frame, kinetic energy formulation is used to factor generalized mass matrix.

As another approach based on velocity transformation, Keat [12] has reported an $\mathcal{O}(n)$ recursive algorithm for the Newton-Euler equations. This work is similar to Spatial Operator Algebra and differs in that constraint forces are calculated only at so called *cut joints* which are, essentially, the minimal set of joints in the absence of which the topology of the system changes from closed-loop to open-loop.

Flexible links and flexible joints have been considered in [13]. For closed kinematic chain systems, [14] obtains dynamical modeling based on the technique given by [15]. Although all of these algorithms are claimed to be computationally efficient, the method they use is still *order* n^3 (specifically, the number of computational operations required at each temporal integration step increase as a cubic function of the number of system generalized coordinates *n*). Multibody dynamical algorithm with *order n* performance (indicating that the number of numerical computations increases as a linear function of the number of generalized coordinates) has been the focus of many researchers [2, 16, 17, 18, 6, 19], since it was first introduced by Vereshchagin [20] in 1974.

What needs to be underlined here is the fact as stated in [21] that "all of the $\mathcal{O}(n)$ algorithms are closely related and have the same inherent structure."

1.2.2 Spatial operators in multibody dynamics

Spatial quantities have been known for many decades. For example, at the beginning of the 20th century, it was employed by Ball [22] in the *theory of screws*. In 1983,

Featherstone [16] developed an $\mathcal{O}(n)$ method using *articulated body inertias* which is derived utilizing the spatial algebra. It is applicable to open chain systems, and it is more efficient than that of Armstrong [2].

In 1987, Guillermo Rodriguez [23] utilized spatial quantities to solve the rigid body dynamics as a two point boundary value problem. This work was inspired from Kalman filtering and Bryson-Frazier smoothing techniques yielding a new $\mathcal{O}(n)$ algorithm for forward and inverse dynamics of multi-body systems forming open-chain and/or closed-chain systems [24, 25]. In 1991, Abhinandan Jain [21] presented a discussion on comparison of several algorithms for serial rigid multibody system dynamics by utilizing the tools provided by the spatial operator algebra(SOA). This helped to establish the bridge between SOA and other multibody dynamics algorithms. Applications of SOA has been presented by Rodriguez, Kreutz-Delgado and Jain [26, 1]. The research given here is rooted in these studies.

Jain and Rodriguez has applied SOA to flexible multibody systems [27], linearized systems [28], molecular dynamics [29], and decomposable systems based on their joints [30, 29]. More recently, sensitivity analysis of SOA has been published [31]. Yen and Jain has published ROAMS: rover analysis modeling and simulation software based on SOA [32].

1.2.3 Underactuated systems

Modeling of underactuated mechanical systems has been studied, such as [33], in the robot dynamics field for more than a decade. Among such work, there are a few papers which address the dynamic modeling of underactuated closed-kinematic-chain systems. Of these, there are some that were misidentified as underactuated systems, such as [34]. When dealing with kinematic loops, one needs to be careful about that it is not sufficient to call it an underactuated system just because there is a passive joint in a system. As stated earlier, there has to be an uncontrolled DOF in the system. If a passive joint has a constraint such that it is kinematically dependent on an actuated joint, then that passive joint does not constitute for an uncontrolled DOF. For instance, let us take a planar four-bar linkage mechanism into consideration. As well-known, there is only one DOF in a planar four-bar linkage mechanism, and therefore actuating only one joint while leaving the other three joints passive makes the system fully

actuated.

Iannitti and Lynch [35] presented a case study in kinematically controllable underactuated systems as a minimum control-switch motions for the snakeboard. Another work given in [36] introduces an underactuated system in the form of biped walking robot. This system was modeled for two separate cases consisting of the swing phase where only one foot is in contact with the ground, and the impact phase where both feet are in contact with the ground. The impact phase was assumed to last for an infinitesimal time and, therefore, was not included in the overall plant model.

There are some notable works on the control of underactuated systems such as the book by Fantoni and Lozano [37], and [38] by Ortega *et.al* introducing a methodology named *interconnection and damping assignment* for the stabilization of a underactuated systems.

1.2.4 Kinematically deficient systems

Although constrained manipulators and kinematically redundant manipulators have been studied extensively, such as the work by Bruyninckx and Khatib [39], kinematically deficient manipulators have not attracted enough attention from the scientific community. Abdel-Malek *et al.* [40] studied the workspace issues of kinematically deficient manipulators. Dynamics of two-finger grippers as kinematically deficient manipulators was studied by Prattichizzo and Bicchi [41]. Teleoperated surgical robots were considered in both kinematically redundant and kinematically deficient cases by Funda et al. [42]. Mobility criterion was considered by Rico *et.al* [43].

1.2.5 Nonholonomic systems

Analytical formalism of Euler and Lagrange was believed to be applicable to any mechanical system until as late as 1894 when Hertz [44] introduced the existence of kinematic constraints that impose no restrictions on the possible configurations. Having the distinction between holonomic and nonholonomic constraints recognized, many researchers (Čaplygin, Volterra, Appell, Maggi, and others) proposed methodologies to solve the dynamics of nonholonomic systems.

In order to analyze a nonholonomic system like a holonomic one, constraint forces are

introduced via the Lagrange multipliers. However, the computation of the multipliers is usually not straight forward. Among others we can mention Hamel [45] who in 1949 developed a method to eliminate the necessity of explicit computation of non working constraint forces. However, Hamel's method introduces other detailed and lengthy computations which require perhaps as much computation as the constraint forces themselves. Later in 1961, Kane [46] developed a method to eliminate non working constraint forces with much less computational effort than that of Hamel. Orthogonal complement based methods of dynamics consist of determining a matrix whose columns span the nullspace of the matrix of velocity constraints. The idea of the orthogonal complement of velocity constraints in the derivation of dynamical equations is not new, for it has been extensively used in multibody dynamics. In 1991 Saha and Angeles [47] make a use of this method in their algorithm.

Dynamics and control of multiple cooperating manipulators with rolling contacts by Deo and Walker [48] models the rolling contact as an unactuated joint of the manipulator. Dynamic Modeling and Adaptive Traction Control for Mobile Robots was studied by Albagul [49]. A mobility analysis method of closed-chain mechanisms with over-constraints and non-holonomic constraints was examined by Kim *et.al.* [50]. From the practical point of view, it needs to be mentioned here that Sorensen's Ph.D. thesis [51] includes implementation on a four-wheel-drive four-wheel-steer vehicle.

1.3 Contributions

The contributions made in this thesis can be classified under the following categories:

- *Kinematically Deficient Cooperating Manipulators:* The numerical problems associated with the computation of the interaction forces and torques, among themselves and/or with the environment, of multiple manipulators at least one of which is kinematically deficient is addressed. A new concept named "pseudo joint" has been introduced as a methodology to solve such complicated systems.

- *Cooperating Underactuated Systems:* The roots of the algorithm on the underactuated systems can be found in [30] which presents the dynamics of underactuated open chain manipulator in order n formulation. Our contribution is to extend

this algorithm to include underactuated manipulators forming closed kinematic loop on a free-flying space platform.

- $\mathcal{O}(n)$ *Formulation:* Mass matrix factorization, which is the core of the $\mathcal{O}(n)$ formulation, has been reformulated to ease the use of it.

- *Nonholonomic systems:* Application of the proposed algorithm to nonholonomic systems enjoys a preeminence among the algorithms known in the literature for its use as a high performance observer of the contact forces between tires and the road.

Next section outlines the organization of this thesis.

1.4 Thesis Outline

Following the introductory material in this chapter, the thesis begins with the dynamics of open and closed kinematic chain systems in chapter 2, where both open and closed-kinematic chain systems are considered to be mounted on a mobile platform instead of a fixed one so that the equation of motions are applicable to a wider set of systems. Later in the thesis, we benefit from this perspective.
The performance of the algorithm is determined by the number of operations necessary for the inversion of the generalized mass matrix. In chapter 3, modified mass matrix factorization and inversion technique based on [1] is explained in detail.
Within a complex topology system, there are two distinct cases that needs to be addressed separately. These are namely underactuated and kinematically deficient structures of closed-kinematic chains. Dynamical modeling theory has been developed for both of these cases in chapter 4 which constitutes for the theoretical foundation of the thesis.
Application and results are given in chapter 5. Finally, chapter 6 provides the concluding remarks.

2. DYNAMICS OF SERIAL AND CLOSED TOPOLOGY SYSTEMS

A system of rigid bodies connected by hinges or sliders form either one or the combinations of three different structures; serial, tree and closed topology systems, an example for each of which is given in Figure 2.1. Any of the two bodies in both serial and tree topology systems has a unique path. The difference in between the two is that a serial topology system has only one terminal body while a tree topology system has multiple terminal bodies. As for the closed topology system, there exist a non-unique path between any two bodies at the system.

Out of the three topologies mentioned above, the serial rigid multibody system is the most basic and the simplest structure. Therefore, it is an ideal platform for laying out the ingredients of the dynamic modeling algorithm used in this thesis. Closed topology systems, on the other hand, constitute for the difficult case where the closure forces and torques need to be computed. Consequently, the dynamical modeling of these two distinct cases will be covered in this chapter.

2.1 Notation

The notation introduced in this section applies not only to this chapter but also to the rest of the thesis.

Let α represent any variable in this thesis. Three indices a, b, c can be used as ${}^{a}_{b}\alpha_{c}$ to mean the following. The superscript a indicates the number of the associated manipulator, the left subscript b indicates the dimension of the variable, and the right subscript c indicates the number of the link (body) being considered.

The algorithm presented here utilizes a basis-free vectorial representation. Vectors in 3 dimensional space are represented with an overarrow ($\vec{x}$). Spatial vectors in 6 dimensional space are represented with two overarrows ($\vec{\vec{x}}$). In mathematical sense, vectors in all other cases are represented as underlined ($\underline{x}$). For matrices, bold capital

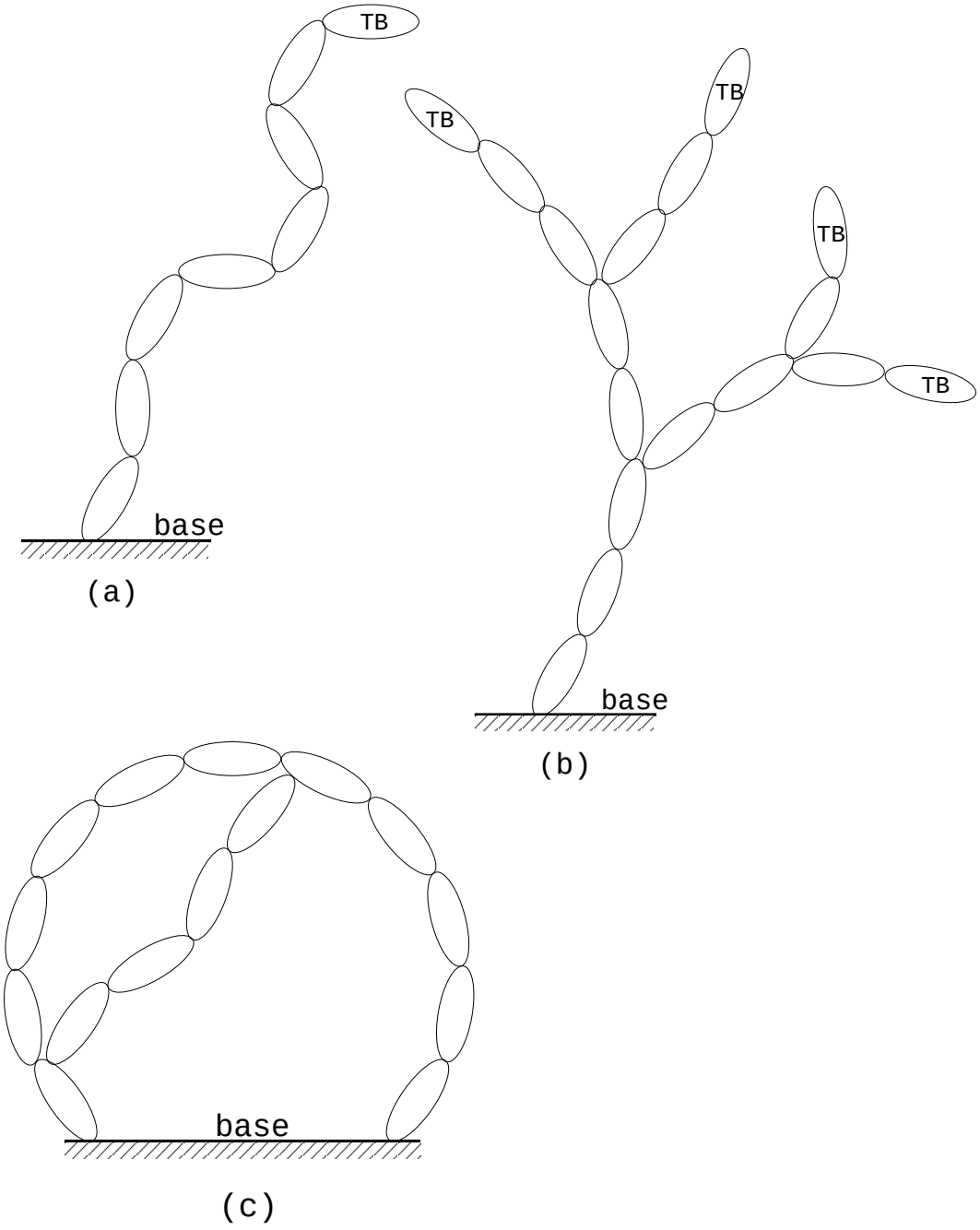

Figure 2.1: Examples of (a) a serial topology system, (b) a tree topology system, and (c) a closed topology system. Here TB stands for “Terminal Body.”

letters ($\mathbf{X}$) or caligraphic fonts ($\mathcal{X}$) are used. Some key vectors used throughout the thesis are displayed in Figure 2.2.

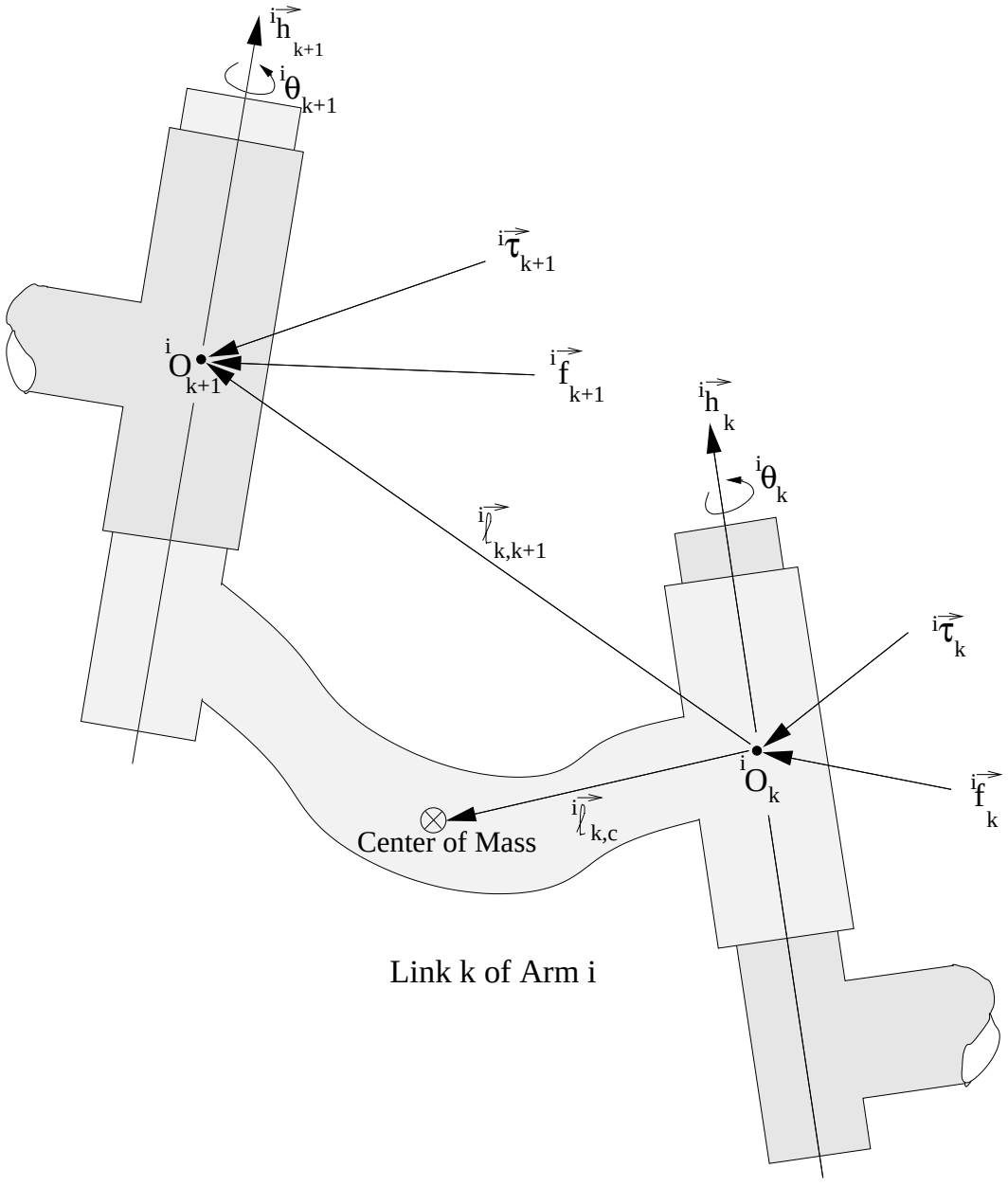

Figure 2.2: Vectors associated with link k of the manipulator i

2.2 Serial Manipulator On A Mobile Platform

A serial manipulator constitutes a serial topology system whose dynamics will be given in this section. Although the dynamics of such systems is well-known and can be found in many textbooks such as [52, 53, 54, 55], here we will present the methodology

very similar to the one introduced in [1] so that the basic ingredients of the dynamic modeling algorithm are introduced. Let us start with the kinematics.

2.2.1 Kinematics

Angular and linear link velocities of the i^{th} manipulator propagate from link $k-1$ to link k for a revolute joint as follows:

$$
\begin{aligned}
{}^{i}\vec{\omega}_k &= {}^{i}\vec{\omega}_{k-1} + {}^{i}\vec{h}_k {}^{i}\dot{\theta}_k && (2.1)\\
{}^{i}\vec{v}_k &= {}^{i}\vec{v}_{k-1} + {}^{i}\vec{\omega}_{k-1} \times {}^{i}\vec{\ell}_{k-1,k} = {}^{i}\vec{v}_{k-1} - {}^{i}\vec{\ell}_{k-1,k} \times {}^{i}\vec{\omega}_{k-1} \\
&= {}^{i}\vec{v}_{k-1} - {}^{i}\mathbf{L}_{k-1,k}\, {}^{i}\vec{\omega}_{k-1} && (2.2)
\end{aligned}
$$

where ${}^{i}\mathbf{L}_{k-1,k} \triangleq ({}^{i}\vec{\ell}_{k-1,k}\times)$ is an operator in the form of a skew symmetric matrix given as

$$
{}^{i}\mathbf{L}_{k-1,k} = \begin{bmatrix} 0 & -{}^{i}\ell_{(k-1,k)_z} & {}^{i}\ell_{(k-1,k)_y} \\ {}^{i}\ell_{(k-1,k)_z} & 0 & -{}^{i}\ell_{(k-1,k)_x} \\ -{}^{i}\ell_{(k-1,k)_y} & {}^{i}\ell_{(k-1,k)_x} & 0 \end{bmatrix}
$$

and $[{}^{i}\ell_{(k-1,k)_x} \;\; {}^{i}\ell_{(k-1,k)_y} \;\; {}^{i}\ell_{(k-1,k)_z}]^T$ is the representation of $\vec{\ell}_{k-1,k}$ in the reference frame. Equations (2.1) and (2.2) can be written in a matrix form as follows:

$$
{}^{i}\vec{\vec{V}}_k = {}^{i}\mathbf{\Phi}_{k,k-1}\, {}^{i}\vec{\vec{V}}_{k-1} + {}^{i}\vec{\vec{H}}_k\, {}^{i}\dot{\theta}_k \qquad (2.3)
$$

where, link spatial velocity is defined as

$$
{}^{i}\vec{\vec{V}}_k \triangleq \begin{bmatrix} {}^{i}\vec{\omega}_k \\ {}^{i}\vec{v}_k \end{bmatrix} \qquad (2.4)
$$

and the propagation operator is defined as

$$
{}^{i}\mathbf{\Phi}_{k,k-1} \triangleq \begin{bmatrix} {}_3\mathbf{I} & {}_3\mathbf{0} \\ -{}^{i}\mathbf{L}_{k-1,k} & {}_3\mathbf{I} \end{bmatrix} \qquad (2.5)
$$

and, finally, axis of rotation spatial vector is defined as

$$
{}^{i}\vec{\vec{H}}_k \triangleq \begin{bmatrix} {}^{i}\vec{h}_k \\ \vec{0} \end{bmatrix} \qquad (2.6)
$$

If it is a prismatic joint, all we have to do is to change the definition of ${}^i\vec{\vec{H}}_k$ in (2.6) as

$$ {}^i\vec{\vec{H}}_k \triangleq \begin{bmatrix} \vec{0} \\ {}^i\vec{h}_k \end{bmatrix} \tag{2.7} $$

Next, we write the spatial velocities of each link from base to tip (outboard) of arm i on a mobile base as

$$ \begin{aligned} {}^i\vec{\vec{V}}_o &= \vec{\vec{V}}_b \\ {}^i\vec{\vec{V}}_1 &= {}^i\mathbf{\Phi}_{1,0}\,{}^i\vec{\vec{V}}_o + {}^i\vec{\vec{H}}_1\,{}^i\dot{\theta}_1 \\ {}^i\vec{\vec{V}}_2 &= {}^i\mathbf{\Phi}_{2,1}\,{}^i\vec{\vec{V}}_1 + {}^i\vec{\vec{H}}_2\,{}^i\dot{\theta}_2 \\ &\vdots \\ {}^i\vec{\vec{V}}_{n_i} &= {}^i\mathbf{\Phi}_{n_i,n_i-1}\,{}^i\vec{\vec{V}}_{n_i-1} + {}^i\vec{\vec{H}}_{n_i}\,{}^i\dot{\theta}_{n_i} \end{aligned} \tag{2.8} $$

where n_i is the number of DOF of the i^{th} manipulator. Figure 2.3, which shows a conceptual serial manipulator on a mobile platform, helps to understand the propagation given in (2.8).

Using the state transition property of the propagation matrix

$$ {}^i\mathbf{\Phi}_{a,b}\,{}^i\mathbf{\Phi}_{b,c} = {}^i\mathbf{\Phi}_{a,c} \tag{2.9} $$

we rewrite the equations in (2.8) so that the spatial velocity terms (except for the base spatial velocity) on the right side of the equations are eliminated

$$ \begin{aligned} {}^i\vec{\vec{V}}_1 &= {}^i\mathbf{\Phi}_{1,0}\vec{\vec{V}}_b + {}^i\vec{\vec{H}}_1\,{}^i\dot{\theta}_1 \\ {}^i\vec{\vec{V}}_2 &= {}^i\mathbf{\Phi}_{2,0}\vec{\vec{V}}_b + {}^i\mathbf{\Phi}_{2,1}{}^i\vec{\vec{H}}_1\,{}^i\dot{\theta}_1 + {}^i\vec{\vec{H}}_2\,{}^i\dot{\theta}_2 \\ &\vdots \\ {}^i\vec{\vec{V}}_{n_i} &= {}^i\mathbf{\Phi}_{n_i,0}\vec{\vec{V}}_b + \cdots + {}^i\mathbf{\Phi}_{n_i,n_i-1}{}^i\vec{\vec{H}}_{n_i-1}\,{}^i\dot{\theta}_{n_i-1} + {}^i\vec{\vec{H}}_{n_i}\,{}^i\dot{\theta}_{n_i} \end{aligned} \tag{2.10} $$

Equations in (2.10) can be written in a matrix form as follows:

$$ {}^i\underline{V} = {}^i\mathbf{\Phi}({}^i\mathbf{H}\,{}^i\underline{\dot{\theta}} + {}^i\mathbf{\Phi}_b\vec{\vec{V}}_b) \tag{2.11} $$

where,

$$ {}^i\underline{V} = \begin{bmatrix} {}^i\vec{\vec{V}}_1 \\ {}^i\vec{\vec{V}}_2 \\ \vdots \\ {}^i\vec{\vec{V}}_{n_i} \end{bmatrix} \qquad {}^i\mathbf{\Phi} = \begin{bmatrix} {}_6\mathbf{I} & {}_6\mathbf{0} & \cdots & {}_6\mathbf{0} \\ {}^i\mathbf{\Phi}_{2,1} & {}_6\mathbf{I} & \cdots & {}_6\mathbf{0} \\ \vdots & \vdots & \ddots & \vdots \\ {}^i\mathbf{\Phi}_{n_i,1} & {}^i\mathbf{\Phi}_{n_i,2} & \cdots & {}_6\mathbf{I} \end{bmatrix} \qquad {}^i\underline{\dot{\theta}} = \begin{bmatrix} {}^i\dot{\theta}_1 \\ {}^i\dot{\theta}_2 \\ \vdots \\ {}^i\dot{\theta}_{n_i} \end{bmatrix} $$

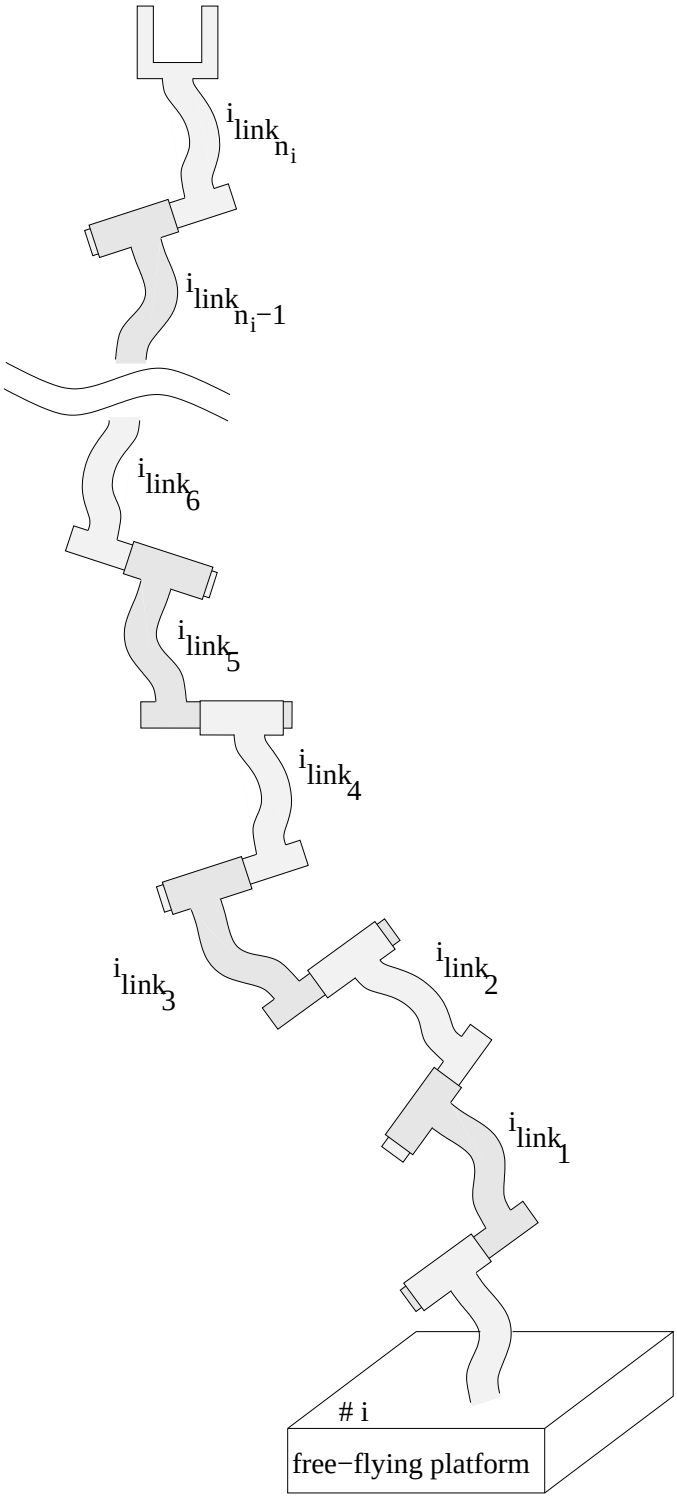

Figure 2.3: Serial manipulator on a free-flying mobile platform

$$ {}^{i}\mathbf{H} = \begin{bmatrix} {}^{i}\mathbf{H}_1 & & & \mathbf{0} \\ & {}^{i}\mathbf{H}_2 & & \\ & & \ddots & \\ \mathbf{0} & & & {}^{i}\mathbf{H}_{n_i} \end{bmatrix} \qquad {}^{i}\mathbf{\Phi}_b = \begin{bmatrix} {}^{i}\mathbf{\Phi}_{1,0} \\ {}_{6}\mathbf{0} \\ \vdots \\ {}_{6}\mathbf{0} \end{bmatrix} $$

Tip velocity is written as

$$ {}^{i}\vec{\vec{V}}_t = {}^{i}\mathbf{\Phi}_t \, {}^{i}\underline{V} \tag{2.12} $$

where,

$$ {}^{i}\mathbf{\Phi}_t = \begin{bmatrix} {}_{6}\mathbf{0} & \cdots & {}_{6}\mathbf{0} & {}^{i}\mathbf{\Phi}_{n_i+1,n_i} \end{bmatrix} $$

Substituting equation (2.11) into (2.12), we get

$$ {}^{i}\vec{\vec{V}}_t = {}^{i}\mathcal{J} \, {}^{i}\underline{\dot{\theta}} + {}^{i}\mathbf{\Phi}_{t,b}\vec{\vec{V}}_b \tag{2.13} $$

where ${}^{i}\mathcal{J}$ which is the Jacobian operator of the i^{th} manipulator and ${}^{i}\mathbf{\Phi}_{t,b}$ are defined as

$$ {}^{i}\mathcal{J} \triangleq {}^{i}\mathbf{\Phi}_t \, {}^{i}\mathbf{\Phi} \, {}^{i}\mathbf{H} \qquad {}^{i}\mathbf{\Phi}_{t,b} \triangleq {}^{i}\mathbf{\Phi}_{n_i+1,0} = {}^{i}\mathbf{\Phi}_t {}^{i}\mathbf{\Phi} {}^{i}\mathbf{\Phi}_b $$

This concludes the kinematics of an open-chain manipulator.

2.2.2 Dynamics

In order to move to dynamical analysis, we need to take the time derivative of equations (2.1) and (2.2).

$$ \begin{aligned} {}^{i}\dot{\vec{\omega}}_k &= {}^{i}\dot{\vec{\omega}}_{k-1} + {}^{i}\vec{h}_k {}^{i}\ddot{\theta}_k + {}^{i}\vec{\omega}_k \times {}^{i}\vec{h}_k {}^{i}\dot{\theta}_k \\ &= {}^{i}\dot{\vec{\omega}}_{k-1} + {}^{i}\vec{h}_k {}^{i}\ddot{\theta}_k + {}^{i}\vec{\omega}_k \times ({}^{i}\vec{\omega}_k - {}^{i}\vec{\omega}_{k-1}) \\ &= {}^{i}\dot{\vec{\omega}}_{k-1} + {}^{i}\vec{h}_k {}^{i}\ddot{\theta}_k + {}^{i}\vec{\omega}_{k-1} \times {}^{i}\vec{\omega}_k \end{aligned} \tag{2.14} $$

$$ \begin{aligned} {}^{i}\dot{\vec{v}}_k &= {}^{i}\dot{\vec{v}}_{k-1} + {}^{i}\dot{\vec{\omega}}_{k-1} \times {}^{i}\vec{\ell}_{k-1,k} + {}^{i}\vec{\omega}_{k-1} \times ({}^{i}\vec{\omega}_{k-1} \times {}^{i}\vec{\ell}_{k-1,k}) \\ &= {}^{i}\dot{\vec{v}}_{k-1} - {}^{i}\vec{\ell}_{k-1,k} \times {}^{i}\dot{\vec{\omega}}_{k-1} + {}^{i}\vec{\omega}_{k-1} \times ({}^{i}\vec{\omega}_{k-1} \times {}^{i}\vec{\ell}_{k-1,k}) \end{aligned} \tag{2.15} $$

Equations (2.14) and (2.15) can be written in a matrix form as follows:

$$ {}^{i}\dot{\vec{\vec{V}}}_k = {}^{i}\mathbf{\Phi}_{k,k-1} {}^{i}\dot{\vec{\vec{V}}}_{k-1} + {}^{i}\vec{\vec{H}}_k \, \ddot{\theta}_k + {}^{i}\vec{\vec{a}}_k \tag{2.16} $$

where ${}^i\vec{\vec{a}}_k$ is the spatial bias accelerations.

$${}^i\vec{\vec{a}}_k = \begin{bmatrix} {}^i\vec{\omega}_{k-1} \times {}^i\vec{\omega}_k \\ {}^i\vec{\omega}_{k-1} \times ({}^i\vec{\omega}_{k-1} \times {}^i\vec{\ell}_{k-1,k}) \end{bmatrix}$$

Stacking up all of the link accelerations of arm i using equation (2.16), we get

$${}^i\underline{\dot{V}} = {}^i\mathbf{\Phi}({}^i\mathbf{H}\,{}^i\underline{\ddot{\theta}} + {}^i\underline{a} + {}^i\mathbf{\Phi}_b\dot{\vec{\vec{V}}}_b) \tag{2.17}$$

Now, we will write the propagation of link torques and forces. This cannot be done outboard because of the boundary conditions. Hence, it will be done inboard. In this thesis, the term outboard is used to mean the traverse from base towards tip, and inboard is used to mean the traverse from tip towards base.

$${}^i\vec{\mathcal{T}}_k = {}^i\vec{\mathcal{T}}_{k+1} + {}^i\vec{\ell}_{k,k+1} \times \vec{f}_{k+1} + {}^i\vec{\ell}_{k,c} \times {}^i\dot{\vec{v}}_k\,{}^im_k + \frac{d}{dt}({}^i\mathcal{I}_k\,{}^i\vec{\omega}_k) \tag{2.18}$$

On the right hand side of equation (2.18), the first and the second terms come from joint $k+1$, the third term is due to translation, and the last term is due to rotation.
Similar to torque propagation, the following is written for the link forces:

$${}^i\vec{f}_k = {}^i\vec{f}_{k+1} + {}^im_k\frac{d}{dt}({}^i\vec{v}_k + {}^i\vec{\omega}_k \times {}^i\vec{\ell}_{k,c}) \tag{2.19}$$

Equations (2.18) and (2.19) can be written in a matrix form as follows:

$${}^i\vec{\vec{F}}_k = {}^i\mathbf{\Phi}^T_{k+1,k}\,{}^i\vec{\vec{F}}_{k+1} + {}^i\mathbf{M}_k\,{}^i\dot{\vec{\vec{V}}}_k + {}^i\vec{\vec{b}}_k \tag{2.20}$$

where ${}^i\vec{\vec{F}}_k$ is the link spatial forces, ${}^i\mathbf{M}_k$ is the link mass matrix, and ${}^i\vec{\vec{b}}_k$ is the link spatial forces remainder terms, as defined below:

$${}^i\vec{\vec{F}}_k = \begin{bmatrix} {}^i\vec{\mathcal{T}}_k \\ {}^i\vec{f}_k \end{bmatrix} \qquad {}^i\mathbf{M}_k = \begin{bmatrix} {}^i\mathcal{I}_k & {}^im_k\,{}^i\mathbf{L}_{k,c} \\ -{}^im_k\,{}^i\mathbf{L}_{k,c} & {}_3\mathbf{I}\,{}^im_k \end{bmatrix}$$

$${}^i\vec{\vec{b}}_k = \begin{bmatrix} {}^i\vec{\omega}_k \times {}^i\mathcal{I}_k\,{}^i\vec{\omega}_k \\ {}^im_k\,{}^i\vec{\omega}_k \times ({}^i\vec{\omega}_k \times {}^i\vec{\ell}_{k,c}) \end{bmatrix}$$

Stacking up all the link spatial forces of arm i using equation (2.20), we get

$${}^i\underline{F} = {}^i\mathbf{\Phi}^T({}^i\mathbf{M}\,{}^i\underline{\dot{V}} + {}^i\underline{b} + {}^i\mathbf{\Phi}_t^T\,{}^i\vec{\vec{F}}_t) \tag{2.21}$$

where

$$ {}^{i}\underline{F} = \begin{bmatrix} {}^{i}\vec{F}_1 \\ \vdots \\ {}^{i}\vec{F}_{n_i} \end{bmatrix} \qquad {}^{i}\mathbf{M} = \begin{bmatrix} {}^{i}\mathbf{M}_1 & & \mathbf{0} \\ & \ddots & \\ \mathbf{0} & & {}^{i}\mathbf{M}_{n_i} \end{bmatrix} \qquad {}^{i}\underline{b} = \begin{bmatrix} {}^{i}\vec{b}_1 \\ \vdots \\ {}^{i}\vec{b}_{n_i} \end{bmatrix} $$

Next, we substitute equation (2.17) into (2.21),

$$ {}^{i}\underline{F} = {}^{i}\mathbf{\Phi}^T({}^{i}\mathbf{M}\,{}^{i}\mathbf{\Phi}\,{}^{i}\mathbf{H}\,{}^{i}\underline{\ddot{\theta}} + {}^{i}\mathbf{M}\,{}^{i}\mathbf{\Phi}\,{}^{i}\underline{a} + {}^{i}\mathbf{M}\,{}^{i}\mathbf{\Phi}\,{}^{i}\mathbf{\Phi}_b\,{}^{i}\dot{\vec{V}}_b + {}^{i}\underline{b} + {}^{i}\mathbf{\Phi}_t^T\,{}^{i}\vec{F}_t) \tag{2.22} $$

Here, we are going to utilize the fact that the applied torques are the projection of the link spatial forces along the axes of rotation. This is mathematically stated as:

$$ {}^{i}\underline{\mathcal{T}} = {}^{i}\mathbf{H}^T\,{}^{i}\underline{F} \tag{2.23} $$

Therefore, premultiplying the equation (2.22) by ${}^{i}\mathbf{H}^T$, the left hand side becomes the applied torques. This yields the inverse dynamics of arm i as follows:

$$ {}^{i}\underline{\mathcal{T}} = {}^{i}\mathcal{M}\,{}^{i}\underline{\ddot{\theta}} + {}^{i}\underline{C} + {}^{i}\mathcal{M}_b\,{}^{i}\dot{\vec{V}}_b + {}^{i}\mathcal{J}^T\,{}^{i}\vec{F}_t \tag{2.24} $$

where

$$ \begin{aligned} {}^{i}\mathcal{M} &= {}^{i}\mathbf{H}^T\,{}^{i}\mathbf{\Phi}^T\,{}^{i}\mathbf{M}\,{}^{i}\mathbf{\Phi}\,{}^{i}\mathbf{H} \\ {}^{i}\underline{C} &= {}^{i}\mathbf{H}^T\,{}^{i}\mathbf{\Phi}^T\,({}^{i}\mathbf{M}\,{}^{i}\mathbf{\Phi}\,{}^{i}\underline{a} + {}^{i}\underline{b}) \\ {}^{i}\mathcal{M}_b &= {}^{i}\mathbf{H}^T\,{}^{i}\mathbf{\Phi}^T\,{}^{i}\mathbf{M}\,{}^{i}\mathbf{\Phi}\,{}^{i}\mathbf{\Phi}_b \end{aligned} $$

Here, ${}^{i}\mathcal{M}$ is the generalized mass matrix, ${}^{i}\underline{C}$ is the bias terms including coriolis and gravity, ${}^{i}\mathcal{M}_b$ is the mass matrix regarding the dynamic interaction between the base and the i^{th} arm.

2.3 Cooperating Manipulators On A Mobile Platform

Dynamical modeling of cooperating manipulators is a subset of dynamical modeling of cooperating manipulators on a mobile platform whose conceptual drawing is shown in Figure 2.4. In this section, we will study this larger set.

Mobile platform, also known as *free flying platform*, refers to, in this thesis, a platform that is free to move without constraints. Its bias spatial force, spatial force and generalized mass matrix are given as:

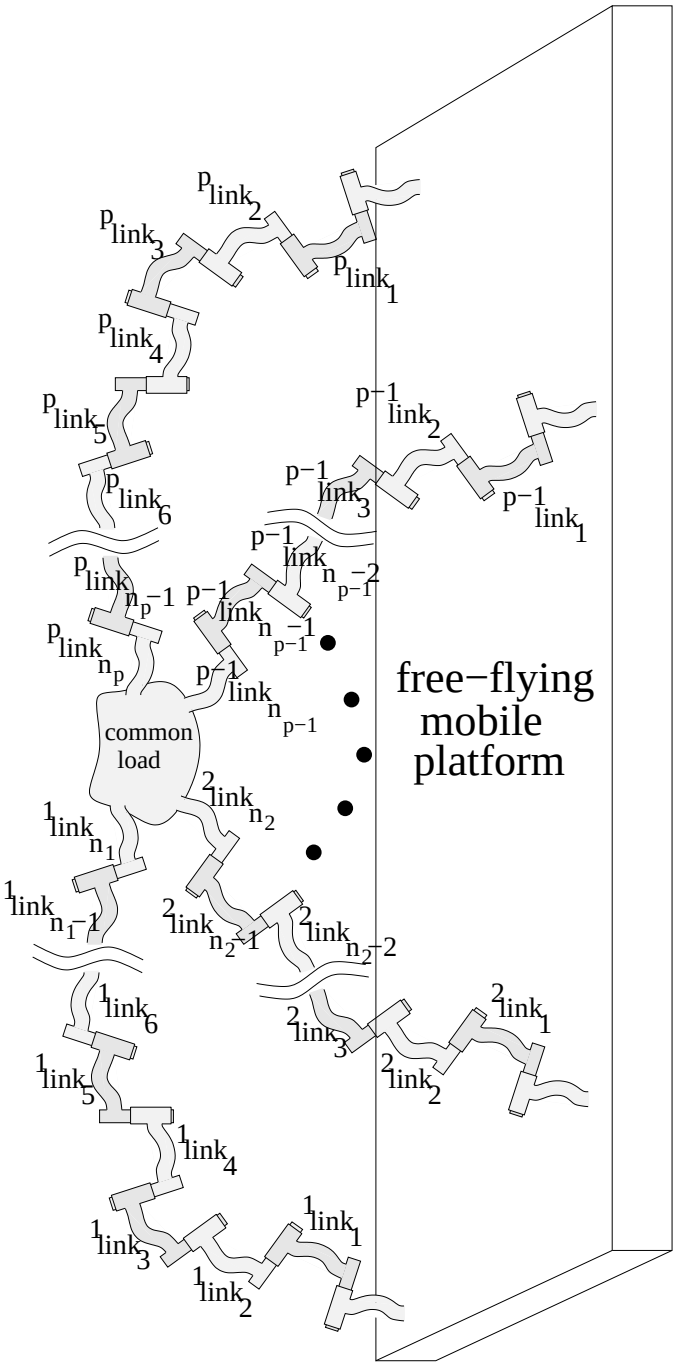

Figure 2.4: Cooperating manipulators with rigid grasp on a free-flying mobile platform

$$\vec{\vec{b}}_b = \begin{bmatrix} \vec{\omega}_b \times \mathcal{I}_b \vec{\omega}_b \\ m_b \vec{\omega}_b \times (\vec{\omega}_b \times \vec{\ell}_{b,c}) \end{bmatrix} \tag{2.25}$$

$$\vec{\vec{F}}_b = \begin{bmatrix} \vec{\mathcal{T}}_b \\ \vec{f}_b \end{bmatrix} \tag{2.26}$$

$$\mathbf{M}_b = \begin{bmatrix} \mathcal{I}_b & m_b \mathbf{L}_{b,c} \\ -m_b \mathbf{L}_{b,c} & {}_3\mathbf{I} m_b \end{bmatrix} \tag{2.27}$$

where, $\mathbf{L}_{b,c}$ is the zero matrix if the origin of the base frame is chosen such that it is coincident with the center of mass of the platform. Otherwise, $\mathbf{L}_{b,c}$ is the skew-symmetric matrix representing the operator $\vec{\ell}_{b,c}\times$, *i.e.*, the cross product of the vector from the origin of the base frame to the center of mass of the platform.

In order to get the dynamical model, we need to stack the accelerations given for an individual manipulator in (2.17) for all the manipulators in the system. Letting p be the number of arms (manipulators) on a mobile platform, we have

$$\dot{\underline{V}} = \mathbf{\Phi}(\mathbf{H}\ddot{\underline{\theta}} + \underline{a}) \tag{2.28}$$

where,

$$\underline{V} = \begin{bmatrix} \vec{\vec{V}}_b \\ {}^1\underline{V} \\ {}^2\underline{V} \\ \vdots \\ {}^p\underline{V} \end{bmatrix} \qquad \underline{\dot{\theta}} = \begin{bmatrix} \vec{\vec{V}}_b \\ {}^1\underline{\dot{\theta}} \\ {}^2\underline{\dot{\theta}} \\ \vdots \\ {}^p\underline{\dot{\theta}} \end{bmatrix} \qquad \underline{\ddot{\theta}} = \begin{bmatrix} \dot{\vec{\vec{V}}}_b \\ {}^1\underline{\ddot{\theta}} \\ {}^2\underline{\ddot{\theta}} \\ \vdots \\ {}^p\underline{\ddot{\theta}} \end{bmatrix} \qquad \underline{a} = \begin{bmatrix} \vec{\vec{a}}_b \\ {}^1\underline{a} \\ {}^2\underline{a} \\ \vdots \\ {}^p\underline{a} \end{bmatrix}$$

$$\mathbf{\Phi} = \begin{bmatrix} {}_6\mathbf{I} & \mathbf{0} & \mathbf{0} & \cdots & \mathbf{0} \\ {}^1\mathbf{\Phi}\ {}^1\mathbf{\Phi}_b & {}^1\mathbf{\Phi} & \mathbf{0} & \cdots & \mathbf{0} \\ {}^2\mathbf{\Phi}\ {}^2\mathbf{\Phi}_b & \mathbf{0} & {}^2\mathbf{\Phi} & \cdots & \mathbf{0} \\ \vdots & \vdots & \vdots & \ddots & \vdots \\ {}^p\mathbf{\Phi}\ {}^p\mathbf{\Phi}_b & \mathbf{0} & \mathbf{0} & \cdots & {}^p\mathbf{\Phi} \end{bmatrix} \qquad \mathbf{H} = \begin{bmatrix} {}_6\mathbf{I} & \mathbf{0} & \mathbf{0} & \cdots & \mathbf{0} \\ \mathbf{0} & {}^1\mathbf{H} & \mathbf{0} & \cdots & \mathbf{0} \\ \mathbf{0} & \mathbf{0} & {}^2\mathbf{H} & \cdots & \mathbf{0} \\ \vdots & \vdots & \vdots & \ddots & \vdots \\ \mathbf{0} & \mathbf{0} & \mathbf{0} & \cdots & {}^p\mathbf{H} \end{bmatrix}$$

Gravity is introduced to the system by assigning

$$\vec{\vec{a}}_b = \begin{bmatrix} \vec{0} \\ \vec{g} \end{bmatrix} \tag{2.29}$$

where $\vec{g}$ is the gravitational acceleration vector. We first look at the spatial force propagation for all of the arms.

$$\underline{F} = \mathbf{\Phi}^T(\mathbf{M}\dot{\underline{V}} + \underline{b} + \mathbf{\Phi}_t^T \underline{F}_t) \tag{2.30}$$

where,

$$\underline{F} = \begin{bmatrix} \vec{\vec{F}}_b \\ {}^1\underline{F} \\ {}^2\underline{F} \\ \vdots \\ {}^p\underline{F} \end{bmatrix} \qquad \underline{b} = \begin{bmatrix} \vec{\vec{b}}_b \\ {}^1\underline{b} \\ {}^2\underline{b} \\ \vdots \\ {}^p\underline{b} \end{bmatrix} \qquad \underline{F}_t = \begin{bmatrix} {}^1\vec{\vec{F}}_t \\ {}^2\vec{\vec{F}}_t \\ \vdots \\ {}^p\vec{\vec{F}}_t \end{bmatrix}$$

$$\mathbf{M} = \begin{bmatrix} \mathbf{M}_b & \mathbf{0} & \mathbf{0} & \cdots & \mathbf{0} \\ \mathbf{0} & {}^1\mathbf{M} & \mathbf{0} & \cdots & \mathbf{0} \\ \mathbf{0} & \mathbf{0} & {}^2\mathbf{M} & \cdots & \mathbf{0} \\ \vdots & \vdots & \vdots & \ddots & \vdots \\ \mathbf{0} & \mathbf{0} & \mathbf{0} & \cdots & {}^p\mathbf{M} \end{bmatrix} \qquad \mathbf{\Phi}_t = \begin{bmatrix} \mathbf{0} & {}^1\mathbf{\Phi}_t & \mathbf{0} & \cdots & \mathbf{0} \\ \mathbf{0} & \mathbf{0} & {}^2\mathbf{\Phi}_t & \cdots & \mathbf{0} \\ \vdots & \vdots & \vdots & \ddots & \vdots \\ \mathbf{0} & \mathbf{0} & \mathbf{0} & \cdots & {}^p\mathbf{\Phi}_t \end{bmatrix}$$

Just the same way as was done for a single manipulator in (2.23), now we write the following equation to single out the applied torques from (2.30) for the complete system.

$$\underline{\mathcal{T}} = \mathbf{H}^T \underline{F} \tag{2.31}$$

We now obtain the equation of motion in the form of inverse dynamics from (2.30) and (2.31).

$$\underline{\mathcal{T}} = \mathcal{M}\underline{\ddot{\theta}} + \underline{C} + \mathcal{J}^T \underline{F}_t \tag{2.32}$$

where

$$\begin{aligned} \mathcal{M} &\triangleq \mathbf{H}^T\mathbf{\Phi}^T\mathbf{M}\mathbf{\Phi}\mathbf{H} \\ &= \begin{bmatrix} {}^b\mathcal{M}_b & {}^1\mathcal{M}_b^T & {}^2\mathcal{M}_b^T & \cdots & {}^p\mathcal{M}_b^T \\ {}^1\mathcal{M}_b & {}^1\mathcal{M} & \mathbf{0} & \cdots & \mathbf{0} \\ {}^2\mathcal{M}_b & \mathbf{0} & {}^2\mathcal{M} & \cdots & \mathbf{0} \\ \vdots & \vdots & \vdots & \ddots & \vdots \\ {}^p\mathcal{M}_b & \mathbf{0} & \mathbf{0} & \cdots & {}^p\mathcal{M} \end{bmatrix} \end{aligned} \tag{2.33}$$

$$^{b}\mathcal{M}_b = \mathbf{M}_b + \sum_{i=1}^{p} {}^{i}\Phi_b^T \; {}^{i}\Phi^T \; {}^{i}\mathcal{M} \; {}^{i}\Phi \; {}^{i}\Phi_b \tag{2.34}$$

$$\begin{aligned} \underline{C} &\triangleq \mathbf{H}^T\mathbf{\Phi}^T\mathbf{M}\mathbf{\Phi}\underline{a} + \mathbf{H}^T\mathbf{\Phi}^T\underline{b} \\ &= \begin{bmatrix} \underline{C_b} \\ {}^{1}\underline{C} \\ {}^{2}\underline{C} \\ \vdots \\ {}^{p}\underline{C} \end{bmatrix} \end{aligned} \tag{2.35}$$

$$\underline{C_b} = \mathbf{M}_b\vec{\vec{a}}_b + \vec{\vec{b}}_b + \sum_{i=1}^{p} {}^{i}\Phi_b^T \; {}^{i}\Phi^T \left({}^{i}\mathcal{M} \; {}^{i}\Phi({}^{i}\Phi_b\vec{\vec{a}}_b + {}^{i}\underline{a}) + {}^{i}\underline{b} \right) \tag{2.36}$$

and the Jacobian

$$\begin{aligned} \mathcal{J} &\triangleq \mathbf{\Phi}_t\mathbf{\Phi}\mathbf{H} \\ &= \begin{bmatrix} {}^{1}\mathbf{\Phi}_{t,b} & {}^{1}\mathcal{J} & \mathbf{0} & \cdots & \mathbf{0} \\ {}^{2}\mathbf{\Phi}_{t,b} & \mathbf{0} & {}^{2}\mathcal{J} & \cdots & \mathbf{0} \\ \vdots & \vdots & \vdots & \ddots & \vdots \\ {}^{p}\mathbf{\Phi}_{t,b} & \mathbf{0} & \mathbf{0} & \cdots & {}^{p}\mathcal{J} \end{bmatrix} \end{aligned} \tag{2.37}$$

Therefore, the equation of motion regarding the forward dynamics is obtained as

$$\ddot{\underline{\theta}} = \mathcal{M}^{-1}\left(\underline{\mathcal{T}} - \underline{C} - \mathcal{J}^T\underline{F_t}\right) \tag{2.38}$$

2.3.1 Computation of the term $\dot{\mathcal{J}}\dot{\theta}$

Tip velocity for an arm was given in (2.12). This can be written for the complete system as

$$\underline{V_t} = \mathbf{\Phi}_t\underline{V} \tag{2.39}$$

where

$$\underline{V_t} = \begin{bmatrix} {}^{1}\vec{\vec{V}}_t \\ {}^{2}\vec{\vec{V}}_t \\ \vdots \\ {}^{p}\vec{\vec{V}}_t \end{bmatrix}$$

Taking the time derivative of (2.39) and utilizing (2.28) and (2.37), we can write the tip accelerations as

$$\begin{aligned}
\underline{\dot{V}_t} &= \mathbf{\Phi}_t \underline{\dot{V}} + \dot{\mathbf{\Phi}}_t \underline{V} \\
\underline{\dot{V}_t} &= \mathbf{\Phi}_t \mathbf{\Phi}(\mathbf{H}\underline{\ddot{\theta}} + \underline{a}) + \dot{\mathbf{\Phi}}_t \underline{V} \\
&= \mathcal{J}\underline{\ddot{\theta}} + \mathbf{\Phi}_t \mathbf{\Phi}\underline{a} + \dot{\mathbf{\Phi}}_t \mathbf{\Phi}\mathbf{H}\underline{\dot{\theta}} \qquad (2.40)
\end{aligned}$$

Since $\underline{V_t} = \mathcal{J}\underline{\dot{\theta}}$ by definition, we can take the time derivative of it and compare the result by (2.40):

$$\begin{aligned}
\underline{\dot{V}_t} &= \mathcal{J}\underline{\ddot{\theta}} + \dot{\mathcal{J}}\underline{\dot{\theta}} \qquad (2.41) \\
&= \mathcal{J}\underline{\ddot{\theta}} + \mathbf{\Phi}_t \mathbf{\Phi}\underline{a} + \dot{\mathbf{\Phi}}_t \mathbf{\Phi}\mathbf{H}\underline{\dot{\theta}} \qquad (2.42)
\end{aligned}$$

As a result of a comparison between (2.41) and (2.42), we can conclude that

$$\dot{\mathcal{J}}\underline{\dot{\theta}} = \mathbf{\Phi}_t \mathbf{\Phi}\underline{a} + \dot{\mathbf{\Phi}}_t \mathbf{\Phi}\mathbf{H}\underline{\dot{\theta}} \qquad (2.43)$$

2.3.2 Computation of the tip forces

In order to obtain the dynamical model of the cooperating manipulators, we need to consider a common payload forming loops or closed kinematic chains. In this case, the tip forces need to be calculated. Let us first take a look at the kinematic constraint due to holding the common load. As displayed at Figure 2.5, the idea is to propagate the tip velocities to a common point.

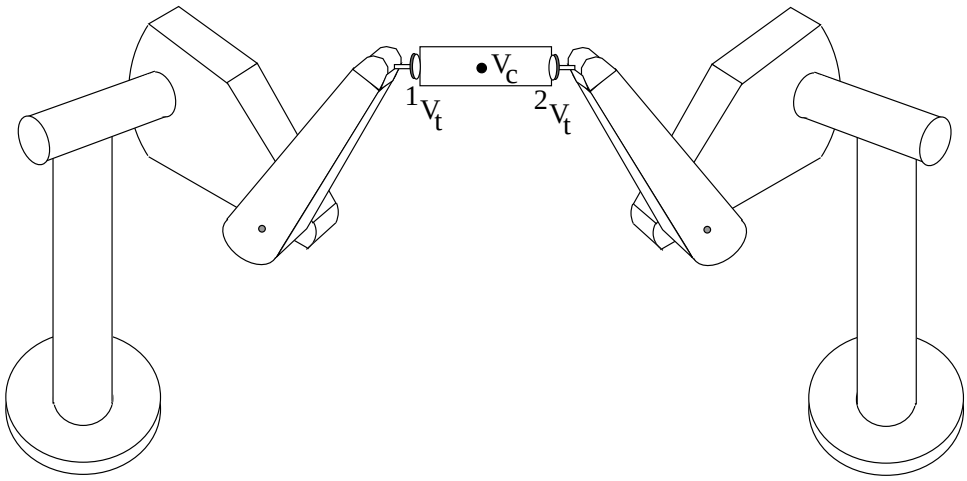

Figure 2.5: An example of cooperating manipulators holding a common object

$$\underline{V}_t = \mathcal{J}\dot{\underline{\theta}} = \mathbf{A}\vec{\vec{V}}_c \tag{2.44}$$

Kinematic constraint given by equation (2.44) has a dual pair on the dynamical side:

$$\mathbf{A}^T\underline{F}_t = \vec{\vec{F}}_c \tag{2.45}$$

where $\vec{\vec{F}}_c$ is the spatial force vector due to common load whose mass, acceleration and bias force are represented as $\mathbf{M}_c, \dot{\underline{V}}_c, \underline{b}_c$. Hence, the spatial force due to common load interaction is also equal to

$$\vec{\vec{F}}_c = \mathbf{M}_c\dot{\vec{\vec{V}}}_c + \vec{\vec{b}}_c \tag{2.46}$$

If we solve (2.46) for $\dot{\vec{\vec{V}}}_c$ and using (2.45) we get

$$\dot{\vec{\vec{V}}}_c = \mathbf{M}_c^{-1}\mathbf{A}^T\underline{F}_t - \mathbf{M}_c^{-1}\vec{\vec{b}}_c \tag{2.47}$$

On the other hand, taking time derivative of (2.44) provides

$$\dot{\underline{V}}_t = \mathcal{J}\ddot{\underline{\theta}} + \dot{\mathcal{J}}\dot{\underline{\theta}} = \mathbf{A}\dot{\vec{\vec{V}}}_c + \vec{\vec{a}}_c \tag{2.48}$$

where $\vec{\vec{a}}_c$ is the bias spatial accelerations of the common load. Here, the term $\dot{\mathcal{J}}\dot{\underline{\theta}}$ is conveniently obtained as shown in (2.43). From (2.47) and (2.48), we can write

$$\mathcal{J}\ddot{\underline{\theta}} = \mathbf{A}\mathbf{M}_c^{-1}\mathbf{A}^T\underline{F}_t - \mathbf{A}\mathbf{M}_c\vec{\vec{b}}_c + \vec{\vec{a}}_c - \dot{\mathcal{J}}\dot{\underline{\theta}} \tag{2.49}$$

While multiplying (2.38) by $\mathcal{J}$ provides

$$\mathcal{J}\ddot{\underline{\theta}} = \mathcal{J}\mathcal{M}^{-1}\bar{\mathcal{T}} - \mathcal{J}\mathcal{M}^{-1}\mathcal{J}^T\underline{F}_t \tag{2.50}$$

By equating (2.49) and (2.50), $\underline{F}_t$ can be solved from

$$\mathbf{\Omega}\underline{F}_t = \mathcal{J}\mathcal{M}^{-1}\mathcal{J}^T - \mathbf{A}\mathbf{M}_c\vec{\vec{b}}_c + \vec{\vec{a}}_c - \dot{\mathcal{J}}\dot{\underline{\theta}} \tag{2.51}$$

where

$$\mathbf{\Omega} = \mathcal{J}\mathcal{M}^{-1}\mathcal{J}^T + \mathbf{A}\mathbf{M}_c^{-1}\mathbf{A}^T \tag{2.52}$$

provided that Ω is full rank.

All of these derivations yield the following equation of motion of forward dynamics

$$\ddot{\underline{\theta}} = \mathbf{D}\bar{\mathcal{T}} + \mathbf{E} \tag{2.53}$$

where

$$\begin{aligned}\mathbf{D} &= \mathcal{M}^{-1} - \mathcal{M}^{-1}\mathcal{J}^T\Omega^{-1}\mathcal{J}\mathcal{M}^{-1} \\ \mathbf{E} &= -\mathcal{M}^{-1}\mathcal{J}^T\Omega^{-1}(\mathbf{A}\mathbf{M}_c^{-1}\vec{\vec{b}}_c - \vec{\vec{a}}_c + \dot{\mathcal{J}}\underline{\dot{\theta}})\end{aligned}$$

Hence, equation of motion for cooperating manipulators on a mobile platform is obtained in a compact form as given in equation (2.53).

2.4 Discussion

Step by step details for obtaining the equation of motion of a serial manipulator as well as a cooperating manipulator on a mobile platform have been provided in this chapter. It needs to be highlighted that no arm can be at a singularity in order to compute the tip forces in a closed kinematic chain. This restriction will be removed later in the thesis.

3. HIGH PERFORMANCE COMPUTATION OF MULTIBODY SYSTEM DYNAMICS

Dynamical modeling of multibody systems, in general, refers to forward dynamics problem which requires inversion of the mass matrix. In generalized coordinates, mass matrix is $n \times n$ matrix where n is the number of links. Generally speaking, n^3 operations are required to invert a nonsparce $n \times n$ matrix. Therefore, its complexity is said to be $\mathcal{O}(n^3)$. If n is a large number, this becomes a major issue regarding the overall performace of the computation. On the other hand, utilizing the properties of the mass matrix, one can reduce the complexity of this process to $\mathcal{O}(n)$. Therefore, ***high performance algorithm*** in particular for the multibody dynamics, refer to the inversion technique of the mass matrix.

A through review of literature on $\mathcal{O}(n)$ was given in Chapter 1 and more detail on the subject can be found in [56]. Out of the algorithms available in the literature, here we will benefit first from the work by Featherstone [16] and then the work by Rodriguez, Jain, and Kreutz [1] in which the formulation is based on the convention of numbering the links from tip towards base (inboard) where the base is called "$n+1$" and the end-effector is called "0" for an n link manipulator. This way of modeling is very uncommon and often times it is considered inconvenient as if Arabic writing were enforced within Latin alphabet. Here, this methodology is modified to incorporate with common manipulator models whose links are numbered from base to tip (outboard). In addition, mobile base parameters are included so that the factorization given in this chapter is consistant with the formulations given in the previous chapter which includes the mobile base.

This chapter is organized in three sections; mass matrix factorization, mass matrix inversion, and discussions.

3.1 Mass Matrix Factorization

The most important step in mass matrix factorization is the definition of *articulated-body inertia*, $\mathcal{I}_{AB}$, introduced by Featherstone [16]. The basic idea is to detach link i from link $i-1$, and relate the relationship between its spatial force and resulting acceleration. Based on Featherstone's idea, we propose the following recursion for the computation of articulated-body inertias:

$$
\begin{aligned}
{}^{i}\mathcal{I}_{AB_k} &= {}^{i}\mathbf{\Psi}_{k+1,k}^{T}\ {}^{i}\mathcal{I}_{AB_{k+1}}\ {}^{i}\mathbf{\Psi}_{k+1,k} + {}^{i}\mathbf{M}_k && (3.1)\\
{}^{i}\mathbf{\Psi}_{k,k-1} &= \left(\mathbf{I} - \frac{{}^{i}\vec{H}_k\ {}^{i}\vec{H}_k^{T}\ {}^{i}\mathcal{I}_{AB_k}^{T}}{{}^{i}\vec{H}_k^{T}\ {}^{i}\mathcal{I}_{AB_k}\ {}^{i}\vec{H}_k}\right) {}^{i}\mathbf{\Phi}_{k,k-1} && (3.2)
\end{aligned}
$$

${}^{i}\mathcal{I}_{AB}$'s are constructed for each manipulator in a recursive manner using (3.1) and (3.2) starting from $k = n_i$ and taking ${}^{i}\mathcal{I}_{AB_{n_i+1}} = \mathbf{0}$. Then k is decremented until $k = 1$ at which step (3.2) is not evaluated. Finally, $\mathcal{I}_{AB}$ is constructed from ${}^{i}\mathcal{I}_{AB}$'s in the form of a block diagonal matrix as

$$
\mathcal{I}_{AB} = \begin{bmatrix}
\mathbf{M}_b & & & \mathbf{0} \\
& {}^{1}\mathcal{I}_{AB} & & \\
& & \ddots & \\
\mathbf{0} & & & {}^{p}\mathcal{I}_{AB}
\end{bmatrix} \qquad (3.3)
$$

Now, we can associate each joint acceleration with its link spacial force through articulated-body inertia.

$$
\underline{F} = \mathcal{I}_{AB}\ \underline{\dot{V}} + \underline{Z} \qquad (3.4)
$$

where $\underline{Z}$ represents the remaining terms due to the spatial forces propagating from the other links. Using (2.31) in (3.4) we get

$$
\underline{\mathcal{T}} = \mathbf{H}^{T}\underline{F} = \mathbf{H}^{T}\mathcal{I}_{AB}\ \underline{\dot{V}} + \mathbf{H}^{T}\underline{Z} \qquad (3.5)
$$

Let ξ be the effective joint force defined as $\xi = \underline{\mathcal{T}} - \mathbf{H}^{T}\underline{Z}$. Hence, we have the following equality

$$
\xi = \mathbf{H}^{T}\mathcal{I}_{AB}\ \underline{\dot{V}} \qquad (3.6)
$$

We are going to utilize (2.28) to substitute for $\underline{\dot{V}}$. From (2.3) we know that ${}^{i}\mathbf{\Phi}$ is a lower-diagonal matrix which implies the fact that the elements of ${}^{i}\underline{\dot{V}}$ are related with their inboard set. On the other hand, we are looking for the term on the relationship between spatial force and acceleration of the joint only without the inboard set, in other words, a block diagonal matrix. Therefore, we need to separate the diagonal from the off-diagonal of ${}^{i}\mathbf{\Phi}$ whose diagonal part is an identity matrix.

$$\begin{aligned}\underline{\dot{V}} &= \mathbf{\Phi}(\mathbf{H}\underline{\ddot{\theta}} + \underline{a}) \\ &= \mathbf{\Phi}(\mathbf{H}\underline{\ddot{\theta}} + \underline{a}) + \mathbf{H}\underline{\ddot{\theta}} - \mathbf{H}\underline{\ddot{\theta}} \\ &= \mathbf{H}\underline{\ddot{\theta}} + (\mathbf{\Phi} - \mathbf{I})\mathbf{H}\underline{\ddot{\theta}} + \mathbf{\Phi}\underline{a}\end{aligned} \tag{3.7}$$

Next we define the *adjacent-link propagation operator of the system*

$$\mathcal{E}_{\phi} = \begin{bmatrix} \mathbf{0} & & & \mathbf{0} \\ {}^{1}\mathbf{\Phi}_{b} & {}^{1}\mathcal{E}_{\phi} & & \\ \vdots & & \ddots & \\ {}^{p}\mathbf{\Phi}_{b} & & & {}^{p}\mathcal{E}_{\phi} \end{bmatrix} \tag{3.8}$$

where,

$${}^{i}\mathcal{E}_{\phi} = \begin{bmatrix} \mathbf{0} & \mathbf{0} & \cdots & \mathbf{0} & \mathbf{0} \\ {}^{i}\mathbf{\Phi}_{2,1} & \mathbf{0} & \cdots & \mathbf{0} & \mathbf{0} \\ \mathbf{0} & {}^{i}\mathbf{\Phi}_{3,2} & \cdots & \mathbf{0} & \mathbf{0} \\ \vdots & \vdots & \ddots & \vdots & \vdots \\ \mathbf{0} & \mathbf{0} & \cdots & {}^{i}\mathbf{\Phi}_{n_i,n_i-1} & \mathbf{0} \end{bmatrix} \tag{3.9}$$

${}^{i}\mathcal{E}_{\phi}^{k}$ is the k^{th} power of ${}^{i}\mathcal{E}_{\phi}$ and is also $-k^{th}$ diagonal of ${}^{i}\mathbf{\Phi}$. This means that ${}^{i}\mathcal{E}_{\phi}^{k}$ is an operator propagating between the two links whose "distance" is k. The term *distance between two links* is defined as the difference of their link numbers. With this definition, now we can write the following equality:

$$\mathbf{\Phi} = \mathbf{I} + \sum_{k=1}^{max} \mathcal{E}_{\phi}^{k} \tag{3.10}$$

where max is the maximum of n_i for $i = 1 \cdots p$. $\mathcal{E}_{\phi}$ is a nilpotent matrix and holds the following property:

$$\mathbf{\Phi} = (\mathbf{I} - \mathcal{E}_{\phi})^{-1} \tag{3.11}$$

If we use (3.10) in (3.7), we get

$$\underline{\dot{V}} = \mathbf{H}\underline{\ddot{\theta}} + \mathcal{E}_\phi \mathbf{H}\underline{\ddot{\theta}} + \left(\sum_{k=2}^{max} \mathcal{E}_\phi^k\right) \mathbf{H}\underline{\ddot{\theta}} + \mathbf{\Phi}\underline{a} \tag{3.12}$$

We use (3.12) in (3.6)

$$\xi = \mathbf{D}\underline{\ddot{\theta}} + \mathbf{H}^T \mathcal{I}_{AB} \mathcal{E}_\phi \mathbf{H}\underline{\ddot{\theta}} + \mathbf{H}^T \mathcal{I}_{AB} \left(\left(\sum_{k=2}^{max} \mathcal{E}_\phi^k\right) \mathbf{H}\underline{\ddot{\theta}} + \mathbf{\Phi}\underline{a} \right) \tag{3.13}$$

where,

$$\mathbf{D} = \mathbf{H}^T \, \mathcal{I}_{AB} \, \mathbf{H} \tag{3.14}$$

Rearranging (3.13) we get

$$\underline{\ddot{\theta}} = \mathbf{D}^{-1}\xi - \mathbf{K}\mathbf{H}\underline{\ddot{\theta}} - \mathbf{D}^{-1}\mathbf{H}^T \mathcal{I}_{AB} \left(\left(\sum_{k=2}^{max} \mathcal{E}_\phi^k\right) \mathbf{H}\underline{\ddot{\theta}} + \mathbf{\Phi}\underline{a} \right) \tag{3.15}$$

where,

$$\mathbf{K} = \mathbf{D}^{-1}\mathbf{H}^T \, \mathcal{I}_{AB} \, \mathcal{E}_\phi \tag{3.16}$$

Now we go back to (3.1) and (3.2) to rewrite them in a more compact way as follows:

$$\mathcal{I}_{AB} = \mathbf{M} + \mathcal{E}_\psi^T \, \mathcal{I}_{AB} \, \mathcal{E}_\psi \tag{3.17}$$

$$\mathcal{E}_\psi = (\mathbf{I} - \mathbf{H}\mathbf{D}^{-1}\mathbf{H}^T \, \mathcal{I}_{AB})\mathcal{E}_\phi \tag{3.18}$$

where,

$$\mathcal{E}_\psi = \begin{bmatrix} \mathbf{0} & & & \mathbf{0} \\ & {}^1\mathcal{E}_\psi & & \\ & & \ddots & \\ \mathbf{0} & & & {}^p\mathcal{E}_\psi \end{bmatrix} \tag{3.19}$$

$${}^i\mathcal{E}_\psi = \begin{bmatrix} \mathbf{0} & \mathbf{0} & \cdots & \mathbf{0} & \mathbf{0} \\ {}^i\mathbf{\Psi}_{2,1} & \mathbf{0} & \cdots & \mathbf{0} & \mathbf{0} \\ \mathbf{0} & {}^i\mathbf{\Psi}_{3,2} & \cdots & \mathbf{0} & \mathbf{0} \\ \vdots & \vdots & \ddots & \vdots & \vdots \\ \mathbf{0} & \mathbf{0} & \cdots & {}^i\mathbf{\Psi}_{n_i,n_i-1} & \mathbf{0} \end{bmatrix} \tag{3.20}$$

Similar to (3.10) and (3.11), the following definition and property holds for $\mathcal{E}_\psi$

$$\psi \stackrel{\triangle}{=} (\mathbf{I} - \mathcal{E}_\psi)^{-1} = \mathbf{I} + \sum_{k=1}^{max} \mathcal{E}_\psi^k \tag{3.21}$$

In addition to the equations written so far, the following lemmas are needed for the factorization of the mass matrix.

Lemma 1

$$\tilde{\mathbf{\Psi}} \stackrel{\triangle}{=} \mathbf{\Psi}\mathcal{E}_\psi = \mathcal{E}_\psi\mathbf{\Psi} = \mathbf{\Psi} - \mathbf{I} \tag{3.22}$$

Proof: From (3.21) we have $\mathcal{E}_\psi = \mathbf{I} - \psi^{-1}$. Pre- and post-multiply $\mathcal{E}_\psi$ by ψ yields the equation in the lemma. ∎

Lemma 2

$$\mathbf{\Psi}^T\mathbf{M}\mathbf{\Psi} = \mathcal{I}_{AB} + \tilde{\mathbf{\Psi}}^T\mathcal{I}_{AB} + \mathcal{I}_{AB}\tilde{\mathbf{\Psi}} \tag{3.23}$$

Proof: From (3.17) we have $\mathbf{M} = \mathcal{I}_{AB} - \mathcal{E}_\psi^T\ \mathcal{I}_{AB}\ \mathcal{E}_\psi$. Pre- and post-multiply $\mathbf{M}$ by ψ^T and ψ, and using (3.22) we get

$$\psi^T\mathbf{M}\psi = (\tilde{\psi}^T + \mathbf{I})\mathcal{I}_{AB}(\tilde{\psi} + \mathbf{I}) - \psi^T\mathcal{E}_\psi^T\mathcal{I}_{AB}\mathcal{E}_\psi\psi$$

yields the equation in the lemma. ∎

Lemma 3

$$\psi^{-1}\mathbf{\Phi} = \mathbf{I} + \mathbf{HK}\mathbf{\Phi} \tag{3.24}$$

$$\mathbf{\Phi}\psi^{-1} = \mathbf{I} + \mathbf{\Phi}\mathbf{HK} \tag{3.25}$$

Proof: From (3.21), (3.18) and (3.16) we have

$$\begin{aligned}\psi^{-1} &= \mathbf{I} - \mathcal{E}_\psi \\ &= (\mathbf{I} - \mathcal{E}_\phi) + \mathbf{HK} \\ &= \mathbf{\Phi}^{-1} + \mathbf{HK}\end{aligned}$$

Pre- and post-multiplying this by $\mathbf{\Phi}$ yields the equations in the lemma. ∎

Lemma 4

$$\mathbf{H}^T\ \mathbf{I}_{AB}\ \mathcal{E}_\psi = \mathbf{0} \tag{3.26}$$

Proof: Let us start with $\mathbf{H}^T\ \mathbf{I}_{AB}\ \mathcal{E}_\phi$. Premultiplying this by $\mathbf{DD}^{-1}$ and then using (3.14) we get

$$\begin{aligned}\mathbf{H}^T\ \mathbf{I}_{AB}\ \mathcal{E}_\phi &= \mathbf{DD}^{-1}\mathbf{H}^T\ \mathbf{I}_{AB}\ \mathcal{E}_\phi \\ &= \mathbf{H}^T\ \mathbf{I}_{AB}\ \mathbf{HD}^{-1}\mathbf{H}^T\ \mathbf{I}_{AB}\ \mathcal{E}_\phi\end{aligned}$$

Taking this in $\mathbf{H}^T\ \mathbf{I}_{AB}$ paranthesis and using (3.18) yields the equation in the lemma. ∎

Lemma 5

$$\mathbf{H}^T\mathbf{\Psi}^T\mathbf{M}\mathbf{\Psi}\mathbf{H} = \mathbf{D} \tag{3.27}$$

Proof: Pre- and post-multiplying (3.23) by $\mathbf{H}^T$ and $\mathbf{H}$, we get

$$\mathbf{H}^T\mathbf{\Psi}^T\mathbf{M}\mathbf{\Psi}\mathbf{H} = \mathbf{H}^T\mathcal{I}_{AB}\mathbf{H} + \mathbf{H}^T\tilde{\mathbf{\Psi}}^T\mathcal{I}_{AB}\mathbf{H} + \mathbf{H}^T\mathcal{I}_{AB}\tilde{\mathbf{\Psi}}\mathbf{H}$$

Using (3.14) and (3.22), we have

$$\mathbf{H}^T\mathbf{\Psi}^T\mathbf{M}\mathbf{\Psi}\mathbf{H} = \mathbf{D} + \mathbf{H}^T\mathbf{\Psi}^T(\mathbf{H}^T\mathcal{I}_{AB}\mathcal{E}_\psi)^T\mathbf{H} + (\mathbf{H}^T\mathcal{I}_{AB}\mathcal{E}_\psi)\mathbf{\Psi}\mathbf{H}$$

(3.26) yields the equation in the lemma. ∎

In the light of the lemmas given above, we can achieve the LDU type factorization of the mass matrix. The followings steps and their explanations afterwards, yield the mass matrix factorization and its proof.

$$\begin{aligned}
\mathcal{M} &= \mathbf{H}^T\mathbf{\Phi}^T\mathbf{M}\mathbf{\Phi}\mathbf{H} && (3.28)\\
&= \mathbf{H}^T(\mathbf{\Psi}^{-1}\mathbf{\Phi})^T\mathbf{\Psi}^T\mathbf{M}\mathbf{\Psi}(\mathbf{\Psi}^{-1}\mathbf{\Phi})\mathbf{H} && (3.29)\\
&= \mathbf{H}^T(\mathbf{I}+\mathbf{H}\mathbf{K}\mathbf{\Phi})^T\mathbf{\Psi}^T\mathbf{M}\mathbf{\Psi}(\mathbf{I}+\mathbf{H}\mathbf{K}\mathbf{\Phi})\mathbf{H} && (3.30)\\
&= [(\mathbf{I}+\mathbf{H}\mathbf{K}\mathbf{\Phi})\mathbf{H}]^T\ \mathbf{\Psi}^T\mathbf{M}\mathbf{\Psi}(\mathbf{I}+\mathbf{H}\mathbf{K}\mathbf{\Phi})\mathbf{H} && (3.31)\\
&= [\mathbf{H}(\mathbf{I}+\mathbf{K}\mathbf{\Phi}\mathbf{H})]^T\ \mathbf{\Psi}^T\mathbf{M}\mathbf{\Psi}\mathbf{H}(\mathbf{I}+\mathbf{K}\mathbf{\Phi}\mathbf{H}) && (3.32)\\
&= (\mathbf{I}+\mathbf{K}\mathbf{\Phi}\mathbf{H})^T\mathbf{H}^T\mathbf{\Psi}^T\mathbf{M}\mathbf{\Psi}\mathbf{H}(\mathbf{I}+\mathbf{K}\mathbf{\Phi}\mathbf{H}) && (3.33)\\
&= (\mathbf{I}+\mathbf{K}\mathbf{\Phi}\mathbf{H})^T\ \mathbf{D}\ (\mathbf{I}+\mathbf{K}\mathbf{\Phi}\mathbf{H}) && (3.34)
\end{aligned}$$

(3.28) is the definition of generalized mass matrix given in (2.33). Pre-multiplying $\mathbf{H}$ by $\mathbf{\Psi}\mathbf{\Psi}^{-1}$ and post-multiplying $\mathbf{H}^T$ by $(\mathbf{\Psi}\mathbf{\Psi}^{-1})^T$, we have (3.29) in which the term $\mathbf{\Psi}^{-1}\mathbf{\Phi}$ is put in paranthesis to help understand the next step, (3.30), where the terms in paranthesis are replaced by $\mathbf{I}+\mathbf{H}\mathbf{K}\mathbf{\Phi}$ according to (3.24). Then (3.31) is obtained using the distribution property of the transpose operator for $\mathbf{H}^T(\mathbf{I}+\mathbf{H}\mathbf{K}\mathbf{\Phi})^T$. Next we use the fact that $(\mathbf{I}+\mathbf{H}\mathbf{K}\mathbf{\Phi})\mathbf{H} = \mathbf{H}(\mathbf{I}+\mathbf{K}\mathbf{\Phi}\mathbf{H})$ to obtain (3.32). Distributing

the transpose over the square paranthesis, we have (3.33). Finally, we use (3.27) to get (3.34), the factorization for which we have been aiming. (3.34) is an LDU type factorization because $\mathbf{I}+\mathbf{K\Phi H}$ is a lower diagonal matrix and $\mathbf{D}$ is a diagonal matrix.

3.2 Mass Matrix Inversion

The following is the key lemma for the inversion of the mass matrix.

Lemma 6

$$(\mathbf{I}+\mathbf{K\Phi H})^{-1} = \mathbf{I}-\mathbf{K\Psi H} \tag{3.35}$$

Proof: We utilize the following Matrix Inversion Lemma which can be found in many textbooks such as [57]:

$$(\mathbf{X}^{-1}-\mathbf{YQ}^{-1}\mathbf{Z})^{-1} = \mathbf{X}^{-1}+\mathbf{X}^{-1}\mathbf{Y}(\mathbf{Q}-\mathbf{ZX}^{-1}\mathbf{Y})^{-1}\mathbf{ZX}^{-1} \tag{3.36}$$

Now, we make the following assignments for the variables in (3.36)

$$\begin{array}{lllll} \mathbf{X} & = & \mathbf{I} & \qquad \mathbf{Z} & = & \mathbf{I} \\ \mathbf{Y} & = & -\mathbf{K\Phi} & \qquad \mathbf{Q} & = & \mathbf{H} \end{array}$$

and we have

$$(\mathbf{I}+\mathbf{K\Phi H})^{-1} = \mathbf{I}-\mathbf{K\Phi}(\mathbf{I}+\mathbf{HK\Phi})^{-1}\mathbf{H} \tag{3.37}$$

Using (3.24) in (3.37) yields the equation in the lemma. ∎

Using (3.35), the factorization given in (3.34) yields the computationally fast inversion of the mass matrix as

$$\mathcal{M}^{-1} = (\mathbf{I}-\mathbf{K\Psi H})\,\mathbf{D}^{-1}\,(\mathbf{I}-\mathbf{K\Psi H})^{T} \tag{3.38}$$

3.3 Discussion

We have studied the factorization and inversion of the generalized mass matrix. However, we need to make it clear that we do not claim the algorithm is completely $\mathcal{O}(n)$ since there are matrices due to constraints need to be inverted as well, and the factorization and inversion technique presented in this chapter do not apply them. This does not prevent it to be *high performance* unless the system is dominated by constraints.

4. DYNAMICAL MODELING OF COMPLEX TOPOLOGY SYSTEMS

A mechanical system is said to be in a *complex topology* when it includes multiple subgroups; the main subgroup forms closed topology and others may form same or different topologies. An example of such a system is shown in Figure 4.1.
The methodology so far presented is modular enough to expand for the modeling of complex topology systems, provided that all of the constraints are properly defined. However, one should note that there are limitations. Each manipulator in the system has to be non-singular and fully actuated. In other words, no arm can be kinematically deficient and/or underactuated. These are fatal shortcomings that make the algorithm not applicable to almost any real life system. In this chapter we will investigate how to overcome these shortcomings.

4.1 Dynamics of Cooperating Underactuated Manipulators

A linear operator $\mathbf{S}$ is constructed by reordering the rows of an identity matrix to rearrange the joint space into four subspaces;

- base,
- actuated joints,
- free joints, and
- flexible joints.

in the order given above. Since $\mathbf{S}$ is an orthogonal matrix, the property $\mathbf{S}^{-1} = \mathbf{S}^T$ holds. When we apply this operator to (2.32), we have

$$(\mathbf{S}\mathcal{M}\mathbf{S}^T)\mathbf{S}\underline{\ddot{\theta}} + \mathbf{S}\underline{C} + \mathbf{S}\mathcal{J}^T\underline{F_t} = \mathbf{S}\underline{\mathcal{T}} \tag{4.1}$$

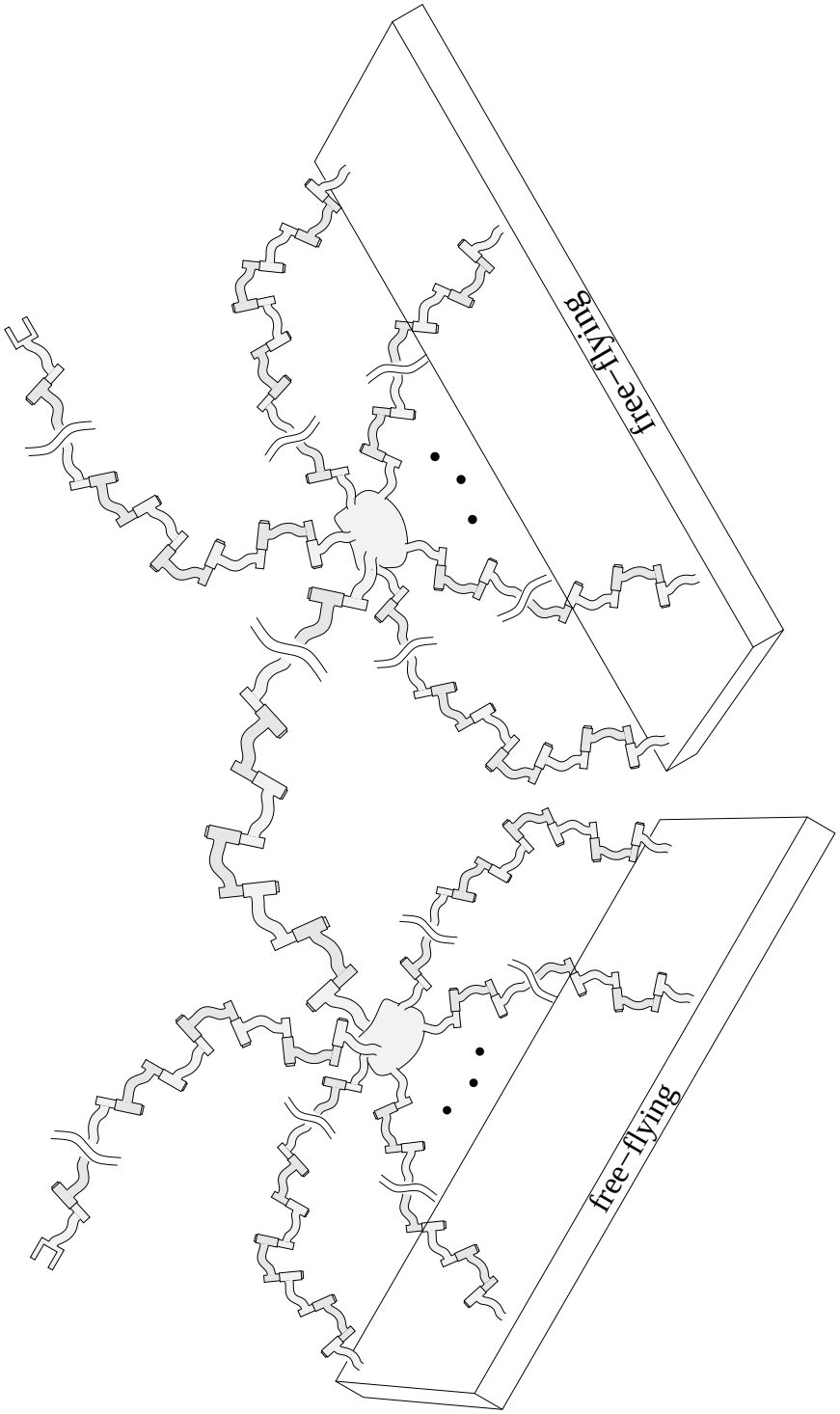

Figure 4.1: An example of a complex topology system

Let $\underline{\theta}_{baf}$ consist of base, actuated and free joint angles and $\underline{\theta}_\ell$ represent only the flexible joint angles. Then, we introduce $\underline{\mathcal{T}}_\ell$ for the torques (or forces) generated by the joint flexibility. Others are similarly defined.

$$\begin{bmatrix} \mathbf{M}_1 & \mathbf{M}_2 \\ \mathbf{M}_3 & \mathbf{M}_4 \end{bmatrix} \begin{bmatrix} \ddot{\underline{\theta}}_{baf} \\ \ddot{\underline{\theta}}_\ell \end{bmatrix} + \begin{bmatrix} \underline{C}_{baf} \\ \underline{C}_\ell \end{bmatrix} + \begin{bmatrix} \mathcal{J}_{baf}^T \\ \mathcal{J}_\ell^T \end{bmatrix} \underline{F}_t = \begin{bmatrix} \underline{\mathcal{T}}_{baf} \\ \underline{\mathcal{T}}_\ell \end{bmatrix} \tag{4.2}$$

We know from the joint flexibility that $\underline{\mathcal{T}}_\ell$ is of the following form

$$\underline{\mathcal{T}}_\ell = -\mathbf{L}_d \dot{\underline{\theta}}_\ell - \mathbf{L}_s \underline{\theta}_\ell \tag{4.3}$$

where $\mathbf{L}_s$ and $\mathbf{L}_d$ are diagonal matrices representing spring and damper characteristics, respectively. Using (4.3) in (4.2) we get,

$$\mathbf{M}_1 \ddot{\underline{\theta}}_{baf} + \mathbf{M}_2 \ddot{\underline{\theta}}_\ell + \underline{C}_{baf} + \mathcal{J}_{baf}^T \underline{F}_t = \underline{\mathcal{T}}_{baf} \tag{4.4}$$

$$\mathbf{M}_3 \ddot{\underline{\theta}}_{baf} + \mathbf{M}_4 \ddot{\underline{\theta}}_\ell + \mathbf{L}_d \dot{\underline{\theta}}_\ell + \mathbf{L}_s \underline{\theta}_\ell + \underline{C}_\ell + \mathcal{J}_\ell^T \underline{F}_t = \underline{0} \tag{4.5}$$

Since $\mathbf{M}_1$ is a positive definite matrix, $\ddot{\underline{\theta}}_{baf}$ can be solved from (4.4).

$$\ddot{\underline{\theta}}_{baf} = \mathbf{M}_1^{-1}(\underline{\mathcal{T}}_{baf} - \mathbf{M}_2 \ddot{\underline{\theta}}_\ell - \underline{C}_{baf} - \mathcal{J}_{baf}^T \underline{F}_t) \tag{4.6}$$

When (4.6) is substituted in (4.5), we get

$$\mathbf{M}_\star \ddot{\underline{\theta}}_\ell + \mathbf{L}_d \dot{\underline{\theta}}_\ell + \mathbf{L}_s \underline{\theta}_\ell + \underline{C}_\star + \mathcal{J}_\star^T \underline{F}_t = \mathbf{B} \underline{\mathcal{T}}_{baf} \tag{4.7}$$

where

$$\mathbf{M}_\star \triangleq \mathbf{M}_4 - \mathbf{M}_3 \mathbf{M}_1^{-1} \mathbf{M}_2 \tag{4.8}$$

$$\underline{C}_\star \triangleq \underline{C}_\ell - \mathbf{M}_3 \mathbf{M}_1^{-1} \underline{C}_{baf} \tag{4.9}$$

$$\mathcal{J}_\star \triangleq \mathcal{J}_\ell - \mathcal{J}_{baf} \mathbf{M}_1^{-1^T} \mathbf{M}_3^T \tag{4.10}$$

$$\mathbf{B} \triangleq -\mathbf{M}_3 \mathbf{M}_1^{-1} \tag{4.11}$$

(4.7) can be reduced from second order to first order differential equation as

$$\mathbf{M}_s \dot{\underline{W}} + \mathbf{L}_{sd} \underline{W} + \underline{C}_s + \mathcal{J}_s^T \underline{F}_t = \mathbf{B}_s \underline{\mathcal{T}}_{baf} \tag{4.12}$$

where

$$\underline{W} = \begin{bmatrix} \underline{\theta}_\ell \\ \underline{\dot{\theta}}_\ell \end{bmatrix} \quad \mathbf{M}_s = \begin{bmatrix} \mathbf{I} & \mathbf{0} \\ \mathbf{0} & \mathbf{M}_\star \end{bmatrix} \quad \mathbf{L}_{sd} = \begin{bmatrix} \mathbf{0} & -\mathbf{I} \\ \mathbf{L}_s & \mathbf{L}_d \end{bmatrix}$$

$$\underline{C}_s = \begin{bmatrix} \underline{0} \\ \underline{C}_\star \end{bmatrix} \qquad \mathcal{J}_s = \begin{bmatrix} \mathbf{0} \\ \mathcal{J}_\star \end{bmatrix} \qquad \mathbf{B}_s = \begin{bmatrix} \mathbf{0} \\ \mathbf{B} \end{bmatrix}$$

Defining

$$\underline{\mathcal{T}}_s \stackrel{\triangle}{=} \mathbf{B}_s \underline{\mathcal{T}}_{baf} - \underline{C}_s \tag{4.13}$$

equation (4.12) becomes

$$\mathbf{M}_s \underline{\dot{W}} + \mathbf{L}_{sd} \underline{W} + \mathcal{J}_s^T \underline{F}_t = \underline{\mathcal{T}}_s \tag{4.14}$$

Now we will continue our model to include closed-kinematic chains.
Joint accelerations can be written as the sum of so called *free accelerations* ($\underline{\ddot{\theta}}^f$) and *correction accelerations* ($\underline{\ddot{\theta}}^\delta$). (For more detail, please refer to [1])

$$\underline{\ddot{\theta}}(\underline{\mathcal{T}}, \underline{F}_t) = \underbrace{\underline{\ddot{\theta}}(\underline{\mathcal{T}}, \underline{0})}_{\underline{\ddot{\theta}}^f} + \underbrace{\underline{\ddot{\theta}}(\underline{0}, \underline{F}_t)}_{\underline{\ddot{\theta}}^\delta} \tag{4.15}$$

Free accelerations, $\underline{\ddot{\theta}}^f$, are nothing more than joint accelerations when the loops (due to cooperation of multiple manipulators) are cut. Therefore, we define $\underline{\theta}_\ell^f$ as the angle of the flexible joints without taking the constraints imposing grasp into account. Similarly, $\underline{W}^f$ is defined as

$$\underline{W}^f = \begin{bmatrix} \underline{\theta}_\ell^f \\ \underline{\dot{\theta}}_\ell^f \end{bmatrix}$$

For such case, equation (4.14) becomes

$$\mathbf{M}_s \underline{\dot{W}}^f + \mathbf{L}_{sd} \underline{W}^f = \underline{\mathcal{T}}_s \tag{4.16}$$

Here $\mathbf{L}_{sd}$ is a constant matrix. The time step of the integrator is chosen small when compared to the time scale of $\mathbf{M}_\star$ which is the time varying term in $\mathbf{M}_s$. Therefore, (4.16) approximately yields the solution as

$$\begin{aligned} \underline{\dot{W}}^f &= \mathbf{M}_s^{-1} \mathbf{L}_{sd} e^{-\mathbf{M}_s^{-1}\mathbf{L}_{sd}(t-t_o)} \mathbf{L}_{sd}^{-1} \mathbf{M}_s \underline{\dot{W}}_o \\ \underline{W}^f &= -e^{-\mathbf{M}_s^{-1}\mathbf{L}_{sd}(t-t_o)} \mathbf{L}_{sd}^{-1} \mathbf{M}_s \underline{\dot{W}}_o + \mathbf{L}_{sd}^{-1} \underline{\mathcal{T}}_s \end{aligned} \tag{4.17}$$

where

$$\mathbf{L}_{sd}^{-1} = \begin{bmatrix} \mathbf{L}_s^{-1}\mathbf{L}_d & \mathbf{L}_s^{-1} \\ -\mathbf{I} & \mathbf{0} \end{bmatrix}$$

Solution of (4.17) gives us an approximation for the free accelerations of flexible joints.

$$\underline{\ddot{\theta}}_\ell^f = \begin{bmatrix} \mathbf{0} & \mathbf{I} \end{bmatrix} \underline{\dot{W}}^f \tag{4.18}$$

Once we know $\underline{\ddot{\theta}}_\ell^f$, we can now obtain the free accelerations of base, actuated and free joints using (4.6)

$$\underline{\ddot{\theta}}_{baf}^f = \mathbf{M}_1^{-1}(\underline{\mathcal{T}}_{baf} - \mathbf{M}_\ell \underline{\ddot{\theta}}_\ell^f - \underline{C}_{baf}) \tag{4.19}$$

Putting the two together, and sorting them back in their original form, gives us the full set of free joint accelerations.

$$\underline{\ddot{\theta}}^f = \mathbf{S}^T \begin{bmatrix} \underline{\ddot{\theta}}_{baf}^f \\ \underline{\ddot{\theta}}_\ell^f \end{bmatrix} \tag{4.20}$$

Now the question is how to solve (4.17) without disturbing the *order n* characteristic of the algorithm.

Let us partition a full rank square matrix $\mathbf{X}$ and its inverse $\mathbf{Y}$.

$$\mathbf{X} = \begin{bmatrix} \mathbf{X}_1 & \mathbf{X}_2 \\ \mathbf{X}_3 & \mathbf{X}_4 \end{bmatrix} \qquad \mathbf{Y} = \begin{bmatrix} \mathbf{Y}_1 & \mathbf{Y}_2 \\ \mathbf{Y}_3 & \mathbf{Y}_4 \end{bmatrix} \tag{4.21}$$

Since they are the inverses of each other, they hold the following relationship.

$$\begin{bmatrix} \mathbf{X}_1 & \mathbf{X}_2 \\ \mathbf{X}_3 & \mathbf{X}_4 \end{bmatrix} \begin{bmatrix} \mathbf{Y}_1 & \mathbf{Y}_2 \\ \mathbf{Y}_3 & \mathbf{Y}_4 \end{bmatrix} = \begin{bmatrix} \mathbf{I} & \mathbf{0} \\ \mathbf{0} & \mathbf{I} \end{bmatrix} \tag{4.22}$$

Here, we are particularly interested in $\mathbf{Y}_4$ for a reason that will be obvious very shortly.

$$\mathbf{Y}_4 = (\mathbf{X}_4 - \mathbf{X}_3\mathbf{X}_1^{-1}\mathbf{X}_2)^{-1} \tag{4.23}$$

Comparing (4.8) with (4.23), we conclude that $\mathbf{M}_\star^{-1}$ is easily obtained from $\mathcal{M}^{-1}$. This shows that the matrix factorization of $\mathbf{M}_\star^{-1}$ can be done as given by (3.38).

Let $\mathbf{Y}_t$ be defined as $\mathbf{Y}_t \triangleq -\mathcal{M}_s^{-1} L_{sd} \Delta t$. Series expansion of $e^{\mathbf{Y}_t}$ is

$$e^{\mathbf{Y}_t} \approx \mathbf{I} + \sum_{n=1}^{k} \frac{\mathbf{Y}_t^n}{n!} \qquad k \to \infty \tag{4.24}$$

As the $\mathcal{L}_2$ norm of $\mathbf{Y}_t$ gets larger, k needs to be incremented enough to prevent unreasonable error. Here, k may be overvalued to eliminate this problem. This yields the computation of $\underline{\ddot{\theta}}^f$.

Now we will concentrate on the computation of $\underline{\ddot{\theta}}^\delta$. For that we will need to obtain the tip forces of the cooperating manipulators. First, the rigid grasping of the common load needs to be taken into consideration. Let the spatial mass matrix, the spatial bias forces and the spatial accelerations of the common load at point c be $\mathbf{M}_c$, $\vec{b}_c$ and $\vec{\alpha}_c$ respectively. Furthermore, the propagation matrix defined from tip of the manipulators to point c of the common load is

$$\mathbf{\Phi}_{t,c} = \begin{bmatrix} {}^1\mathbf{\Phi}_{t,c} \\ {}^2\mathbf{\Phi}_{t,c} \\ \vdots \\ {}^p\mathbf{\Phi}_{t,c} \end{bmatrix}$$

Newton-Euler equation in spatial form is stated for the common load as

$$\mathbf{M}_c\vec{\alpha}_c + \vec{b}_c = \mathbf{\Phi}_{t,c}^T\underline{F}_t \tag{4.25}$$

Tip point accelerations, $\underline{\alpha}_t$, and the acceleration of point c, $\vec{\alpha}_c$, are not all independent due to the grasping.

$$\begin{aligned} \underline{\alpha}_t &= \mathcal{J}\underline{\ddot{\theta}} + \dot{\mathcal{J}}\underline{\dot{\theta}} \\ &= \mathbf{\Phi}_{t,c}\vec{\alpha}_c + \underline{a}_c \end{aligned} \tag{4.26}$$

From (4.25) and (4.26)

$$\mathcal{J}\underline{\ddot{\theta}} = \mathbf{\Phi}_{t,c}\mathbf{M}_c^{-1}\mathbf{\Phi}_{t,c}^T\underline{F}_t - \mathbf{\Phi}_{t,c}\mathbf{M}_c^{-1}\vec{b}_c + \underline{a}_c - \dot{\mathcal{J}}\underline{\dot{\theta}} \tag{4.27}$$

On the other hand, $\mathcal{J}\underline{\ddot{\theta}}$ can also be obtained using (2.32)

$$\mathcal{J}\underline{\ddot{\theta}} = \mathcal{J}\mathcal{M}^{-1}\underline{\mathcal{T}}_a - \mathcal{J}\mathcal{M}^{-1}\mathcal{J}^T\underline{F}_t \tag{4.28}$$

where

$$\underline{\mathcal{T}}_a \triangleq \underline{\mathcal{T}} - \underline{C}$$

Combining (4.27) and (4.28)

$$\mathbf{\Omega}\underline{F}_t = \mathcal{J}\mathcal{M}^{-1}\underline{\mathcal{T}}_a + \mathbf{\Phi}_{t,c}\mathbf{M}_c^{-1}\vec{b}_c - \underline{a}_c + \dot{\mathcal{J}}\underline{\dot{\theta}} \tag{4.29}$$

where

$$\mathbf{\Omega} = \mathcal{J}\mathcal{M}^{-1}\mathcal{J}^T + \mathbf{\Phi}_{t,c}\mathbf{M}_c^{-1}\mathbf{\Phi}_{t,c}^T$$

Correction joint accelerations can now be obtained from:

$$\mathcal{M}\underline{\ddot{\theta}}^{\delta} = -\mathcal{J}^T\underline{F}_t \tag{4.30}$$

Since we now know free and correction accelerations, true joint accelerations follow

$$\underline{\ddot{\theta}} = \underline{\ddot{\theta}}^{f} + \underline{\ddot{\theta}}^{\delta} \tag{4.31}$$

This solves the forward dynamics problem of underactuated cooperating systems.

4.2 Kinematically Deficient Cooperating Manipulators

Kinematically deficient manipulators are those that have fewer degrees of freedom than necessary to achieve any admissible configuration in their operational space. When multiple manipulators, some or all of which are kinematically deficient, cooperate to perform a common task, the constrained forces at the contact points cannot be solved directly due to rank deficiency of the jacobian. This section addresses this challenge associated with the computation of constrained forces at the contact points by introducing a novel approach called "pseudo joint." Forward dynamical model utilizing pseudo joint has been driven for cooperating kinematically deficient manipulators.
Many industrial applications do not require the full kinematic capability to move and rotate the tip point of the manipulator in any direction. Usually, the desired trajectory lies in a subset of this six dimensional operational space. Unless kinematic redundancy is needed for both task space and joint space controls such as obstacle avoidance or joint limit avoidance problems, kinematically deficient manipulators gain superiority over more DOF manipulators in terms of cost, manufacturing, and compactness. In addition, cooperating manipulators bring unprecedented advantage over serial manipulators in terms of precision, load balancing, high payload capacity, etc. Therefore, certain applications require to utilize multiple manipulators that cooperate to perform a common task and are kinematically deficient.

Kinematically redundant manipulators have been studied extensively such as [58], the book by Nakamura. In contrary, kinematically deficient manipulators have not attracted such interest from the research community. Out of the limited number of publications, some confused constrained manipulators with kinematically deficient ones. Constraint manipulators and kinematically redundant manipulators have been studied by Bruyninckx and Khatib [39]. Abdel-Malek et al. [40] studied the workspace issues of kinematically deficient manipulators. Dynamics of two-finger grippers as kinematically deficient manipulators was studied by Prattichizzo and Bicchi [41]. Teleoperated surgical robots were considered in both kinematically redundant and kinematically deficient cases by Funda et al. [42]. The term *nonmanipulable grasp* was used by Murray *et.al.* [53] instead of kinematically deficient manipulator. Their method is based on finding the nonmanipulable directions and reducing the task space. They also use lagrange multipliers in finding the constraint forces.
This section of the thesis is aimed at addressing the numerical problems associated with contact force calculations by introducing a new concept called "*pseudo joint*."

4.2.1 Numerical approach

In order to deal with the rank deficiency problem of the jacobian in the case of singular configuration or with the manipulators having less than six DOF, one may suggest to reduce the size of the task space. To do that, first we need to find the directions towards which the tip of the manipulator cannot move. The information regarding these directions is hidden in jacobian, $\mathcal{J}$, which is a linear operator that maps joint space to task space.
Generally speaking, task space is a 6 dimensional manifold per manipulator. This manifold is formed by $\Re^3$ for rotations and $\Re^3$ for translations. For the sake of simplicity, let us consider only one manipulator in the system without loss of generality. Hence, mathematical reiteration of the previous statement about jacobian is that $\mathcal{J} : \Re^n \rightarrow \Re^6$ or simply $\mathcal{J} \in \Re^{6\times n}$. This mapping is displayed in Figure 4.2 where $\mathcal{N}$ represents the *null space*, and $\mathcal{R}$ represents the *range space*. Clearly, $\mathcal{R}(\mathcal{J})$ is the space in which the tip of the manipulator is free to move. On the other hand, $\mathcal{N}(\mathcal{J}^T)$ is perpendicular to and therefore linearly independent from $\mathcal{R}(\mathcal{J})$. Both of these spaces together form $\Re^6$. Consequently, $\mathcal{N}(\mathcal{J}^T)$ represents the directions towards which the tip of the

manipulator cannot move.

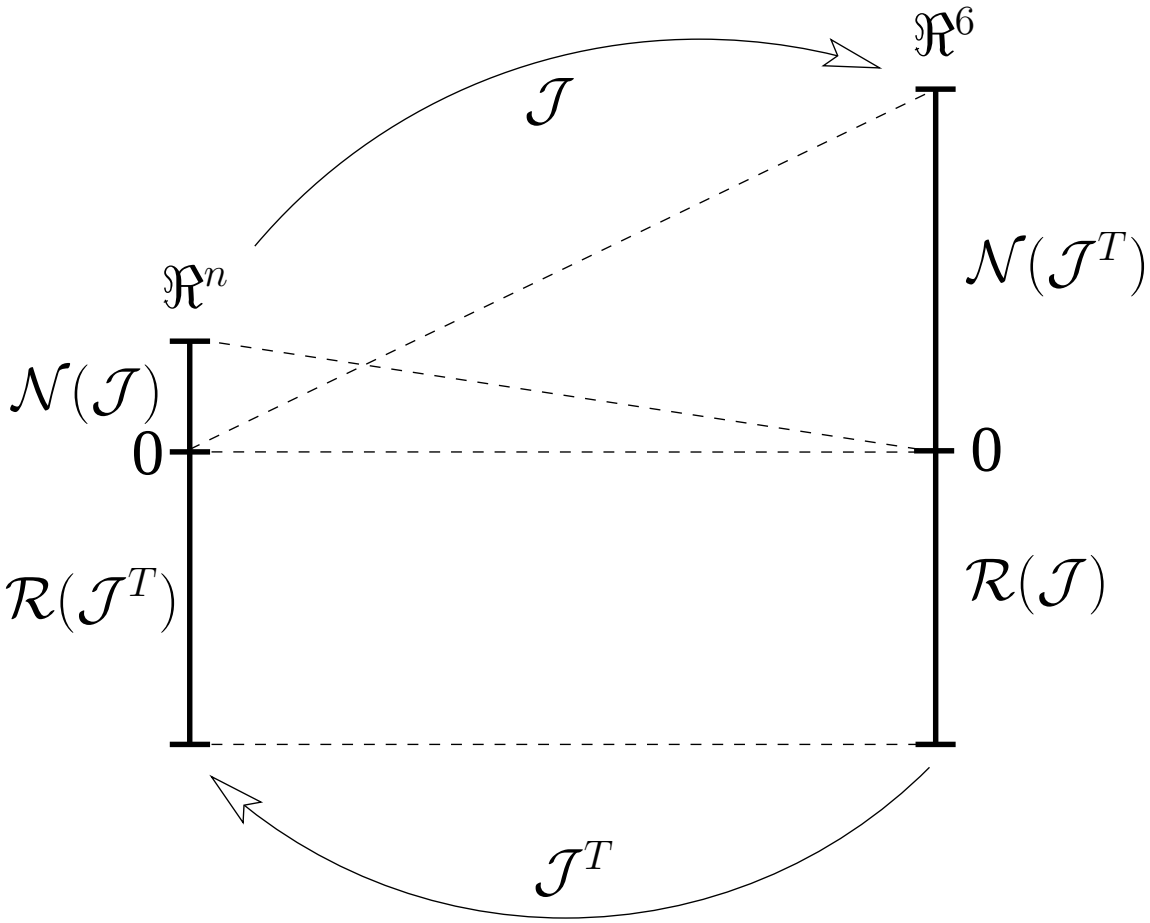

Figure 4.2: Jacobian maps joint space to task space

Now that we know these inadmissible directions, the question is how to find a coordinate transformation matrix R to reduce the task space such that $R\mathcal{J}$ spans it completely. The answer is as follows:

$$R = \mathcal{N}(\mathcal{N}(\mathcal{J}^T)^T)^T \tag{4.32}$$

Using equation (4.32) we can replace the Jacobian by J_r as

$$J_r = RJ \tag{4.33}$$

This is an orthogonal transformation yielding the inverse transformation as

$$J = R^T J_r \tag{4.34}$$

The six step forward dynamic calculations are updated by replacing A_r with A, where

$$A_r = AR \tag{4.35}$$

The drawback of this method is that the computation of null space requires Singular Value Decomposition (SVD) which introduces instability due to the fact that singular vectors are not unique, and may introduce discontinuity. This drawback alone makes this methodology impractical, not to mention the cost associated with the numerical computation of SVD.

4.2.2 Pseudo joint

An easy to implement and computationally efficient alternative approach, is to calculate link internal torques. First we assume as if there were extra joints and then we have to calculate the torques to keep those joints at zero angle at all times as displayed in Figure 4.3.

First kinematic analysis needs to be done to decide at what location of which link pseudo joint to be placed in what direction. This analysis is usually straight forward and easy enough to decide by visual inspection of the manipulator. In the more complicated cases, forward kinematic model is obtained and augmented jacobian is desired to be full rank.

We first need to obtain a linear operator dividing the joint space into two sub spaces; real joints and pseudo joints. Let S do that. S can be obtained easily by rearranging the rows of $n \times n$ identity matrix, where n is the total DOF including pseudo joints. Rearranging the rows of an identity matrix does not disturb its orthogonality property. Therefore, S is an orthogonal matrix and $S^{-1} = S^T$ holds. The rearranged form of the inverse dynamics (2.53) becomes:

$$S\ddot{\theta}_{augmented} = (SDS^T)S\mathcal{T}_{augmented} + SE \tag{4.36}$$

$$\begin{bmatrix} \ddot{\theta} \\ \ddot{\theta}_p \end{bmatrix} = \begin{bmatrix} d_1 & d_2 \\ d_3 & d_4 \end{bmatrix} \begin{bmatrix} \bar{\mathcal{T}} \\ \bar{\mathcal{T}}_p \end{bmatrix} + \begin{bmatrix} e_1 \\ e_2 \end{bmatrix} \tag{4.37}$$

Here, D and E matrices are obtained for the augmented system. By the definition of the pseudo joint we know that $\ddot{\theta}_p = 0$. Therefore, the equation of motion is achieved as:

$$\ddot{\theta} = D_r\bar{\mathcal{T}} + E_r \tag{4.38}$$

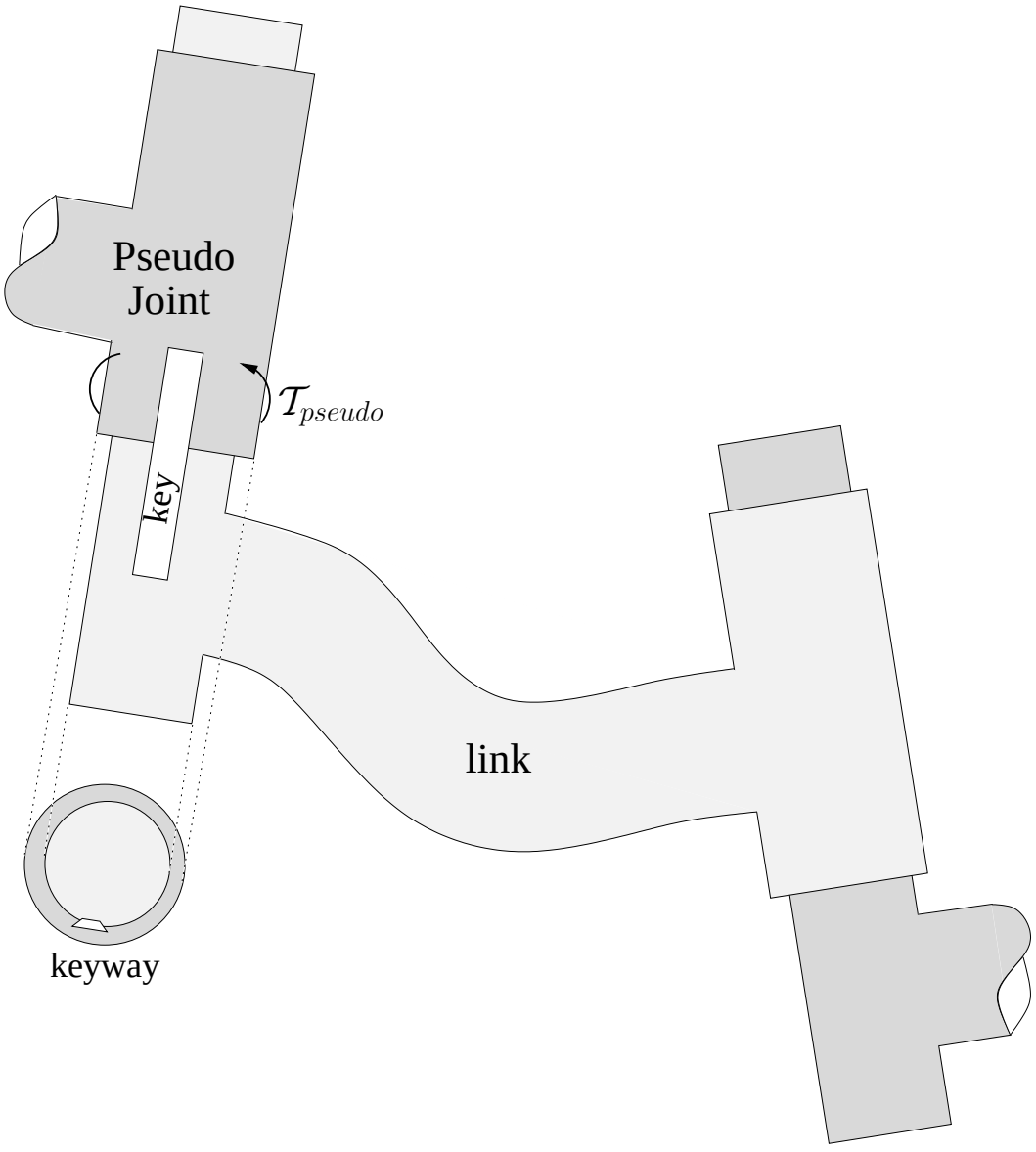

Figure 4.3: Pseudo joint in the form of a joint constrained by a key-bushing mechanism

where

$$D_r = d_1 - d_2 d_4^{-1} d_3$$
$$E_r = e_1 - d_2 d_4^{-1} e_2$$

provided that d_4 is full rank.

How to make d_4 full rank is, in a way, a design issue that needs to be discussed here. First, consider a planar four-bar linkage mechanism shown in Figure 4.4. Let say we want to constrain joints 2 and 3 so that $\ddot{\theta}_2 = 0$ and $\ddot{\theta}_3 = 0$ at all times. Using the methodology presented in this section, one may assign joints 2 and 3 as the pseudo-joints. On the other hand, the four angles; $\theta_1, \theta_2, \theta_3$ and θ_4 shown in Figure 4.4 are all equal to eachother, hence, dependent on one another. Consequently, although there are four joints in the system, only one of them is independent. As a result, if we ensure, for example, $\ddot{\theta}_2$ to remain zero at all times by applying the necessary torque, this will already ensure that $\ddot{\theta}_3$ to be zero as well. In this simplified system we can see that the term d_4 looses rank to mean that there is a dependency in between the pseudo joints.

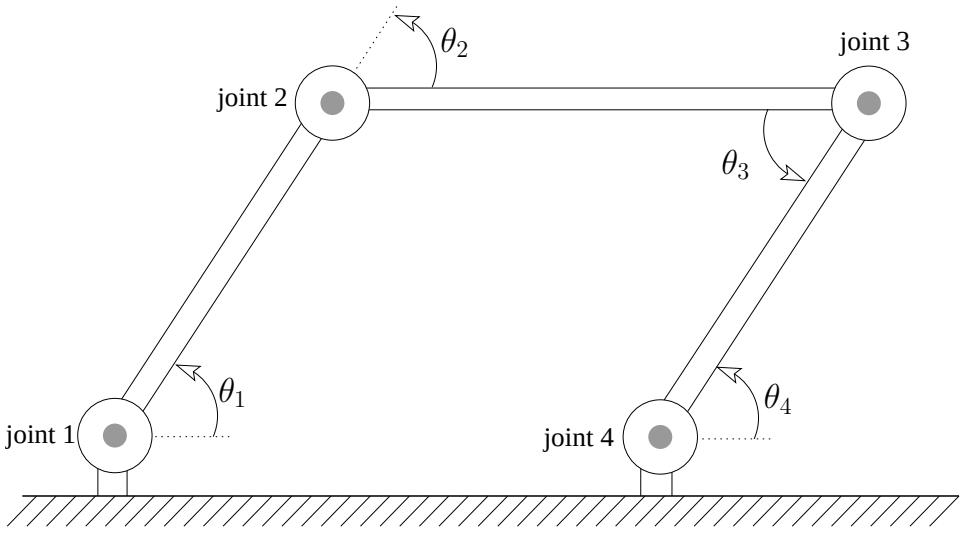

Figure 4.4: Planar four-bar linkage mechanism

If it is desired to apply the method of pseudo-joint to a four-bar mechanism as shown in Figure 4.4, first we need to divide the structure to *arm 1* and *arm 2* to claim that they are cooperating. A logical choice is to divide it from the middle of the bar parallel to the ground. Then we need to add extra joints to each arm to bring each one to a desired number of DOF so that Ω defined in (2.52) becomes invertible. Figure 4.5 displays a

possible configuration where joints 2 and 5 to be chosen as the pseudo joints.

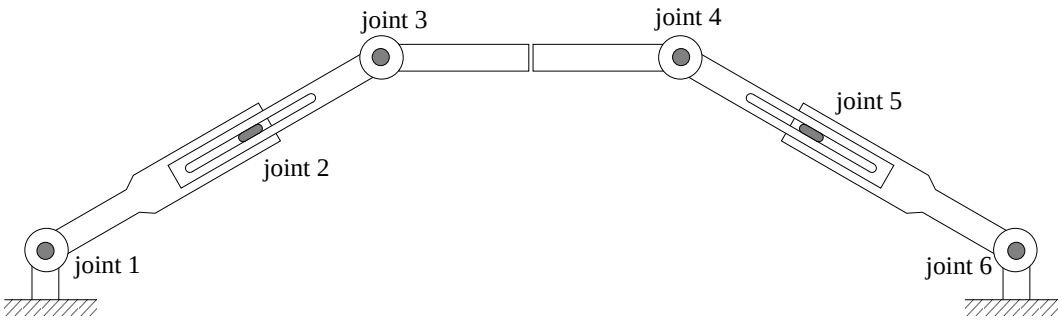

Figure 4.5: Planar four-bar mechanism with slider

4.3 Dynamics of Wheeled Systems Subject to Pure Rolling Constraint

A rolling wheel is a member of nonholonomic systems that are subject to constraints expressed as functions of generalized speeds but not as functions of positions. The root of the term *holonomy* comes from *whole-law* which refers to the system obeying the laws of Lagrangian mechanics, Hamiltonian mechanics and the conservation of momentum. Dynamics of nonholonomic systems, on the other hand, do not obey these laws in general. Instead, Lagrange d'Alembert mechanics, nonholonomic Hamiltonian mechanics and momentum equation are available for nonholonomic systems [59].

Without a doubt, the most common and basic nonholonomic system is a rolling wheel subject to no-slip (pure rolling) constraint. In fact, due to the limitation of the scope, rolling wheel is the only nonholonomic system that has been considered in this thesis. The reason why this section is dedicated for it is because it unleashes a whole new world of dynamical modeling of wheeled mobile robots with a goal to observe the full set of forces and torques at the contact points. This is in contrast to most of the algorithms in the literature regarding the dynamics of wheeled vehicles where constraint forces and torques are eliminated. However, these forces and torques play a crucial role in many applications such as rollover prevention of wheeled ground vehicles.

Figure 4.6 displays rolling wheel subject to no-slip constraint. As seen from this figure, the system has 3 DOF. Its symbolic representation indicating joint assignments as well as tip and base assignments, shown in Figure 4.7, is the key step here. In this modeling approach, the wheel mass and inertia are assigned to the mobile base. These assignments may not be intuitive as intuition may deem joint 1 to be placed together

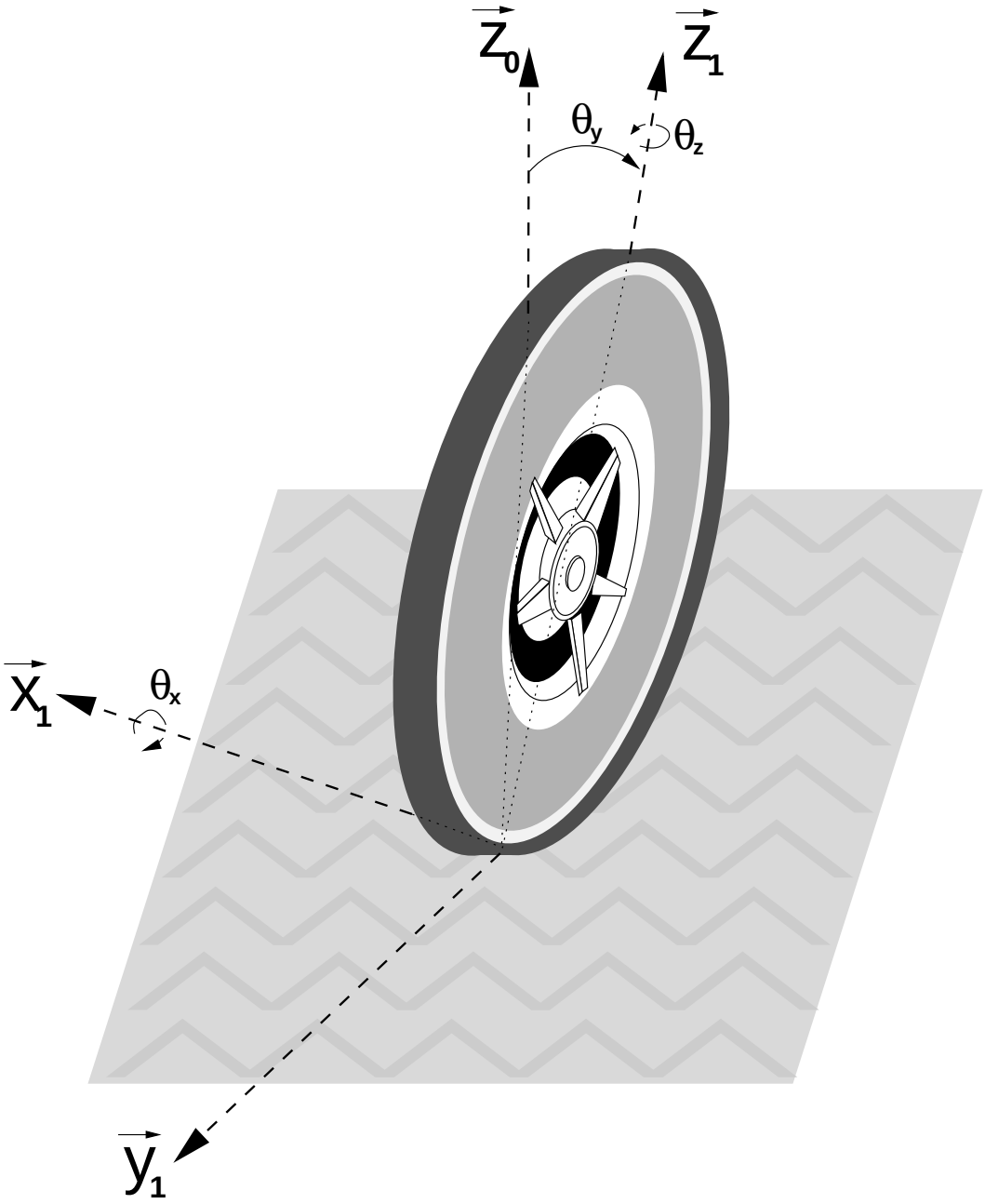

Figure 4.6: Rolling wheel subject to no-slippage constraint

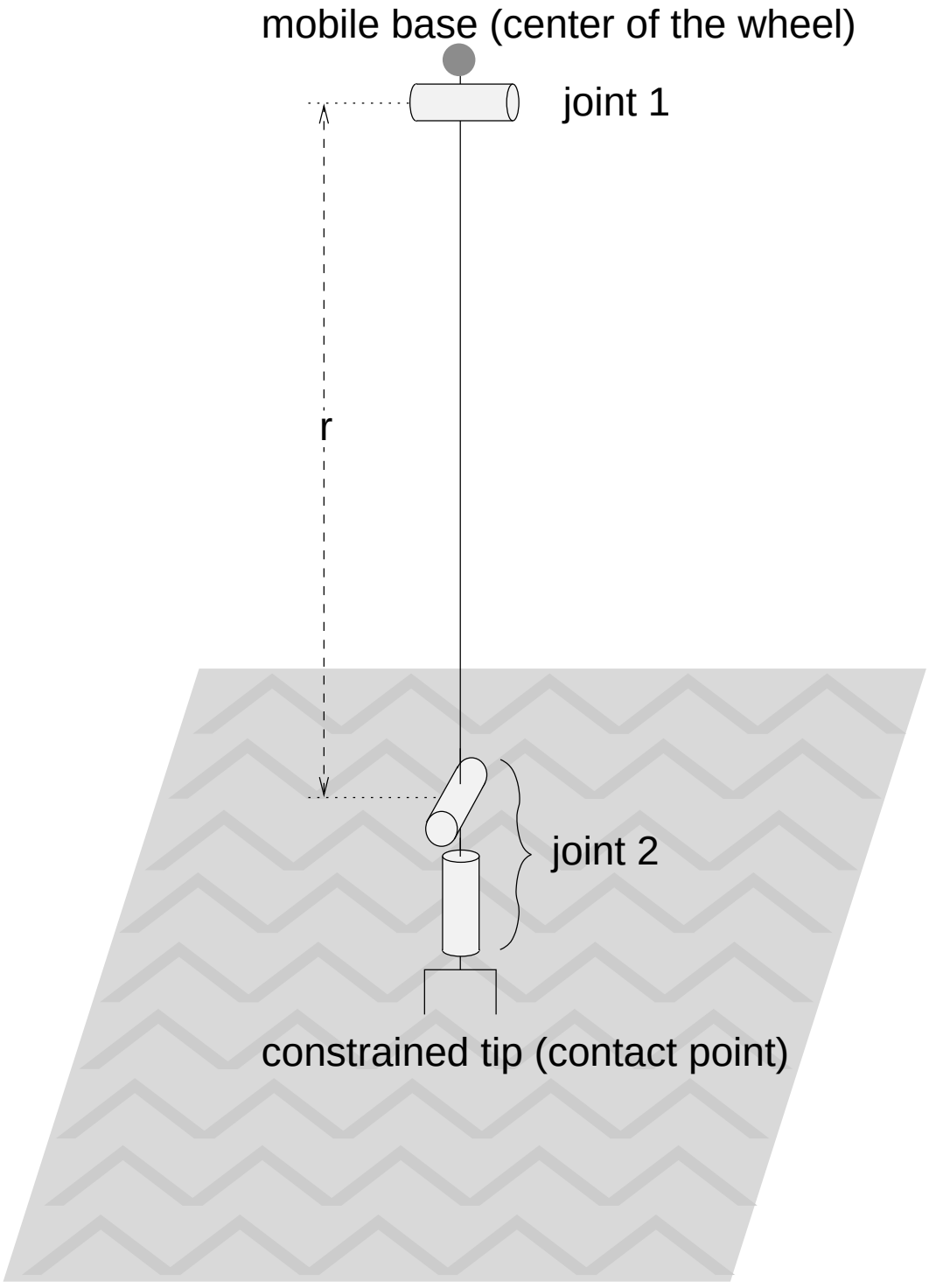

Figure 4.7: Symbolic representation of a rolling wheel where r is the radius of the wheel

with joint 2, and the choice of base and tip to be reversed. There are few publications on the dynamics of wheeled vehicles using robotic formalism such as [60] and [61]. All of such publications known to us follow this intuition which poses problems unless the system to be modeled consists of only the single wheel. These problems will be explained at the end of this section.

Figure 4.8: Unicycle and its symbolic representation

To help understand the methodology, let us consider a unicycle as shown in Figure 4.8. Orthogonal frames obeying *right hand rule* are assigned as shown in Figure 4.9. It

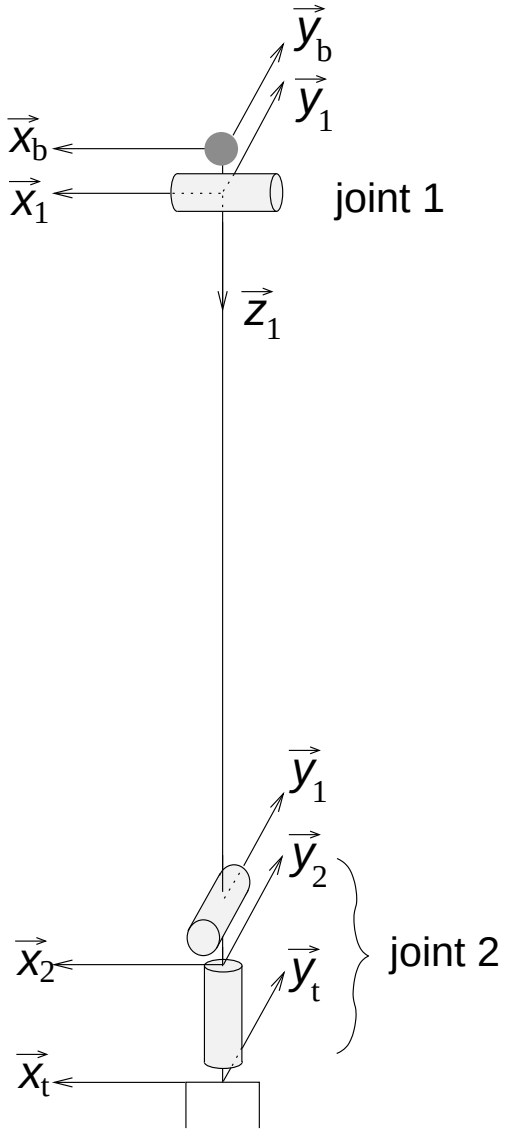

Figure 4.9: Frame assignment for a single wheel or unicycle

needs to be highlighted here that joint 2 has two revolute DOF, and therefore has two axes of rotation; one in $\vec{z}_2$ and the other in $\vec{y}_1$. It may be confusing to those who are accustomed to see each axis of rotation defined in its own body frame. This is not the case here.

Let us start with the constraint analysis. There are two constraints at the tip point; one prevents lateral slip, and the other prevents longitudinal slip. First we will write the lateral one in a form reducible to a *Pfaffian constraint*, *i.e.*, $f(\underline{x})\dot{\underline{x}} = 0$.

$$\tilde{\mathbf{A}}^T \vec{\vec{V}}_t = 0 \tag{4.39}$$

where

$$\tilde{\mathbf{A}} = \begin{bmatrix} \vec{0} \\ \vec{x}_1 \end{bmatrix} \tag{4.40}$$

Now, let $\tilde{\mathbf{A}}$ be the annihilator of $\mathbf{A}$. In other words, let $\mathbf{A}$ be the matrix such that $\tilde{\mathbf{A}}$ spans its null-space. This is stated as

$$\mathbf{A}\tilde{\mathbf{A}} = \mathbf{0} \tag{4.41}$$

Although there is no unique solution of (4.41), one possible choice of A is

$$\mathbf{A} = \begin{bmatrix} \vec{x}_1^T & \vec{0}^T \\ \vec{y}_1^T & \vec{0}^T \\ \vec{z}_1^T & \vec{0}^T \\ \vec{0}^T & \vec{y}_1^T \\ \vec{0}^T & \vec{z}_1^T \end{bmatrix} \tag{4.42}$$

Note that A, as defined in (4.42), is an orthogonal matrix and therefore holds orthogonality property

$$\mathbf{A}\mathbf{A}^T = \mathbf{I} \tag{4.43}$$

There exists a velocity vector $\underline{V_c}$ in a five dimensional manifold to express the tip velocity using (4.39) and (4.41).

$$\vec{\vec{V}}_t = \mathbf{A}^T \underline{V_c} \tag{4.44}$$

Using the longitudinal slip constraint, $\underline{V_c}$ can be expressed as a function of the joint space of the wheel.

$$\underline{V_c} = \mathbf{B}\underline{\dot{\theta}} \tag{4.45}$$

where

$$\underline{\dot{\theta}} = \begin{bmatrix} \vec{\vec{V}}_b \\ \dot{\theta}_1 \\ \dot{\theta}_2 \\ \dot{\theta}_3 \end{bmatrix} \qquad \mathbf{B} = \begin{bmatrix} 0 & 0 & 0 & 0 & 0 & 0 & 0 & 0 & 0 \\ 0 & 0 & 0 & 0 & 0 & 0 & 0 & 0 & 0 \\ 0 & 0 & 0 & 0 & 0 & 0 & 0 & 0 & 0 \\ 0 & 0 & 0 & 0 & 0 & 0 & -r & 0 & 0 \\ 0 & 0 & 0 & 0 & 0 & 0 & 0 & 0 & 0 \end{bmatrix}$$

The constraints considered so far were kinematic. To study the constraint forces let us look at the work done at the tip point and utilize (4.44)

$$\vec{\vec{F}}_t^T \vec{\vec{V}}_t = \vec{\vec{F}}_t^T \mathbf{A}^T \underline{V_c} = \left(\mathbf{A}\vec{\vec{F}}_t\right)^T \underline{V_c} = \underline{F_c}^T \underline{V_c} \tag{4.46}$$

which is true for all $\underline{V_c}$. Here, $\underline{F_c}$ is the externally applied force/torque corresponding to $\underline{V_c}$. From (4.46) we have

$$\underline{F_c} = \mathbf{A}\vec{\vec{F}}_t \tag{4.47}$$

Let us decompose $\vec{\vec{F}}_t$ as

$$\vec{\vec{F}}_t = \underline{F_m} + \underline{F_s} \tag{4.48}$$

where $\underline{F_m} \in \mathcal{R}(\mathbf{A}^T)$ and $\underline{F_s} \in \mathcal{R}(\tilde{\mathbf{A}})$ as shown in Figure 4.10. Here, $\mathcal{R}$ refers to *range space*. As a result of this decomposition, $\vec{\vec{F}}_t$ can be written as

$$\vec{\vec{F}}_t = \mathbf{A}^T\underline{\xi} + \tilde{\mathbf{A}}\eta \tag{4.49}$$

Plugging (4.49) into (4.47) and using (4.43), we get

$$\underline{F_c} = \underline{\xi} \tag{4.50}$$

From (4.49) and (4.50)

$$\vec{\vec{F}}_t = \mathbf{A}^T\underline{F_c} + \tilde{\mathbf{A}}\eta \tag{4.51}$$

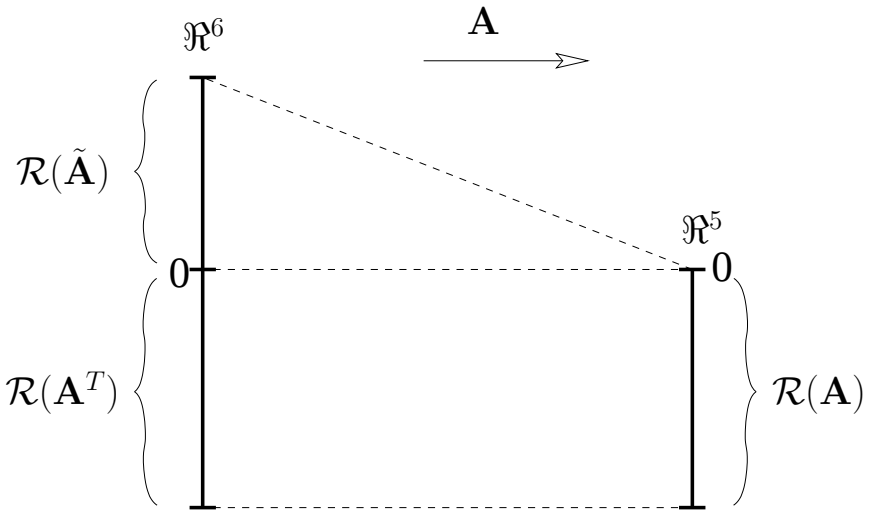

Figure 4.10: Decomposition of the task space

Here η corresponds to the *workless force*. Minimum norm solution would be to set it to zero. This leaves us with

$$\vec{F}_t = \mathbf{A}^T \underline{F}_c \tag{4.52}$$

Similar to (4.46), let us write the work done at the tip point again. This time, we will utilize (4.52), (4.43) and (4.45) in the order given to obtain the equations below.

$$\begin{aligned}
\vec{F}_t^T \vec{V}_t &= (\mathbf{A}^T \underline{F}_c)^T \mathbf{A}^T \underline{V}_c \\
&= \underline{F}_c^T \underline{V}_c \\
&= \underline{F}_c^T \mathbf{B} \underline{\dot{\theta}} \\
&= (\mathbf{B}^T \underline{F}_c)^T \underline{\dot{\theta}} \qquad (4.53) \\
&= \underline{\mathcal{T}}_t^T \underline{\dot{\theta}} \qquad (4.54)
\end{aligned}$$

Here $\underline{\mathcal{T}}_t$ is the induced torque due to the constraint forces. From (4.53) and (4.54)

$$\underline{\mathcal{T}}_t = \mathbf{B}^T \underline{F}_c \tag{4.55}$$

Inverse dynamics equation of the system is

$$\underline{\mathcal{T}}_a + \underline{\mathcal{T}}_t = \mathcal{M}\underline{\ddot{\theta}} + \underline{\mathcal{C}} + \mathcal{J}^T \vec{F}_t \tag{4.56}$$

where $\underline{\mathcal{T}}_a$ is the applied torques. Plugging (4.52) and (4.55) into (4.56), we have

$$\underline{\mathcal{T}}_c = \mathcal{M}\underline{\ddot{\theta}} + (\mathbf{A}\mathcal{J} - \mathbf{B})^T \underline{F}_c \tag{4.57}$$

where $\underline{\mathcal{T}}_c = \underline{\mathcal{T}}_a - \underline{\mathcal{C}}$.

Forward dynamics equation is obtained from (4.57) as

$$\underline{\ddot{\theta}} = \mathcal{M}^{-1}\left(\underline{\mathcal{T}}_c - (\mathbf{A}\mathcal{J} - \mathbf{B})^T \underline{F}_c\right) \tag{4.58}$$

Now, let us go back to kinematics. From (4.44) and (4.45), and using the jacobian operator, we have

$$\vec{\dot{V}}_t = \mathbf{A}^T\mathbf{B}\underline{\dot{\theta}} = \mathcal{J}\underline{\dot{\theta}} \tag{4.59}$$

Taking the time derivative of (4.59)

$$\dot{\vec{V}}_t = \mathbf{A}^T\mathbf{B}\underline{\ddot{\theta}} + \dot{\mathbf{A}}^T\mathbf{B}\underline{\dot{\theta}} = \mathcal{J}\underline{\ddot{\theta}} + \dot{\mathcal{J}}\underline{\dot{\theta}} \tag{4.60}$$

We know from Section 2.3.1 that

$$\dot{\mathcal{J}}\underline{\dot{\theta}} = \mathbf{\Phi}_t\mathbf{\Phi}\underline{a} + \vec{\dot{a}}_t \tag{4.61}$$

Here, $\vec{\dot{a}}_t$ is zero because the length of the link between the last joint ant the tip is zero. Using (4.61) and rearranging (4.60) we have

$$(\mathcal{J} - \mathbf{A}^T\mathbf{B})\underline{\ddot{\theta}} = \dot{\mathbf{A}}^T\mathbf{B}\underline{\dot{\theta}} - \mathbf{\Phi}_t\mathbf{\Phi}\underline{a} \tag{4.62}$$

Premultiplying (4.62) by $\mathbf{A}$ yields

$$(\mathbf{A}\mathcal{J} - \mathbf{B})\underline{\ddot{\theta}} = \mathbf{A}\dot{\mathbf{A}}^T\mathbf{B}\underline{\dot{\theta}} - \mathbf{A}\mathbf{\Phi}_t\mathbf{\Phi}\underline{a} \tag{4.63}$$

On the other hand, premultiplying (4.58) by $\mathbf{A}\mathcal{J} - \mathbf{B}$, we have

$$(\mathbf{A}\mathcal{J} - \mathbf{B})\underline{\ddot{\theta}} = (\mathbf{A}\mathcal{J} - \mathbf{B})\mathcal{M}^{-1}\underline{\mathcal{T}}_c - (\mathbf{A}\mathcal{J} - \mathbf{B})\mathcal{M}^{-1}(\mathbf{A}\mathcal{J} - \mathbf{B})^T\underline{F}_c \tag{4.64}$$

Equating (4.63) and (4.64) yields the solution for $\underline{F}_c$

$$\underline{F}_c = \mathbf{\Omega}^{-1}\left(\mathbf{A}\mathbf{\Phi}_t\mathbf{\Phi}\underline{a} + (\mathbf{A}\mathcal{J} - \mathbf{B})\mathcal{M}^{-1}\underline{\mathcal{T}}_c - \mathbf{A}\dot{\mathbf{A}}^T\mathbf{B}\underline{\dot{\theta}}\right) \tag{4.65}$$

where

$$\mathbf{\Omega} = (\mathbf{A}\mathcal{J} - \mathbf{B})\mathcal{M}^{-1}(\mathbf{A}\mathcal{J} - \mathbf{B})^T \tag{4.66}$$

It is clear that $\mathbf{\Omega}$ needs to be full rank in order to have a solution. Generally speaking, this is directly related with the rank of the jacobian, hence the number of DOF of each manipulator in the system and their singularity issues. If our wheel model were similar

to those available in the literature on the dynamics of wheeled vehicles using robotic formalism such as [60] and [61], the jacobian would be 6×3 and we would suffer from rank deficiency in $\mathbf{\Omega}$. As we gain full 6 DOF from the mobile base, our jacobian for a single wheel is 6×9. At last but not least, we need to mention that having 3 DOF at the contact is a poor choice because the tip forces cannot be computed correctly if link 1 posses an angular acceleration corresponding to wheel rotation. As is done in our approach, this angular acceleration should apply to base only. To comprehend the methodology, one can think of the following analogy. Consider a unicycle in space without gravity and without contact to any surface. Now, shrink that mass and inertia of the wheel to a point and call that *the base*. The rest is to impose constraints.

4.4 Discussion

Dynamic modeling of cooperating kinematically deficient manipulators yielding full set of force, torque and acceleration distributions including those at the constraint uncovers a very important domain of multibody dynamics. *Pseudo Joint* is a stable yet efficient method to deal with such systems. The best way, probably, is to demonstrate the use of the algorithm on some examples. Next chapter is dedicated for this purpose.

5. CASE STUDIES

This chapter includes both theory and application. It enjoys the theoretical foundations established in the previous chapter, and utilizes them in practical cases. While doing that, through explanation of the theoretical details on how to apply the algorithm is the goal of this chapter. It starts with general underactuated cooperating manipulators in space manipulation and continues on the dynamical modeling of two-wheeled cart. The following sections include the dynamics of four-wheel steered and four-wheel driven mobile robot and a four-wheeled full-suspension passanger vehicle dynamics.

5.1 General Underactuated Cooperating Manipulators in Space Manipulation

The example system on which the algorithm will be explained is chosen to be simple enough so that the reader can easily follow the algorithm without getting lost in the structural details. The task space of the 3 DOF arm shown in Figure 5.1 is only 2 dimensional. Here, we will define the third coordinate as

$$\vec{z} = \vec{x} \times \vec{y}$$

Angular velocity of the joints will always be parallel to $\vec{z}$ and linear velocity of the joints will always remain in the plane of $(\vec{x}, \vec{y})$. Therefore, the spatial velocity of the kth joint of the ith arm can be written as:

$$^{i}V_k = \begin{bmatrix} ^{i}\omega_k \\ ^{i}v_k \end{bmatrix} \in \mathcal{R}^{3\times 1} \tag{5.1}$$

Spatial velocity defined in (5.1) holds the following relationship with its counterpart in 3 dimensional space.

$$^{i}V_k = A\,^{i}\vec{\vec{V}}_k \qquad ^{i}\vec{\vec{V}}_k \in \mathcal{R}^{6\times 1} \tag{5.2}$$

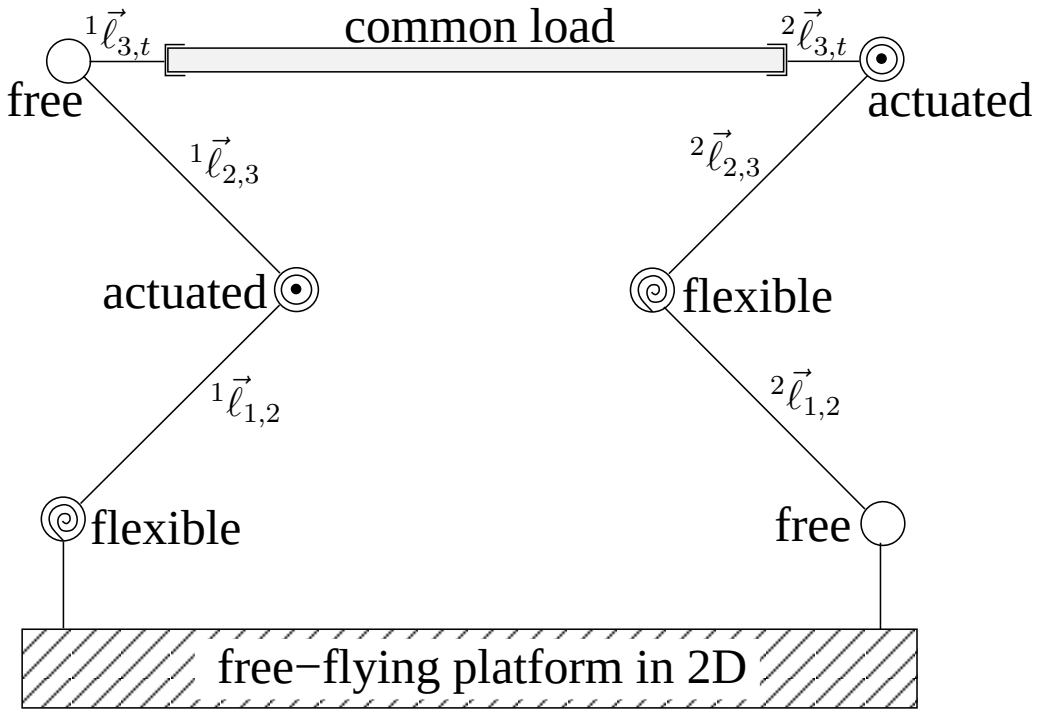

Figure 5.1: Initial configuration

where,

$$A = \begin{bmatrix} 0 & 0 & 1 & 0 & 0 & 0 \\ 0 & 0 & 0 & 1 & 0 & 0 \\ 0 & 0 & 0 & 0 & 1 & 0 \end{bmatrix}$$

Let ${}^{i}\mathbf{\Phi}_{k+1,k}$ be a linear operator that translates ${}^{i}\vec{V}_k$ to ${}^{i}\vec{V}_{k+1}$. In 2 dimensional space, we will represent this operator as ${}^{i}\phi_{k+1,k}$.

$${}^{i}\phi_{k+1,k} = A\,{}^{i}\mathbf{\Phi}_{k+1,k}A^T = \begin{bmatrix} 1 & 0 & 0 \\ -{}^{i}\ell_{k_y} & 1 & 0 \\ {}^{i}\ell_{k_x} & 0 & 1 \end{bmatrix} \tag{5.3}$$

The rest of the elements of the spatial algebra in 2 and 3 dimensional analysis have similar relationships as given in equations (5.2) and (5.3).

The closed chain system consisting of two arms and a common load is shown at its initial configuration in Figure 5.1 in which joints are drawn differently according to their actuation. There is no actuation provided to so called “free joints”. Flexible joint, on the other hand, has a spring and a damper attached to it.

In this proposed system, all the links and the common load are rigid bodies. The contacts between the common load and the arms are also rigid.

Joints are numbered in an increasing order from base to tip. Base is common for both arm 1 and 2 and it is numbered zero. The third joint of Arm 1 and the first joint of Arm 2 are free joints. The first joint of Arm 1 and the second joint of Arm 2 are flexible joints. The second joint of Arm 1 and the third joint of Arm 2 are actuated joints.

Velocity of the base:

$$^{1}V_o = {}^{2}V_o = V_o \tag{5.4}$$

Acceleration of the base:

$$^{1}\alpha_o = {}^{2}\alpha_o = \alpha_o \tag{5.5}$$

The forces on the base:

$$f_o = {}^{1}\phi_{1,0}^{T}\,{}^{1}f_1 + {}^{2}\phi_{1,0}^{T}\,{}^{2}f_1 + M_o\alpha_o + b_o \tag{5.6}$$

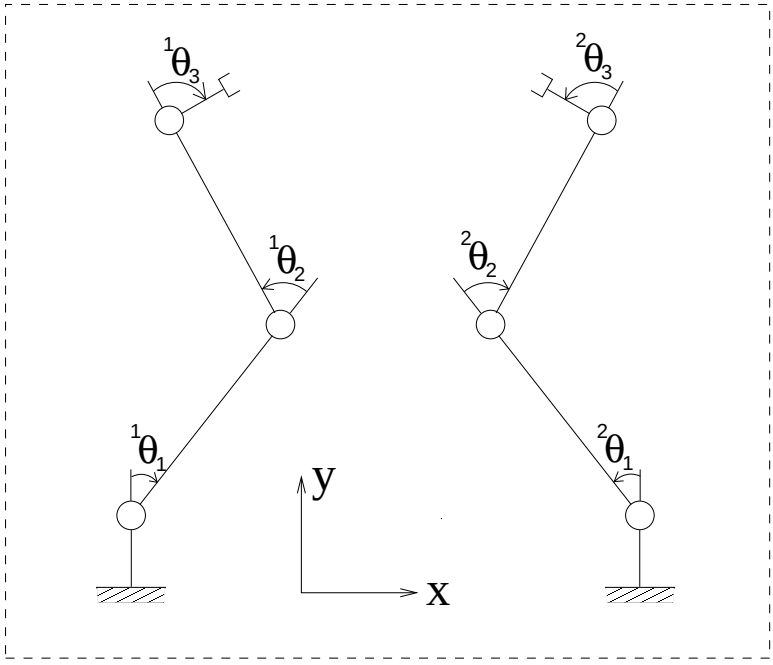

Figure 5.2: Joint angles

The propagation matrix for each arm is:

$$
{}^{i}\phi = \begin{bmatrix}
1 & 0 & 0 & 0 & 0 & 0 & 0 & 0 & 0 \\
0 & 1 & 0 & 0 & 0 & 0 & 0 & 0 & 0 \\
0 & 0 & 1 & 0 & 0 & 0 & 0 & 0 & 0 \\
1 & 0 & 0 & 1 & 0 & 0 & 0 & 0 & 0 \\
-{}^{i}\ell_{1_y} & 1 & 0 & 0 & 1 & 0 & 0 & 0 & 0 \\
{}^{i}\ell_{1_x} & 0 & 1 & 0 & 0 & 1 & 0 & 0 & 0 \\
1 & 0 & 0 & 1 & 0 & 0 & 1 & 0 & 0 \\
-({}^{i}\ell_{1_y} + {}^{i}\ell_{2_y}) & 1 & 0 & -{}^{i}\ell_{2_y} & 1 & 0 & 0 & 1 & 0 \\
({}^{i}\ell_{1_x} + {}^{i}\ell_{2_x}) & 0 & 1 & {}^{i}\ell_{1_x} & 0 & 1 & 0 & 0 & 1
\end{bmatrix}
$$

Since it is a planar system and all of the joints are revolute joints, the axis of rotation stays constant. Therefore, the axis of rotation matrix for either arm is:

$$
{}^{i}H = \begin{bmatrix}
1 & 0 & 0 & 0 & 0 & 0 & 0 & 0 & 0 \\
0 & 0 & 0 & 1 & 0 & 0 & 0 & 0 & 0 \\
0 & 0 & 0 & 0 & 0 & 0 & 1 & 0 & 0
\end{bmatrix}^{T}
$$

The spatial acceleration bias term and the spatial force bias terms for either arm is:

$$
{}^{i}a = \begin{bmatrix}
0 \\ 0 \\ 0 \\ 0 \\ -{}^{i}\dot{\theta}_1^2\, {}^{i}\ell_{1_x} \\ -{}^{i}\dot{\theta}_1^2\, {}^{i}\ell_{1_y} \\ 0 \\ -{}^{i}\dot{\theta}_2^2\, {}^{i}\ell_{2_x} \\ -{}^{i}\dot{\theta}_2^2\, {}^{i}\ell_{2_y}
\end{bmatrix}
\qquad
{}^{i}b = -\frac{1}{2}\begin{bmatrix}
0 \\ {}^{i}\dot{\theta}_1^2\, {}^{i}\ell_{1_x} \\ {}^{i}\dot{\theta}_1^2\, {}^{i}\ell_{1_y} \\ 0 \\ {}^{i}\dot{\theta}_2^2\, {}^{i}\ell_{2_x} \\ {}^{i}\dot{\theta}_2^2\, {}^{i}\ell_{2_y} \\ 0 \\ {}^{i}\dot{\theta}_3^2\, {}^{i}\ell_{3_x} \\ {}^{i}\dot{\theta}_3^2\, {}^{i}\ell_{3_y}
\end{bmatrix}
$$

Propagation to base and propagation to tip operators are respectively:

$$
{}^{i}\sigma_b = \begin{bmatrix} 1 & 0 & 0 \\ -{}^{i}\ell_{b_y} & 1 & 0 \\ {}^{i}\ell_{b_x} & 0 & 1 \\ 0 & 0 & 0 \\ 0 & 0 & 0 \\ 0 & 0 & 0 \\ 0 & 0 & 0 \\ 0 & 0 & 0 \\ 0 & 0 & 0 \end{bmatrix} \qquad {}^{i}\sigma_t = \begin{bmatrix} 0 & 0 & 0 \\ 0 & 0 & 0 \\ 0 & 0 & 0 \\ 0 & 0 & 0 \\ 0 & 0 & 0 \\ 0 & 0 & 0 \\ 1 & {}^{i}\ell_{3_y} & {}^{i}\ell_{3_x} \\ 0 & 1 & 0 \\ 0 & 0 & 1 \end{bmatrix}^T
$$

Mass matrix will be given next. It is assumed that each link has a uniform mass distribution and the vector from the joint to the center of mass of each link is the half of the link vector. ${}^{i}\mathcal{I}_k$ is the moment of inertia of link k of manipulator i defined at the point ${}^{i}O_k$ on the axis of rotation. Mass matrix for each manipulator is in the following form:

$$
{}^{i}M_k = \begin{bmatrix} {}^{i}\mathcal{I}_k & \frac{1}{2}\,{}^{i}m_k\,{}^{i}\ell_{k_y} & -\frac{1}{2}\,{}^{i}m_k\,{}^{i}\ell_{k_x} \\ \frac{1}{2}\,{}^{i}m_k\,{}^{i}\ell_{k_y} & {}^{i}m_k & 0 \\ -\frac{1}{2}\,{}^{i}m_k\,{}^{i}\ell_{k_x} & 0 & {}^{i}m_k \end{bmatrix}
$$

$$
{}^{i}M = \begin{bmatrix} {}^{i}M_1 & 0 & 0 \\ 0 & {}^{i}M_2 & 0 \\ 0 & 0 & {}^{i}M_3 \end{bmatrix}
$$

Mass matrix for the base and the mass matrix for the complete system which is formed by stacking up the mass matrices for the base and the arms are given as follows:

$$
M_b = \begin{bmatrix} \mathcal{I}_b & 0 & 0 \\ 0 & m_b & 0 \\ 0 & 0 & m_b \end{bmatrix} \qquad M = \begin{bmatrix} M_b & 0 & 0 \\ 0 & {}^{1}M & 0 \\ 0 & 0 & {}^{2}M \end{bmatrix}
$$

Spatial acceleration bias term, spatial force bias term, propagation to tip operator, propagation operator, axis of motion matrix and the separator operator for the complete

system are formed as:

$$a = \begin{bmatrix} 0 \\ {}^1a \\ {}^2a \end{bmatrix} \qquad b = \begin{bmatrix} 0 \\ {}^1b \\ {}^2b \end{bmatrix} \qquad \sigma_t = \begin{bmatrix} 0 & {}^1\sigma_t & 0 \\ 0 & 0 & {}^2\sigma_t \end{bmatrix}$$

$$\phi = \begin{bmatrix} {}_{3\times3}I & 0 & 0 \\ {}^1\phi\,{}^1\sigma_b & {}^1\phi & 0 \\ {}^2\phi\,{}^2\sigma_b & 0 & {}^2\phi \end{bmatrix} \qquad H = \begin{bmatrix} {}_{3\times3}I & 0 & 0 \\ 0 & {}^1H & 0 \\ 0 & 0 & {}^2H \end{bmatrix}$$

$$S = \begin{bmatrix} 1 & 0 & 0 & 0 & 0 & 0 & 0 & 0 & 0 \\ 0 & 1 & 0 & 0 & 0 & 0 & 0 & 0 & 0 \\ 0 & 0 & 1 & 0 & 0 & 0 & 0 & 0 & 0 \\ 0 & 0 & 0 & 0 & 1 & 0 & 0 & 0 & 0 \\ 0 & 0 & 0 & 0 & 0 & 0 & 0 & 0 & 1 \\ 0 & 0 & 0 & 0 & 0 & 1 & 0 & 0 & 0 \\ 0 & 0 & 0 & 0 & 0 & 0 & 1 & 0 & 0 \\ 0 & 0 & 0 & 1 & 0 & 0 & 0 & 0 & 0 \\ 0 & 0 & 0 & 0 & 0 & 0 & 0 & 1 & 0 \end{bmatrix}$$

Simulation results associated with the given system can be found in Appendix A.

5.2 Two Wheeled Cart

The system consists of two independently actuated wheels that are connected by a rod, as shown in Figure 5.3.

As explained in Section 4.3, each wheel is modeled as a one-link mechanism having 3 DOF. Each actuator introduces one DOF at the wheel center, making four DOF per arm. Although the sum of the number of DOF each joint has in the system is eight, only two of them are independently actuated. However, the degree of underactuation in the system is only one (not six) due to the no-slip constraint reducing the overall DOF. The explained configuration is shown in Figure 5.4 where the mass and inertia of wheel i are assigned to ${}^i\text{link}_1$ ($i = 1, 2$) as in the case of a unicycle explained in Section 4.3.

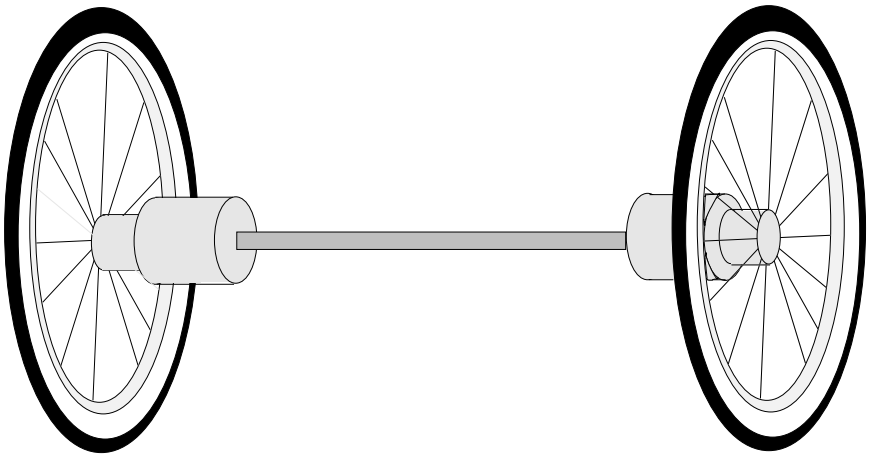

Figure 5.3: Two-wheeled cart: pictorial representation

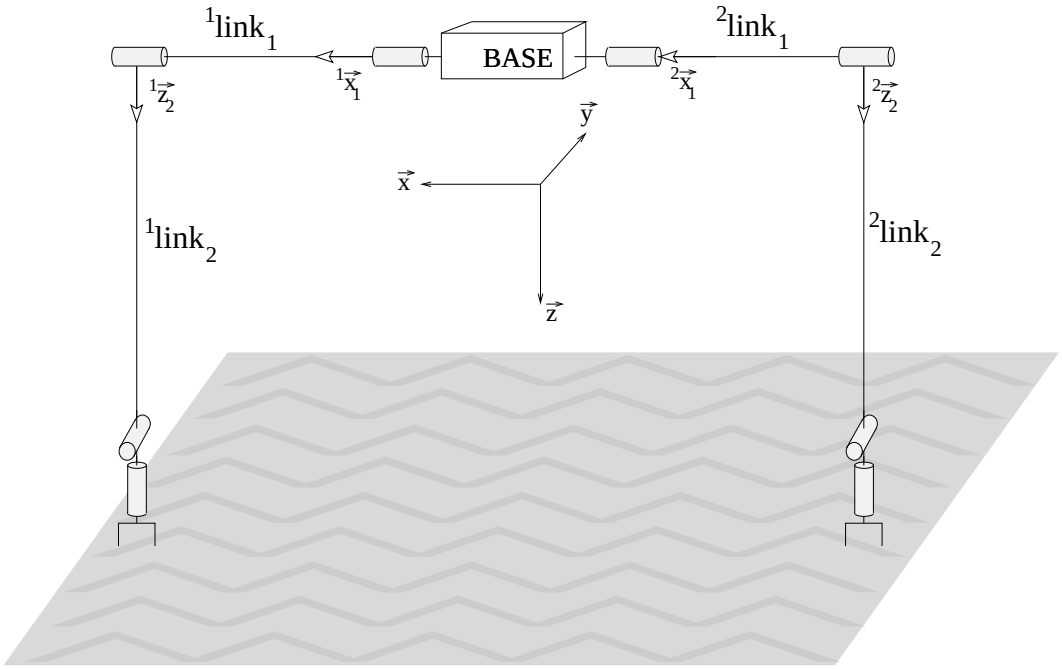

Figure 5.4: Two-wheeled cart: manipulator representation

Frames are assigned in the same way for both arms as follows: Base frame, frame 0, is attached to the axle. Frame 1 is on the actuator. Frame 2 is attached to a one-DOF joint at the wheel center. Frame 3 is a two-DOF revolute joint, and its origin coincides with that of the tool frame which is the contact point to the ground.

Equation of motion is obtained similar, to some extend, to that of a single wheel introduced in Section 4.3. In order to keep the continuity within this section, there will be some repetitions with Section 4.3, but we believe that the differences are great enough not to mind the similarities.

Here, we present two approaches for the dynamical modeling. The main difference is in the definition of the axis of rotation. For the first approach the axis of rotation matrix is defined per arm as

$$ {}^{i}\mathbf{H} = \begin{bmatrix} {}^{i}\vec{x}_1 & \vec{0} & \vec{0} & \vec{0} \\ \vec{0} & \vec{0} & \vec{0} & \vec{0} \\ \vec{0} & {}^{i}\vec{x}_2 & \vec{0} & \vec{0} \\ \vec{0} & \vec{0} & \vec{0} & \vec{0} \\ \vec{0} & \vec{0} & {}^{i}\vec{y}_2 & {}^{i}\vec{z}_3 \\ \vec{0} & \vec{0} & \vec{0} & \vec{0} \end{bmatrix} \tag{5.7} $$

where ${}^{i}\vec{x}_1$ and ${}^{i}\vec{x}_2$ are unit vectors along the rod (axel), ${}^{i}\vec{y}_2$ is in the travel direction of the wheel and ${}^{i}\vec{z}_3$ is the normal vector of the tangent plane of the contact point with the ground.

Now, we start with the lateral slip condition.

$$ {}^{1}\vec{x}_2^{T}\ \vec{v}_t\ =\ {}^{2}\vec{x}_2^{T}\ {}^{2}\vec{v}_t \tag{5.8} $$

We can express (5.8) in a form reducible to a Pfaffian constraint

$$ \tilde{\mathbf{A}}^{T}\underline{V}_t = 0 \tag{5.9} $$

where

$$ \tilde{\mathbf{A}} = \begin{bmatrix} \vec{0} \\ {}^{1}\vec{x}_2 \\ \vec{0} \\ -{}^{2}\vec{x}_2 \end{bmatrix} \tag{5.10} $$

Now, let $\tilde{\mathbf{A}}$ be the annihilator of $\mathbf{A}$. In other words, let $\mathbf{A}$ be the matrix such that $\tilde{\mathbf{A}}$ spans its null-space. This is stated as

$$\mathbf{A}\tilde{\mathbf{A}} = \mathbf{0} \tag{5.11}$$

Although there is no unique solution of (5.11), one possible choice of A is

$$\mathbf{A} = \begin{bmatrix} {}^1\vec{x}_2^T & \vec{0}^T & \vec{0}^T & \vec{0}^T \\ {}^1\vec{y}_2^T & \vec{0}^T & \vec{0}^T & \vec{0}^T \\ {}^1\vec{z}_2^T & \vec{0}^T & \vec{0}^T & \vec{0}^T \\ \vec{0}^T & \vec{0}^T & {}^2\vec{x}_2^T & \vec{0}^T \\ \vec{0}^T & \vec{0}^T & {}^2\vec{y}_2^T & \vec{0}^T \\ \vec{0}^T & \vec{0}^T & {}^2\vec{z}_2^T & \vec{0}^T \\ \vec{0}^T & \frac{{}^1\vec{x}_2^T}{\sqrt{2}} & \vec{0}^T & \frac{{}^2\vec{x}_2^T}{\sqrt{2}} \\ \vec{0}^T & {}^1\vec{y}_2^T & \vec{0}^T & \vec{0}^T \\ \vec{0}^T & {}^1\vec{z}_2^T & \vec{0}^T & \vec{0}^T \\ \vec{0}^T & \vec{0}^T & \vec{0}^T & {}^2\vec{y}_2^T \\ \vec{0}^T & \vec{0}^T & \vec{0}^T & {}^2\vec{z}_2^T \end{bmatrix} \tag{5.12}$$

Note that A, as defined in (5.12), is an orthogonal matrix and therefore holds orthogonality property

$$\mathbf{A}\mathbf{A}^T = \mathbf{I} \tag{5.13}$$

There exists a velocity vector $\underline{V_c}$ in an eleven dimensional manifold to express the tip velocity using (5.9) and (5.11).

$$\underline{V_t} = \mathbf{A}^T\underline{V_c} \tag{5.14}$$

Using the longitudinal slip constraint, $\underline{V_c}$ can be expressed as a function of the joint space of the wheel.

$$\underline{V_c} = \mathbf{B}\underline{\dot{\theta}} \tag{5.15}$$

where

$$\underline{\dot{\theta}} = \begin{bmatrix} \vec{\vec{V}}_b \\ {}^1\underline{\dot{\theta}} \\ {}^2\underline{\dot{\theta}} \end{bmatrix} \qquad \mathbf{B} = \begin{bmatrix} 0 & 0 & 0 & 0 & 0 & 0 & 0 & 0 & 0 & 0 & 0 & 0 & 0 & 0 \\ 0 & 0 & 0 & 0 & 0 & 0 & 0 & 0 & 0 & 0 & 0 & 0 & 0 & 0 \\ 0 & 0 & 0 & 0 & 0 & 0 & 0 & 0 & 0 & 0 & 0 & 0 & 0 & 0 \\ 0 & 0 & 0 & 0 & 0 & 0 & 0 & 0 & 0 & 0 & 0 & 0 & 0 & 0 \\ 0 & 0 & 0 & 0 & 0 & 0 & 0 & 0 & 0 & 0 & 0 & 0 & 0 & 0 \\ 0 & 0 & 0 & 0 & 0 & 0 & 0 & 0 & 0 & 0 & 0 & 0 & 0 & 0 \\ 0 & 0 & 0 & 0 & 0 & 0 & 0 & 0 & 0 & 0 & 0 & 0 & 0 & 0 \\ 0 & 0 & 0 & 0 & 0 & 0 & 0 & -r & 0 & 0 & 0 & 0 & 0 & 0 \\ 0 & 0 & 0 & 0 & 0 & 0 & 0 & 0 & 0 & 0 & 0 & 0 & 0 & 0 \\ 0 & 0 & 0 & 0 & 0 & 0 & 0 & 0 & 0 & 0 & 0 & -r & 0 & 0 \\ 0 & 0 & 0 & 0 & 0 & 0 & 0 & 0 & 0 & 0 & 0 & 0 & 0 & 0 \end{bmatrix}$$

where r is the radius of the wheel.

The rest of the formulations here are very similar to those in Section 4.3. We will skip the intermediate steps and write down the more significant ones.

Tip force can be decomposed as

$$\underline{F}_t = \mathbf{A}^T \underline{F}_c + \tilde{\mathbf{A}}\underline{\eta} \tag{5.16}$$

Here $\underline{\eta}$ corresponds to the squeeze force. Minimum norm solution would be to set it to zero.

Forward dynamics equation becomes

$$\underline{\ddot{\theta}} = \mathcal{M}^{-1}\left(\underline{\mathcal{T}}_c - (\mathbf{A}\mathcal{J} - \mathbf{B})^T \underline{F}_c\right) \tag{5.17}$$

where $\underline{\mathcal{T}}_c = \underline{\mathcal{T}}_a - \underline{\mathcal{C}}$, and $\underline{\mathcal{T}}_a$ is the applied torques.

Finally, we have

$$\underline{F}_c = \mathbf{\Omega}^{-1}\left(\mathbf{A}\mathbf{\Phi}_t\mathbf{\Phi}\underline{a} + (\mathbf{A}\mathcal{J} - \mathbf{B})\mathcal{M}^{-1}\underline{\mathcal{T}}_c - \mathbf{A}\dot{\mathbf{A}}^T\mathbf{B}\underline{\dot{\theta}}\right) \tag{5.18}$$

where

$$\mathbf{\Omega} = (\mathbf{A}\mathcal{J} - \mathbf{B})\mathcal{M}^{-1}(\mathbf{A}\mathcal{J} - \mathbf{B})^T \tag{5.19}$$

An alternative approach is the following. Let us change the defining of the axis of rotation matrix from (5.7) to

$$
{}^{i}\mathbf{H} = \begin{bmatrix}
{}^{i}\vec{x}_1 & \vec{0} & \vec{0} & \vec{0} \\
\vec{0} & \vec{0} & \vec{0} & \vec{0} \\
\vec{0} & {}^{i}\vec{x}_2 & \vec{0} & \vec{0} \\
\vec{0} & \vec{0} & \vec{0} & \vec{0} \\
\vec{0} & \vec{0} & {}^{i}\vec{y}_2 & {}^{i}\vec{z}_3 \\
\vec{0} & r\,{}^{i}\vec{y}_2 & \vec{0} & \vec{0}
\end{bmatrix} \tag{5.20}
$$

This means that the longitudinal slip condition is augmented in the Jacobian. Hence, there is no need to externally enforce the system to obey it. This small modification of the matrix $\mathbf{H}$ results in the removal of the matrix $\mathbf{B}$ from the equation of motion. Therefore, we have

$$
\begin{aligned}
\mathbf{\Omega} &= \mathbf{A}\mathcal{J}\mathcal{M}^{-1}\mathcal{J}^{T}\mathbf{A}^{T} \\
\underline{F_t} &= \mathbf{A}^{T}\mathbf{\Omega}^{-1}\mathbf{A}\left(\mathcal{J}\mathcal{M}^{-1}\underline{\mathcal{T}_c} + \mathbf{\Phi}_t\mathbf{\Phi}\underline{a}\right) \\
\underline{\ddot{\theta}} &= \mathcal{M}^{-1}\left(\underline{\mathcal{T}_c} - \mathcal{J}^{T}\underline{F_t}\right)
\end{aligned}
$$

Simulation results associated with this system can be found in Appendix B.

5.3 Four-Wheel-Drive Four-Wheel-Steer Mobile Manipulator

Mechanical and electrical design details of the four-wheel-driven and four-wheel-steered mobile robot manufactured as a mobile platform for the Mitsubishi PA10-7C robotic arm can be found in [62] and shown in Figure 5.9. We will model the platform only. A photograph of the mobile platform without the manipulator is displayed in Figure 5.5 and a generated image using a computer aided three dimensional design package is shown in Figure 5.6.

Let us concentrate only on the backbone, leg and wheel part of the system as shown in Figure 5.7 which helps us understand the analogy between multiple constrained manipulators and the actual system, where “the base” is the backbone, and each leg

Figure 5.5: A photograph of the 4x4x4 mobile robot

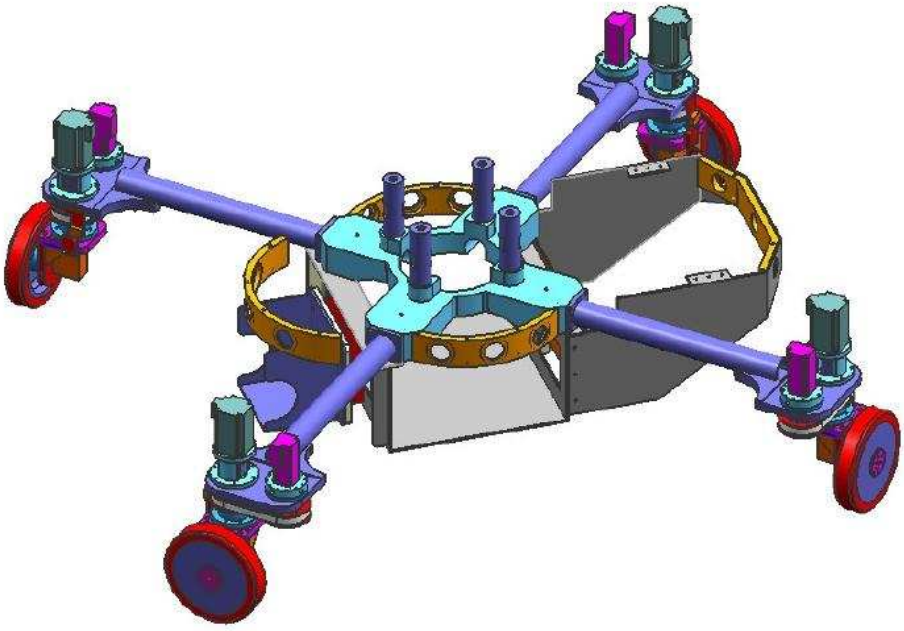

Figure 5.6: Computer generated image of the 4x4x4 mobile robot

and the wheel are constituted by a manipulator. Manipulator representation of the system is given in Figure 5.8. The unconstrained system has 26 DOF in total; 6 from the base, and 5 from each arm.

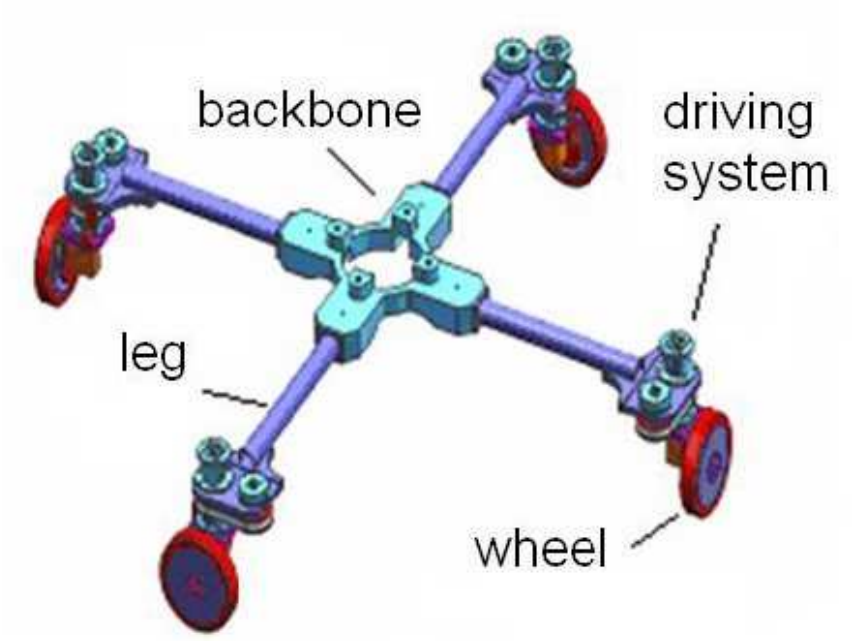

Figure 5.7: Backbone, leg and wheel parts of the mobile robot

Dynamical modeling formulation of the four-wheel-driven and four-wheel-steered mobile robot is very similar to that of the two-wheeled cart explained in the previous section except that this system has four "arms" instead of two. The most important part is to come up with the constraint matrix, $\tilde{\mathbf{A}}$. As the system gets complicated, it gets harder to predict it. An easy way to obtain it is to use the rational basis null space of $\mathcal{J}^T$ in MATLAB for once. It yields the following independent constraints:

$$ {}^1\vec{x}_3^T \, {}^1\vec{v}_t = {}^2\vec{x}_3^T \, {}^2\vec{v}_t \tag{5.21} $$

$$ {}^3\vec{x}_3^T \, {}^3\vec{v}_t = {}^4\vec{x}_3^T \, {}^4\vec{v}_t \tag{5.22} $$

$$ {}^3\vec{z}_3^T \, {}^3\vec{v}_t = {}^4\vec{z}_3^T \, {}^4\vec{v}_t \tag{5.23} $$

Simulation results associated with this system can be found in Appendix C.

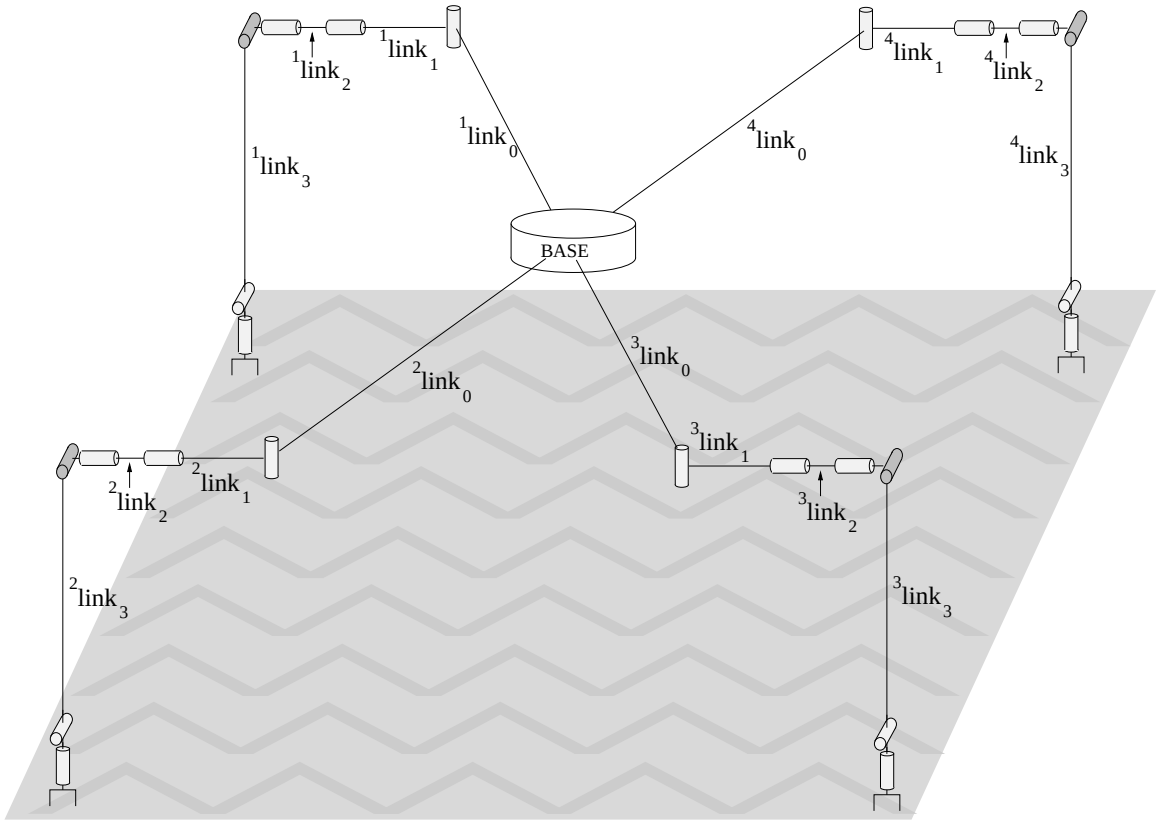

Figure 5.8: Manipulator representation of the mobile robot

5.4 Four Wheeled Passenger Vehicle with Full Suspension Mechanism

The proposed model of vehicle will be explained for separate parts first of which is the tire model. Tire characteristics are known to be highly nonlinear and very complicated. Since the motivation here is to demonstrate the use of the algorithm, the point contact tire model [63] is employed. The algorithm, on the other hand, can be extended to include more complicated tire models.

The joint at the point contact has 3 rotational DOF. Pneumatic characteristics of tire are represented by spring and damper pairs in both vertical and horizontal directions. The end effector shown in Fig.5.10 corresponds to the center of the wheel.

As shown in Fig.5.11, the suspension model has 5-DOF. All of the rotational joints are represented with a cylinder whose axis is aligned with the axis of rotation. A small circle in the cylinder indicates that there is a torsional spring and a damper attached to that joint. Figure 5.12 shows the trapezoidal geometry of the steering mechanism. This design closely approximates the Ackerman condition.

Finally, in Fig.5.13, the full model of a vehicle is given. The total number of DOF is

Figure 5.9: Mobile manipulator with Mitsubishi PA10-7C

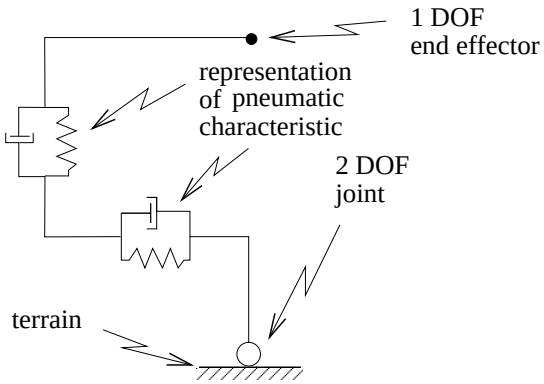

Figure 5.10: Tire model

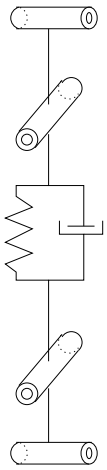

Figure 5.11: Suspension model

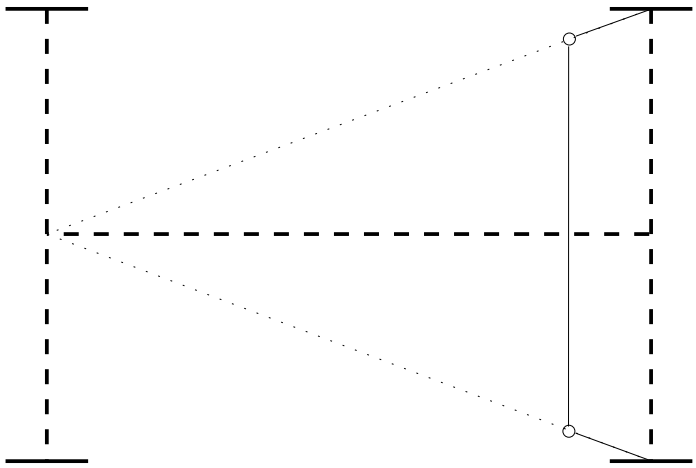

Figure 5.12: Trapezoidal geometry to partially satisfy the Ackerman condition

51; however, as to be shown later, only 24 of them are independent.

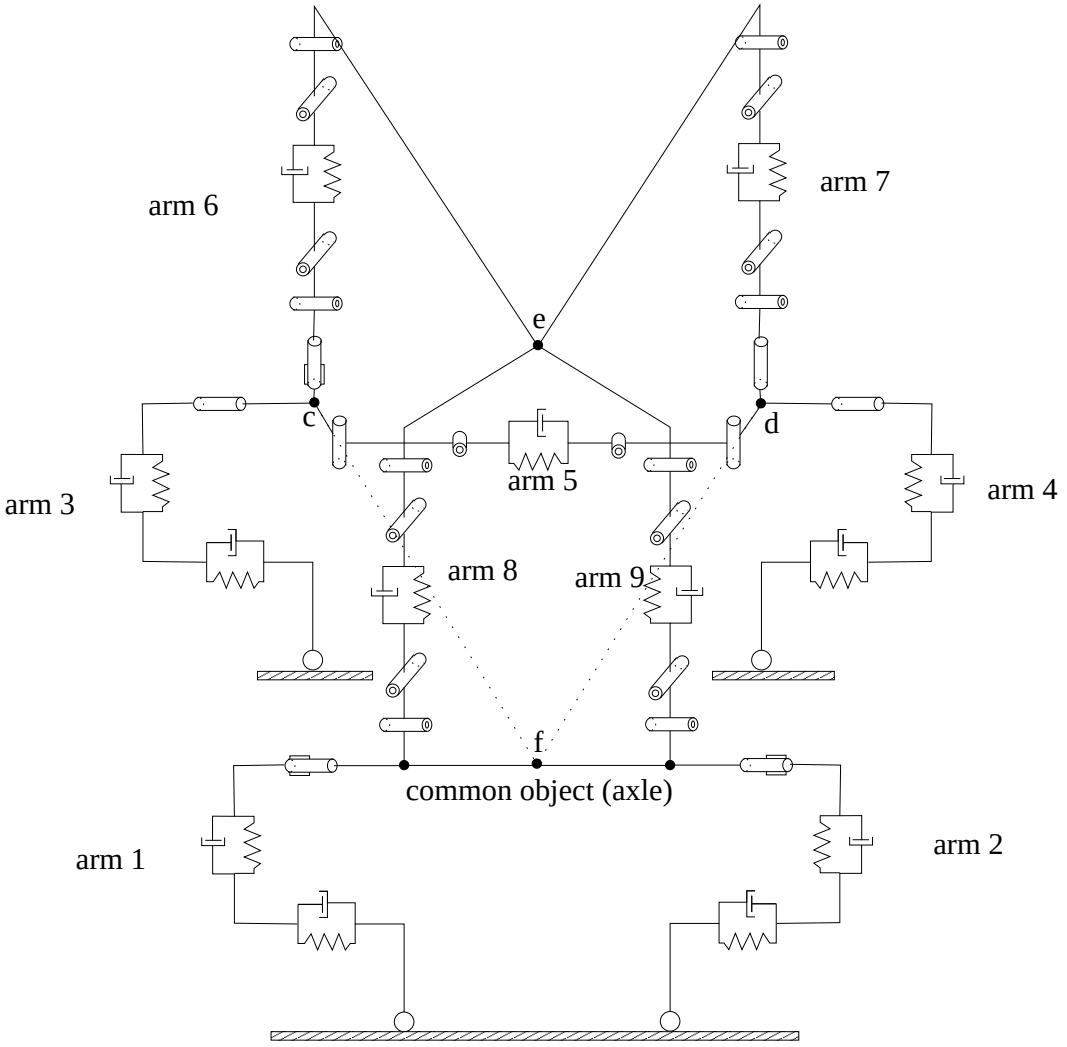

Figure 5.13: Full model of a four-wheeled full suspension vehicle

Let V_{b_+} and V_{b_-} represent the base spatial velocities of all the arms on the arm side, and on the base side respectively. No slip condition requires both velocities to be the same. Let them be equal to V_b.

$$\begin{bmatrix} V_{b_-} \\ V_{b_+} \end{bmatrix} = \begin{bmatrix} I \\ I \end{bmatrix} V_b \tag{5.24}$$

Let V^c be the stacked up spatial velocities of contact points where the bases and the tips of arms meet. Let V^s consist of the time derivatives of each of the four wheels' vertical displacements due to the surface geometry of the terrain. Since these displacements

are known to be vertical, each elements of V^s, ${}^iv_s$, is scalar.

$$
\begin{aligned}
V^c &= \begin{bmatrix} V_c^T & V_d^T & V_e^T & V_f^T \end{bmatrix}^T \\
V^s &= \begin{bmatrix} {}^1v_s & {}^2v_s & {}^3v_s & {}^4v_s \end{bmatrix}^T
\end{aligned}
$$

Base velocity part of the kinematic constraints can be written as:

$$
V_{b\_} = \begin{bmatrix} A_{bs0} & A_{0bc} \end{bmatrix} \begin{bmatrix} V^s \\ V^c \end{bmatrix} \tag{5.25}
$$

$$
\begin{aligned}
A_{bs} &= \begin{bmatrix} i & 0 & 0 & 0 \\ 0 & i & 0 & 0 \\ 0 & 0 & i & 0 \\ 0 & 0 & 0 & i \end{bmatrix} \quad A_{bc} = \begin{bmatrix} I & 0 & 0 & 0 \\ I & 0 & 0 & 0 \\ 0 & I & 0 & 0 \\ 0 & 0 & 0 & \phi_{1,f} \\ 0 & 0 & 0 & \phi_{2,f} \end{bmatrix} \\
i &= \begin{bmatrix} 0 & 0 & 0 & 0 & 0 & 1 \end{bmatrix}^T \\
A_{bs0} &= \begin{bmatrix} A_{bs}^T & 0 \end{bmatrix}^T \quad A_{0bc} = \begin{bmatrix} 0 & A_{bc}^T \end{bmatrix}^T
\end{aligned}
$$

Tip velocity part of the kinematic constraints are:

$$
V_t = A_{tc} V^c \tag{5.26}
$$

$$
A_{tc} = \begin{bmatrix} 0 & 0 & I & 0 & 0 & 0 & 0 & 0 & 0 \\ 0 & 0 & 0 & I & I & 0 & 0 & 0 & 0 \\ 0 & 0 & 0 & 0 & 0 & I & I & I & I \\ \phi_{1,f}^T & \phi_{2,f}^T & 0 & 0 & 0 & 0 & 0 & 0 & 0 \end{bmatrix}^T
$$

Putting (5.25) and (5.26) together,

$$
\begin{bmatrix} V_{b\_} \\ V_t \end{bmatrix} = \begin{bmatrix} A_b \\ A_t \end{bmatrix} \begin{bmatrix} V^s \\ V^c \end{bmatrix} \tag{5.27}
$$

where $A_b = \begin{bmatrix} A_{bs0} & A_{0bc} \end{bmatrix}$, $A_t = \begin{bmatrix} 0 & A_{tc} \end{bmatrix}$. Kinematic constraints are fully obtained from (5.24) and (5.27).

Spatial velocities of the joints with respect to an inertial frame can be obtained by using velocity propagation.

$$
V = \phi H \dot{\theta} + \phi \sigma_b V_{b\_} \tag{5.28}
$$

Furthermore, tip velocities of arms can be calculated.

$$\begin{aligned} V_t &= \sigma_t V \\ &= \mathcal{J}\dot{\theta} + \phi_{t,b} V_{b_-} \\ &= \mathcal{J}\dot{\theta} + \phi_{t,b} A_{bs0} V^s + \phi_{t,b} A_{0bc} V^c \end{aligned} \tag{5.29}$$

From (5.26):

$$V^c = A_{tc}^{\dagger} V_t \quad A_{tc}^{\dagger} = (A_{tc}^T A_{tc})^{-1} A_{tc}^T \tag{5.30}$$

Substituting (5.30) in (5.29)

$$V_t = L_t \mathcal{J}\dot{\theta} + L_s V^s \tag{5.31}$$

where $L_t = \left(I - \phi_{t,b} A_{0bc} A_{tc}^{\dagger}\right)^{-1}$, $L_s = L_t \phi_{t,b} A_{bs0}$. Let us take time derivative of (5.31)

$$\alpha_t = L_t \mathcal{J}\ddot{\theta} + L_t \dot{\mathcal{J}}\dot{\theta} + \dot{L}_t \mathcal{J}\dot{\theta} + L_s \alpha^s + \dot{L}_s V^s \tag{5.32}$$

Using the known equality, $\dot{\mathcal{J}}\dot{\theta} = \sigma_t \phi a + a_t$, finally we get

$$\alpha_t = L_t \mathcal{J}\ddot{\theta} + \dot{L}_t \mathcal{J}\dot{\theta} + L_s \alpha^s + \dot{L}_s V^s + L_t(\sigma_t \phi a + a_t) \tag{5.33}$$

Now let us focus on the base accelerations. Taking the time derivative of (5.25)

$$\alpha_{b_-} = A_{bs0}\alpha^s + A_{0bc}\alpha^c + \dot{A}_{0bc} V^c \tag{5.34}$$

Substituting (5.31) in (5.30)

$$V^c = A_{tc}^{\dagger}(L_t \mathcal{J}\dot{\theta} + L_s V^s) \tag{5.35}$$

Taking time derivative of (5.30) and substituting (5.31)

$$\alpha^c = A_{tc}^{\dagger}\alpha_t + \dot{A}_{tc}^{\dagger}(L_t \mathcal{J}\dot{\theta} + L_s V^s) \tag{5.36}$$

Substituting (5.35) and (5.36) in (5.34)

$$\alpha_{b_-} = A_{0bc} A_{tc}^{\dagger}\alpha_t + L_u L_t \mathcal{J}\dot{\theta} + A_{bs0}\alpha^s + L_u L_s V^s \tag{5.37}$$

where $L_u = A_{0bc}\dot{A}_{tc}^{\dagger} + \dot{A}_{0bc} A_{tc}^{\dagger}$. Plugging (5.33) in (5.37), now we can obtain the equation for base accelerations in terms of $\ddot{\theta}$, $\dot{\theta}$, α^s and V^s.

$$\alpha_{b_-} = L_a \mathcal{J}\ddot{\theta} + L_b \mathcal{J}\dot{\theta} + L_c \alpha^s + L_d V^s + L_e \tag{5.38}$$

$$
\begin{aligned}
L_a &= A_{0bc}A_{tc}^{\dagger}L_t \\
L_b &= L_u L_t + A_{0bc}A_{tc}^{\dagger}\dot{L}_t \\
L_c &= A_{bs0} + A_{0bc}A_{tc}^{\dagger}L_s \\
L_d &= L_u L_s + A_{0bc}A_{tc}^{\dagger}\dot{L}_s \\
L_e &= A_{0bc}A_{tc}^{\dagger}L_t(\sigma_t\phi a + a_t) = L_a(\sigma_t\phi a + a_t)
\end{aligned}
$$

Now we will investigate the feasible sets of $\dot{\theta}$. Combining (5.26) and (5.31), and pre-multiplying both sides of the result by $\widetilde{A_{tc}}$, we get:

$$
\widetilde{A_{tc}}L_t\mathcal{J}\dot{\theta} = V^r \qquad V^r = -\widetilde{A_{tc}}L_s V^s \tag{5.39}
$$

To uniquely determine the dependent joint velocities in terms of the independent ones, the elements of the joint space, $\dot{\theta}$, are reordered in a way that these elements are grouped into independent and dependent subspaces using the matrix S^a formed by rearranging the rows of an identity matrix. As the choice of these subspaces is not unique, one can determine his/her choice based on preference and the structure.

$$
\widetilde{A_{tc}}L_t\mathcal{J}S^{a^{-1}}S^a\dot{\theta} = V^r
$$

With the following definitions, (5.40) is obtained.

$$
\widetilde{A_{tc}}L_t\mathcal{J}S^{a^{-1}} = \begin{bmatrix} E^{\text{dep}} & E^{\text{ind}} \end{bmatrix} \quad S^a\dot{\theta} = \begin{bmatrix} \dot{\theta}^{\text{dep}} \\ \dot{\theta}^{\text{ind}} \end{bmatrix}
$$

$$
\dot{\theta}^{\text{dep}} = E^{\text{dep}^{-1}}(-E^{\text{ind}}\dot{\theta}^{\text{ind}} + V^r) \tag{5.40}
$$

If E^{dep} is not full rank, it means that the choice of S^a is wrong. Similar equation to (5.40) can be written for accelerations too. In order to do that, let us first take the time derivative of (5.26).

$$
\alpha_t = A_{tc}\alpha^c + \dot{A}_{tc}V^c \tag{5.41}
$$

From(5.33) and (5.41)

$$
A_{tc}\alpha^c + \dot{A}_{tc}V^c = L_t\mathcal{J}\ddot{\theta} + \dot{L}_t\mathcal{J}\dot{\theta} + L_s\alpha_s + \dot{L}_sV_s + L_t\sigma_t\phi a + L_t a_t \tag{5.42}
$$

Using (5.35) in (5.42), and pre-multiplying it with $\widetilde{A_{tc}}$

$$
\widetilde{A_{tc}}L_t\mathcal{J}\ddot{\theta} = \widetilde{A_{tc}}(\dot{A}_{tc}A_{tc}^{\dagger}L_t - \dot{L}_t)\mathcal{J}\dot{\theta} + \alpha^r \tag{5.43}
$$

where

$$\alpha^r = -\widetilde{A_{tc}}(L_s\alpha_s + (\dot{L}_s - \dot{A}_{tc}A_{tc}^{\dagger}L_s)V_s + L_t\sigma_t\phi a + L_t a_t)$$

Let us apply the operator S^a to separate the dependent and independent variables.

$$\widetilde{A_{tc}}L_t\mathcal{J}S^{a^{-1}}S^a\ddot{\theta} = \widetilde{A_{tc}}(\dot{A}_{tc}A_{tc}^{\dagger}L_t - \dot{L}_t)\mathcal{J}S^{a^{-1}}S^a\dot{\theta} + \alpha^r$$

Assigning

$$\widetilde{A_{tc}}(\dot{A}_{tc}A_{tc}^{\dagger}L_t - \dot{L}_t)\mathcal{J}S^{a^{-1}} = \begin{bmatrix} C^{\text{dep}} & C^{\text{ind}} \end{bmatrix}$$

Finally we get

$$\ddot{\theta}^{\text{dep}} = E^{\text{dep}^{-1}}(-E^{\text{ind}}\ddot{\theta}^{\text{ind}} + C^r\dot{\theta}^{\text{ind}} + \alpha^r + C^{\text{dep}}E^{\text{dep}^{-1}}V^r) \tag{5.44}$$

where $C^r = C^{\text{ind}} - C^{\text{dep}}E^{\text{dep}^{-1}}E^{\text{ind}}$.

Dynamic constraints have a dual relationship with the kinematic constraints. Dual of (5.24) is

$$\begin{bmatrix} I & I \end{bmatrix}\begin{bmatrix} F_{b_-} \\ F_{b_+} \end{bmatrix} = F_b \tag{5.45}$$

where F_b is a spatial force whose torque component represents the frictional term that slows down rolling wheel. Dual of (5.27) is

$$\begin{bmatrix} A_b^T & A_t^T \end{bmatrix}\begin{bmatrix} F_{b_-} \\ F_t \end{bmatrix} = \begin{bmatrix} F^s \\ F^c \end{bmatrix} \tag{5.46}$$

where

$$F^s = \begin{bmatrix} {}^1f_s \\ {}^2f_s \\ {}^3f_s \\ {}^4f_s \end{bmatrix} \quad F^c = K^f(M_f\alpha_f + b_f) \quad K^f = \begin{bmatrix} 0 \\ 0 \\ 0 \\ I \end{bmatrix}$$

From the acceleration propagation we can obtain all the accelerations as:

$$\alpha = \phi(H\ddot{\theta} + a + \sigma_b\alpha_{b_-}) \tag{5.47}$$

Now we can substitute (5.38) in (5.47)

$$\alpha = \phi((H + \sigma_b L_a\mathcal{J})\ddot{\theta} + \sigma_b L_b\mathcal{J}\dot{\theta} + \sigma_b L_c\alpha^s + \sigma_b L_d V^s + \sigma_b L_e + a) \tag{5.48}$$

General force equation is

$$F = \phi^T(M\alpha + b) + \phi^T\sigma_t^T F_t \tag{5.49}$$

Base forces can be written as:

$$F_{b_+} = \sigma_b^T F \tag{5.50}$$

Using (5.50) and (5.49)

$$F_{b_+} = \sigma_b^T\phi^T(M\alpha + b) + \phi_{t,b}^T F_t \tag{5.51}$$

We can write two dynamic constraints using (5.45)

$$A_{bs0}^T F_{b_-} = F^s \qquad A_{0bc}^T F_{b_-} + A_{tc}^T F_t = F^c \tag{5.52}$$

using (5.52) and annihilator of A_{tc}, $\widetilde{A_{tc}}$

$$F_t = A_{tc}^{\dagger^T}(F^c - A_{0bc}^T F_{b_-}) + \widetilde{A_{tc}}^T F_{ta} \tag{5.53}$$

Using (5.45), let us substitute (5.51) in (5.53).

$$\begin{aligned} F_t &= A_{tc}^{\dagger^T} F^c + (\phi\sigma_b A_{0bc} A_{tc}^\dagger)^T(M\alpha + b) + \\ &\quad (\phi_{t,b} A_{0bc} A_{tc}^\dagger)^T F_t + \widetilde{A_{tc}}^T F_{ta} - (A_{0bc}A_{tc}^\dagger)^T F_b \end{aligned}$$

Finally we get

$$F_t = (\phi\sigma_b L_a)^T(M\alpha + b) + (A_{tc}^\dagger L_t)^T F^c + (\widetilde{A_{tc}} L_t)^T F_{ta} - L_a^T F_b \tag{5.54}$$

Let us substitute (5.54) in (5.49)

$$\begin{aligned} F &= [\phi(I + \sigma_b L_a \sigma_t \phi)]^T(M\alpha + b) + (A_{tc}^\dagger L_t \sigma_t \phi)^T F^c + \\ &\quad (\widetilde{A_{tc}} L_t \sigma_t \phi)^T F_{ta} - (L_a \sigma_t \phi)^T F_b \end{aligned} \tag{5.55}$$

Next, substituting (5.48) in (5.55) we get the force equation in terms of the joint accelerations

$$\begin{aligned} F =& (I + \sigma_b L_a \sigma_t \phi)^T \phi^T \Big[M\phi \Big((H + \sigma_b L_a \mathcal{J})\ddot{\theta} + \\ & \sigma_b \Big(L_b \mathcal{J}\dot{\theta} + L_c \alpha^s + L_d V^s + L_e \Big) + a \Big) + b \Big] + \\ & (A_{tc}^\dagger L_t \sigma_t \phi)^T F^c - (L_a \sigma_t \phi)^T F_b + (\widetilde{A_{tc}} L_t \sigma_t \phi)^T F_{ta} \end{aligned} \tag{5.56}$$

The torques on the links can be extracted as $\mathcal{T} = H^T F$. Hence,

$$\mathcal{T} = \mathcal{M}\ddot{\theta} + \mathcal{C}\dot{\theta} + \mathcal{L}_a\alpha^s + \mathcal{L}_b V^s + \mathcal{D} + \mathcal{B}_b^T F_b + \mathcal{B}_t^T F_{ta} \tag{5.57}$$

$$\begin{aligned}
\mathcal{M}&=(H + \sigma_b L_a \mathcal{J})^T \phi^T M \phi (H + \sigma_b L_a \mathcal{J}) \\
\mathcal{C}&=(H + \sigma_b L_a \mathcal{J})^T \phi^T M \phi \sigma_b L_b \mathcal{J} \\
\mathcal{L}_a&=(H + \sigma_b L_a \mathcal{J})^T \phi^T M \phi \sigma_b L_c \\
\mathcal{L}_b&=(H + \sigma_b L_a \mathcal{J})^T \phi^T M \phi \sigma_b L_d \\
\mathcal{D}&=(H + \sigma_b L_a \mathcal{J})^T \phi^T (M\phi(\sigma_b L_e + a) + b) + \\
&\quad (A_{tc}^{\dagger} L_t \mathcal{J})^T F^c \\
\mathcal{B}_b&=-L_a \mathcal{J} \qquad \mathcal{B}_t = \widetilde{A_{tc}} L_t \mathcal{J}
\end{aligned}$$

Now the equation of motion can be obtained as

$$\ddot{\theta} = \mathcal{M}^{-1}(\mathcal{T} - \mathcal{C}\dot{\theta} - \mathcal{L}_a\alpha^s - \mathcal{L}_b V^s - \mathcal{D} + \mathcal{B}_b^T F_b - \mathcal{B}_t^T F_{ta}) \tag{5.58}$$

Taking the time derivative of (5.39) and substituting (5.58) in that, we obtain

$$F_{ta} = G_a\mathcal{T} + G_b F_b + G_c\dot{\theta} + G_d\alpha^s + G_e V^s + G_f \tag{5.59}$$

$$\begin{aligned}
G_a&=(\mathcal{B}_t \mathcal{M}^{-1} \mathcal{B}_t^T)^{-1} \mathcal{B}_t \mathcal{M}^{-1} \\
G_b&=(\mathcal{B}_t \mathcal{M}^{-1} \mathcal{B}_t^T)^{-1} \mathcal{B}_t \mathcal{M}^{-1} \mathcal{B}_b^T \\
G_c&=(\mathcal{B}_t \mathcal{M}^{-1} \mathcal{B}_t^T)^{-1} (\widetilde{A_{tc}} \dot{L}_t \mathcal{J} + \dot{\widetilde{A_{tc}}} L_t \mathcal{J} - \mathcal{B}_t \mathcal{M}^{-1} \mathcal{C}) \\
G_d&=(\mathcal{B}_t \mathcal{M}^{-1} \mathcal{B}_t^T)^{-1} (\widetilde{A_{tc}} L_s - \mathcal{B}_t \mathcal{M}^{-1} \mathcal{L}_a) \\
G_e&=(\mathcal{B}_t \mathcal{M}^{-1} \mathcal{B}_t^T)^{-1} (\dot{\widetilde{A_{tc}}} L_s - \mathcal{B}_t \mathcal{M}^{-1} \mathcal{L}_b) \\
G_f&=(\mathcal{B}_t \mathcal{M}^{-1} \mathcal{B}_t^T)^{-1} (\widetilde{A_{tc}} L_t(\sigma_t \phi a + a_t) - \mathcal{B}_t \mathcal{M}^{-1} \mathcal{D})
\end{aligned}$$

As for the suspension dynamics, we substitute (5.59) in (5.58)

$$\ddot{\theta} = N_a\mathcal{T} + N_b F_b + N_c\dot{\theta} + N_d\alpha^s + N_e V^s + N_f \tag{5.60}$$

$$\begin{aligned}
N_a&=\mathcal{M}^{-1}(I - \mathcal{B}_t^T G_a) \quad N_b = \mathcal{M}^{-1}(\mathcal{B}_b^T - \mathcal{B}_t^T G_b) \\
N_c&=-\mathcal{M}^{-1}(\mathcal{C} + \mathcal{B}_t^T G_c) \quad N_d = -\mathcal{M}^{-1}(\mathcal{L}_a + \mathcal{B}_t^T G_d) \\
N_e&=-\mathcal{M}^{-1}(\mathcal{L}_b + \mathcal{B}_t^T G_e) \quad N_f = -\mathcal{M}^{-1}(\mathcal{D} + \mathcal{B}_t^T G_f)
\end{aligned}$$

Assigning $B(F_b, \alpha_s, V_s) = N_b F_b + N_d \alpha_s + N_e V_s + N_f$

$$\ddot{\theta} = N_a\mathcal{T} + N_c\dot{\theta} + B$$

Now, let us separate the joint variables subject to dynamic effect of suspension mechanism from the others. To do that, we first reorder the equations.

$$S^b\ddot{\theta} = S^b N_a S^{b^{-1}} S^b \mathcal{T} + S^b N_c S^{b^{-1}} S^b \dot{\theta} + S^b B$$

Here, S^b is obtained by rearranging the rows of a 54×54 identity matrix. Separation is done as follows:

$$\begin{aligned}
S^b\ddot{\theta} &= \begin{bmatrix} \ddot{\theta}^{\text{susp}} \\ \ddot{\theta}^{\text{nosusp}} \end{bmatrix} & S^b\dot{\theta} &= \begin{bmatrix} \dot{\theta}^{\text{susp}} \\ \dot{\theta}^{\text{nosusp}} \end{bmatrix} \\
S^b N_a S^{b^{-1}} &= \begin{bmatrix} N_{a_1} & N_{a_2} \\ N_{a_3} & N_{a_4} \end{bmatrix} & S^b N_c S^{b^{-1}} &= \begin{bmatrix} N_{c_1} & N_{c_2} \\ N_{c_3} & N_{c_4} \end{bmatrix} \\
S^b\mathcal{T} &= \begin{bmatrix} \mathcal{T}^{\text{susp}} \\ \mathcal{T}^{\text{nosusp}} \end{bmatrix} & S^b B &= \begin{bmatrix} B^{\text{susp}} \\ B^{\text{nosusp}} \end{bmatrix}
\end{aligned}$$

Suspension dynamics equation is

$$M^{\text{susp}}\ddot{\theta}^{\text{susp}} = -d\,\dot{\theta}^{\text{susp}} - k\,\theta^{\text{susp}} \tag{5.61}$$

where d and k are damper and spring constants respectively.

$$\begin{aligned}
\begin{bmatrix} \ddot{\theta}^{\text{susp}} \\ \ddot{\theta}^{\text{nosusp}} \end{bmatrix} = &\begin{bmatrix} N_{a_2} \\ N_{a_4} \end{bmatrix} \mathcal{T}^{\text{nosusp}} + \begin{bmatrix} B^{\text{susp}} \\ B^{\text{nosusp}} \end{bmatrix} + \\
&\begin{bmatrix} -N_{a_1} d + N_{c_1} & N_{c_2} \\ -N_{a_3} d + N_{c_3} & N_{c_4} \end{bmatrix} \begin{bmatrix} \dot{\theta}^{\text{susp}} \\ \dot{\theta}^{\text{nosusp}} \end{bmatrix} + \\
&\begin{bmatrix} -N_{a_1} k & 0 \\ -N_{a_3} k & 0 \end{bmatrix} \begin{bmatrix} \theta^{\text{susp}} \\ \theta^{\text{nosusp}} \end{bmatrix}
\end{aligned} \tag{5.62}$$

Let the following be defined as:

$$P_a = S^{b^{-1}} \begin{bmatrix} N_{a_2} \\ N_{a_4} \end{bmatrix} \qquad P_c = S^{b^{-1}} \begin{bmatrix} N_{a_1} k & 0 \\ N_{a_3} k & 0 \end{bmatrix} S^b$$

$$P_b = S^{b^{-1}} \begin{bmatrix} N_{a_1} d + N_{c_1} & N_{c_2} \\ N_{a_3} d + N_{c_3} & N_{c_4} \end{bmatrix} S^b$$

Now, the equation of motion can be modified to include suspension dynamics.

$$\ddot{\theta} = P_a \mathcal{T}^{\text{nosusp}} + P_b \dot{\theta} + P_c \theta + B \tag{5.63}$$

Let S^c, and S^d be sorting matrices.

$$S^c\ddot{\theta} = S^c P_a S^{d^{-1}} S^d \mathcal{T}^{\text{nosusp}} + S^c P_b S^{c^{-1}} S^c \dot{\theta} + S^c P_c S^{c^{-1}} S^c \theta + S^c B$$

$$\begin{bmatrix} \ddot{\theta}^{\text{pseudo}} \\ \ddot{\theta}^{\text{true}} \end{bmatrix} = \begin{bmatrix} P_{a_1} & P_{a_2} \\ P_{a_3} & P_{a_4} \end{bmatrix} \begin{bmatrix} \mathcal{T}^{\text{pseudo}} \\ \mathcal{T}^{\text{nosusp\_true}} \end{bmatrix} + \begin{bmatrix} P_{b_1} & P_{b_2} \\ P_{b_3} & P_{b_4} \end{bmatrix} \begin{bmatrix} \dot{\theta}^{\text{pseudo}} \\ \dot{\theta}^{\text{true}} \end{bmatrix} + \begin{bmatrix} P_{c_1} & P_{c_2} \\ P_{c_3} & P_{c_4} \end{bmatrix} \begin{bmatrix} \theta^{\text{pseudo}} \\ \theta^{\text{true}} \end{bmatrix} + \begin{bmatrix} B^{\text{pseudo}} \\ B^{\text{true}} \end{bmatrix} \tag{5.64}$$

By definition $\ddot{\theta}^{\text{pseudo}} = 0$, $\dot{\theta}^{\text{pseudo}} = 0$, $\theta^{\text{pseudo}} = 0$

$$\mathcal{T}^{\text{pseudo}} = -P_{a_1}^{-1}(P_{a_2}\mathcal{T}^{\text{nosusp\_true}} + P_{b_2}\dot{\theta}^{\text{true}} + P_{c_2}\theta^{\text{true}} + B^{\text{pseudo}})$$

Including pseudo joint torques in the equation of motion, we get:

$$\ddot{\theta}^{\text{true}} = Y_a \mathcal{T}^{\text{nosusp\_true}} + Y_b \dot{\theta}^{\text{true}} + Y_c \theta^{\text{ true}} + Y_d \tag{5.65}$$

$$\begin{aligned} Y_a &= P_{a_4} - P_{a_3} P_{a_1}^{-1} P_{a_2} & Y_b &= P_{b_4} - P_{a_3} P_{a_1}^{-1} P_{b_2} \\ Y_c &= P_{c_4} - P_{a_3} P_{a_1}^{-1} P_{c_2} & Y_d &= B^{\text{true}} - P_{a_3} P_{a_1}^{-1} B^{\text{pseudo}} \end{aligned}$$

Let us write (5.65) in the form of first order ODE:

$$\begin{bmatrix} \ddot{\theta}^{\text{true}} \\ \dot{\theta}^{\text{true}} \end{bmatrix} = \begin{bmatrix} Y_b & Y_c \\ I & 0 \end{bmatrix} \begin{bmatrix} \dot{\theta}^{\text{true}} \\ \theta^{\text{true}} \end{bmatrix} + \begin{bmatrix} Y_a \mathcal{T}^{\text{nosusp\_true}} + Y_d \\ 0 \end{bmatrix} \tag{5.66}$$

Simulation results associated with this system can be found in [64].

5.5 Discussion

Both theory and application has been presented in this chapter. It utilized the theoretical foundations established in the previous chapter, and applied them in practical cases. The selection of these cases were done so that the complex system dynamical modeling is demonstrated without making it too complicated for the reader to follow. The simulation results are in the appendices.

6. CONCLUDING REMARKS

The research presented in this thesis provides the tools necessary for the analysis of complex topology system dynamics and concentrates on the development of a framework for the dynamical modeling of wheeled ground vehicles. The contributions were in the fields of cooperating underactuated systems, kinematically deficient cooperating manipulators and the nonholonomic systems as well as mass matrix factorization and inversion techniques. Although they may seem to be distinct areas, they are, in fact, the significant players under one umbrella; multibody dynamics. Therefore, to understand how these areas all fit together is essential for evaluating the paramount importance of this work. Vehicle dynamical simulation can be a good example to see that each aforementioned field constitutes as an ingredient of an algorithm for high fidelity and hight efficiency.

We conclude this dissertation with a summary of the work together with proposals for problems suggesting future research.

6.1 Summary

The focus of this dissertation was the development of dynamical modeling algorithm capable of handling complex topology systems. Considerable efforts have been made to apply the presented methodology to wheeled ground vehicles with the goal of achieving high fidelity simulations while attaining high performance. To achieve this outcome, we first started with unconstrained problems for the sake of simplicity from the reader's point of view. Then we moved to cooperating manipulator dynamics and included the base dynamics as a free-flying platform. There were two important cases which we addressed in detail; 1) The case when there are unactuated joints in the system forming a closed kinematic chain where the number of actuators are less then the number of DOF of the system. 2) The case which can be briefly stated as the singu-

larity issues. The jacobian is required to be a full rank matrix so that the tip forces of cooperating manipulators can be computed. If a manipulator is at a singularity, the jacobian looses rank and prevents the computation of tip forces, hence the dynamics. We introduced both a numerical and an analytical method to overcome this problem, and explained that analytical approach was superior to the numerical one. With the mass matrix factorization and inversion in $\mathcal{O}(n)$ and the application of the algorithm to nonholonomic systems made it a complete tool for complex topology systems.

A complex topology systems, from our perspective, is regarded as a system composed of multiple "*arms*" treated as if they were robotic arms. For example a bicycle can very well be considered as a cooperating manipulator if each wheel is regarded as a manipulator subject to nonholonomic constraint. To be able to compute the traction forces between the wheel and the terrain and even perform a stress analysis on the spokes of the wheel motivated us. These traction forces are crucial for roll-over estimation and, therefore, to compute them has a major value.

Application of the algorithm to an example underactuated system was demonstrated with simulation results. Two wheeled cart, and four wheel steered and driven (4x4x4) system were the next case studies. Finally the full dynamical model of a passenger vehicle was shown.

6.2 Future Directions

Trucking industry can gain substantial economic benefits through use of larger trucks, there has been rapidly growing interest in using multitrailer vehicles to obtain higher cargo volume while retaining the practical benefit of good maneuverability. On the other hand, multitrailer vehicles are known to suffer from special dynamic characteristics that can limit their stability and emergency maneuverability.

This dynamic characteristic leads a concern over the potential for degradation of the safety quality of highways. Some noted problems are reduced yaw stability and susceptibility to roll-over in steady turn, slower response and possible instability during braking, reduced level of sensory feedback of trailer conditions, off tracking, amplified trailer response to rapid steering, and oscillatory sway due to road disturbances. In addition to these problems, due to their isolation in the cabin, most drivers of such

vehicles do not receive early sensory feedback of imminent roll-over.

This research can be extended as the basis of the development of a framework for the control of multitrailer vehicles. Establishing the feasibility of providing the drivers of articulated vehicles with information on the roll stability of their trailer can be the goal of such work.

In this regard, the developed algorithm can be applied, for example, to a triple-trailer-tractor vehicle to obtain highly accurate analytical dynamical model on any given terrain. To give an idea, this system would consist of 166 joints with 48 independent degrees of freedom in total. Given the steering torque, driving torque and terrain structure, the forward dynamics algorithm obtains the velocities, the accelerations, the forces and torques of all joints. Among these, contact forces between tires and the road can be used to prevent roll-over by adjusting the speed. Tire slip in both longitudinal and lateral directions and frictional characteristic of terrain [65] can be included in the model.

LITERATURE CITED

[1] **Rodriguez, G.**, **Jain, A.**, **and Kreutz, K.**, 1992. Spatial operator algebra for multibody systems dynamics, *The Journal of the Astronautical Sciences*, **40,** 27–50.

[2] **Armstrong, W. W.**, 1979. Recursive solutions to the equations of motion of an n-link manipulator, In *Proceedings of the Fifth World Congress on the Theory of Machines and Mechanisms*, Montreal, pp. 1342–1346.

[3] **Walker, M. W. and Orin, D. E.**, 1982. Efficient dynamic computer simulation of robotic mechanisms, *Journal of Dynamics System Measurement and Control*, **104,** 205–211.

[4] **Kane, T. R. and Wang, C. F.**, 1965. On the derivation of equations of motion, *J. Soc. Indust. Appl. Math.*, **13,** 487–492.

[5] **Kane, T. R. and Levinson, D. A.**, 1985. *Dynamics: Theory and Applications.* McGraw-Hill, New York.

[6] **Rosenthal, Dan E.**, 1990. An order *n* formulation for robotic systems, *The Journal of the Astronautical Sciences*, **38,** 511–529.

[7] **Anderson, K. S.**, 1992. An order *n* formulation for the motion simulation of general multi-rigid-body constrained systems, *Computers & Structures*, **43,** 565–579.

[8] **Lotstedt, P.**, 1979. On a penalty function method for the simulation of mechanical systems subject to constraints Technical Report TRITA-NA-7919, Royal Institute of Techology, Stockholm.

[9] **Baumgarte, J.**, 1972. Stabilization of constraint and integrals of motion in dynamical systems, *Comp. Meth. Applied Mechanical Engineering*, **1,** 1–16.

[10] **Park, K. C. and Chiou, J. C.**, 1988. Stabilization of computational procedures for constrained dynamical systems, *Journal of Guidance*, **11,** 365–370.

[11] **Kalantzis, S.**, **Modi, V. J.**, **Pradhan, S.**, **and Misra, A. K.**, 1998. Order-n formulation and dynamics of multibody tethered systems, *Journal of Guidance, Control, and Dynamics*, **21,** 277–285.

[12] **Keat, J. E.**, 1990. Multibody system order*n* dynamics formulation based on velocity transform method, *Journal of Guidance*, **13,** 207–212.

[13] **Subudhi, B. and S., Morris A.**, 2002. Dynamic modelling, simulation and control of a manipulator with flexible links and joints, *Robotics and Autonomous Systems*, **41,** 257–270.

[14] **Menini, L.**, **Tornambè, A.**, **and Zaccarian, L.**, 1998. Modelling and control of an under-actuated closed kinematic chain, *IEE Proceedings on Control Theory and Applications*, **145,** 1–8.

[15] **Nakamura, Y. and Ghodoussi, M.**, 1989. Dynamics computation of closed-link robot mechanisms with nonredundant and redundant actuators, *IEEE Transactions on Robotics and Automation*, **5,** 294–302.

[16] **Featherstone, R.**, 1983. The calculation of robot dynamics using articulated-body inertias, *The International Journal of Robotics Research*, **2,** 13–30.

[17] **Bae, D. S. and Haug, E. J.**, 1987. A recursive formation for constrained mechanical system dynamics: Part I, Open loop systems, *Mechanisms, Structures, and Machines*, **15,** 359–382.

[18] **Bae, D. S. and Haug, E. J.**, 1987. A recursive formation for constrained mechanical system dynamics: Part II, Closed loop systems, *Mechanisms, Structures, and Machines*, **15,** 481–506.

[19] **Anderson, K. S. and Critchley, J. H.**, 2003. Improved order-n performance algorithm for the simulation of constrained multi-rigid-body systems, *Multibody Systems Dynamics*, **9,** 185–212.

[20] **Vereshchagin, A. F.**, 1974. Computer simulation of the dynamics of complicated mechanisms of robot-manipulators, *Engineering Cybernetics*, **12,** 65–70.

[21] **Jain, A.**, 1991. Unified formulation of dynamics for serial rigid multibody systems, *Journal of Guidance*, **14,** 531–542.

[22] **Ball, R. S.**, 1900. *A Treatise on the Theory of Screws* Cambridge University Press, London.

[23] **Rodriguez, G.**, 1987. Kalman filtering, smoothing and recursive robot arm forward and inverse dynamics, *IEEE Journal of Robotics and Automation*, **3,** .

[24] **Rodriguez, G.**, 1989. Recursive forward dynamics for multiple robot arms moving a common task object, *IEEE Transactions on Robotics and Automation*, **5,** .

[25] **Rodriguez, G.**, 1990. Random field estimation approach to robot dynamics, *IEEE Transactions on Systems, Man, and Cybernetics*, **20,** 1081–1093.

[26] **Rodriguez, G.**, **Kreutz-Delgado, K.**, **and Jain, A.**, 1991. Spatial operator algebra for manipulator modeling and control, *International Journal of Robotics Research*, **10,** 371–381.

[27] **Jain, A. and Rodriguez, G.**, 1992. Recursive flexible multibody system dynamics using spatial operators, *Journal of Guidance, Control and Dynamics*, **15,** 1453–1466.

[28] **Jain, A. and Rodriguez, G.**, 1993. Linearization of manipulator dynamics using spatial operators, *IEEE Transactions on Systems, Man, and Cybernetics*, **23,** 239–248.

[29] **Jain, A.**, **Vaidehi, N.**, **and Rodriguez, G.**, 1993. A fast recursive algorithm for molecular dynamics simulation, *Journal of Computational Physics*, **106,** 258–268.

[30] **Jain, A. and Rodriguez, G.**, 1993. An analysis of the kinematics and dynamics of under-actuated manipulators, *IEEE Transactions on Robotics and Automation*, **9,** 411–422.

[31] **Jain, A. and Rodriguez, G.**, 1999. Sensitivity analysis for multibody systems using spatial operators, In *International conference on scientific computation and differential equations*, Fraser Island, Queensland, Australia, August.

[32] **Yen, J. and Jain, A.**, 1999. Roams: Rover analysis modeling and simulation software, In *International symposium on artificial intelligence, robotics and automation in space (i-SAIRAS'99)*, Noordwijk, Netherlands, June.

[33] **Scherm, Norbert and Heimann, Bodo**, 2000. Dynamics and control of underactuated manipulation systems: A discrete-time approach, *Robotics and Autonomous Systems*, **30,** 237–248.

[34] **Liu, Y.**, **Xu, Y.**, **and Bergerman, M.**, 1999. Cooperation control of multiple manipulators with passive joints, *IEEE Transactions on Robotics and Automation*, **15,** 258–267.

[35] **Iannitti, S. and Lynch, K.M.**, 2004. Minimum control-switch motions for the snakeboard: A case study in kinematically controllable underactuated systems, *IEEE Transactions on Robotics*, **20,** 994–1006.

[36] **Westervelt, E. R.**, **Grizzle, J. W.**, **and Koditschek, D. E.**, 2003. Hybrid zero dynamics of planar biped walkers, *IEEE Transactions on Automatic Control*, **48,** 42–56.

[37] **Fantoni, I. and Lozano, R.**, 2002. *Non-linear Control for Underactuated Mechanical Systems* Springer.

[38] **Ortega, R.**, **Spong, M.**, **Gomez-Estern, F.**, **and G., Blankenstein**, 2002. Stabilization of a class of underactuated mechanical systems via interconnection and damping assignment, *IEEE Transactions on Automatic Control*, **47,** 1218–1233.

[39] **Bruyninckx, H. and O., Khatib**, 2000. Gauss' priciple and the dynamics of redundant and constrained manipulators, In *Proceedings of the IEEE International Conference on Robotics & Automation*, San Francisco, CA, pp. 2563–2568.

[40] **Abdel-Malek, K.**, **Yeh, H.**, **and Khairallah, N.**, 1999. Workspace, void, and volume determination of the general 5dof manipulator, *Mechanics of Structures and Machines*, **27,** 91–117.

[41] **Prattichizzo, D. and Bicchi, A.**, 1996. Specifying consistent control goals for kinematically defective manipulation systems, In *Proceedings of the IEEE International Conference on Robotics and Automation*, Mineapolis, MN, USA, pp. 3532–3537.

[42] **Funda, J.**, **Taylor, R.**, **Eldridge, B.**, **Gomory, S.**, **and Gruben, K.**, 1996. Constrained cartesian motion control for teleoperated surgical robots, *IEEE Transactions on Robotics and Automation*, **12,** 453–465.

[43] **Rico, J.M.**, **Aguilera, L.D.**, **Gallardo, J.**, **Rodriguez, R.**, **Orozco, H.**, **and Barrera, J.M.**, 2006. A more general mobility criterion for parallel platforms, *Journal of Mechanical Design*, **128,** 207–219.

[44] **Hertz, H.**, 1894. *Die Prinzipien der Mechanik in neuem Zusammenhange dargestellt* Gesamelte Werke, Band III. Barth, Leipzig.

[45] **Hamel, G.**, 1949. *Theoretische Mechanik : Eine einheitliche Einführung in die gesamte Mechanik* Springer-Verlag, Berlin.

[46] **Kane, T. R.**, 1961. Dynamics of nonholonomic systems, *ASME Journal of Applied Mechanics*, **28,** 574–578.

[47] **Saha, S. and Angeles, J.**, 1991. Dynamics of nonholonomic mechanical using a natural orthogonal complement, *ASME Journal of Applied Mechanics*, **58,** 238–243.

[48] **Deo, A. S. and Walker, I. D.**, 1996. Dynamics and control of multiple cooperating manipulators with rolling contacts, *Journal of Robotic Systems*, **13,** 619–648.

[49] **Albagul, A. and Wahyudi**, 2004. Dynamic modelling and adaptive traction control for mobile robots, *International Journal of Advanced Robotic Systems*, **1,** 149–154.

[50] **Kim, W.**, **Choi, K.**, **and Yi, B.**, 2004. A mobility analysis method of closed-chain mechanisms with over-constraints and non-holonomic constraints, In *Proceedings of the international conference on robotics & automation (ICRA)*, New Orleans, LA, USA, pp. 2801–2807.

[51] **Sorensen, M. J.**, 2005. *Feedback Control of a Class of Nonholonomic Hamiltonian Systems* PhD thesis, Aalborg University, Denmark.

[52] **Spong, Mark W.**, **Hutchinson, S.**, **and Vidyasagar, M.**, 2006. *Robot Modeling and Control* John Willey & Sons.

[53] **Murray, R. M.**, **Li, Z.**, **and Sastry, S. S.**, 1994. *A Mathematical Introduction to Robotic Manipulation* CRC Press.

[54] **Sciavicco, L. and Siciliano, B.**, 2001. *Modelling and Control of Robot Manipulators* Springer, 2nd edition.

[55] **Craig, J. J.**, 2003. *Introduction to Robotics : Mechanics and Control* Prentice Hall, 3rd edition.

[56] **Lilly, K. W.**, 1993. *Efficient Dynamic Simulation of Robotic Mechanisms* Kluwer Academic Publishers.

[57] **Brogan, W.**, 1991. *Modern Control Theory* Prentice Hall, New Jersey.

[58] **Nakamura, Y.**, 1991. *Advanced Robotics Redundancy and Optimization* Addison-Wesley Publishing Company.

[59] **Bloch, A.**, 2003. *Nonholonomic Mechanics and Control* Springer.

[60] **Holmberg, R. and Khatib, O.**, 2000. Development and control of a holonomic mobile robot for mobile manipulation tasks, *International Journal of Robotics Research*, **19,** 1066–1074.

[61] **Venture, G.**, **Ripert, P.**, **Khalil, W.**, **Gautier, M.**, **and Bodson, P.**, 2006. Modeling and identification of passenger car dynamics using robotics formalism, *IEEE Transactions on Intelligent Transportation Systems*, **7,** 349–359.

[62] **Gurol, B.**, **Dal, M.**, **Yesiloglu, S. M.**, **and Temeltas, H.**, 2007. Mechanical and electrical design of a four-wheel-drive, four-wheel-steer mobile manipulator with pa-10 arm, In *IEEE International Electric Machines and Drives Conference*, Antalya, Turkey, May.

[63] **Captain, K. M.**, **Boghani, A. B.**, **and Wormley, D.N.**, 1979. Analytical tire models for dynamic vehicle simulation, *Vehicle System Dynamics.*, **8,** 1–32.

[64] **Yesiloglu, S. M. and Temeltas, H.**, 2006. Dynamic modeling of four-wheel full-suspension vehicle, In *Proceedings of the 8th International IFAC Symposium on Robot Control (SYROCO)*, Santa Cristina Convent, Italy, September.

[65] **Gustafsson, F.**, 1997. Slip-based tire-road friction estimation, *Automatica*, **33,** 1087–1099.

A. SIMULATION RESULTS: GENERAL UNDERACTUATED COOPERATING MANIPULATORS IN SPACE MANIPULATION

Using the methodology presented in Chapter 5.1, the system was simulated using MATLAB on a Pentium 4 computer. Torques are applied at the second joint of arm 1 and at the third joint of arm 2 in the form of a ramp function for five seconds as shown in Figure A.1 and then the system is let to swing by its own on a free flying platform in 2D without gravity.

A.1 Results

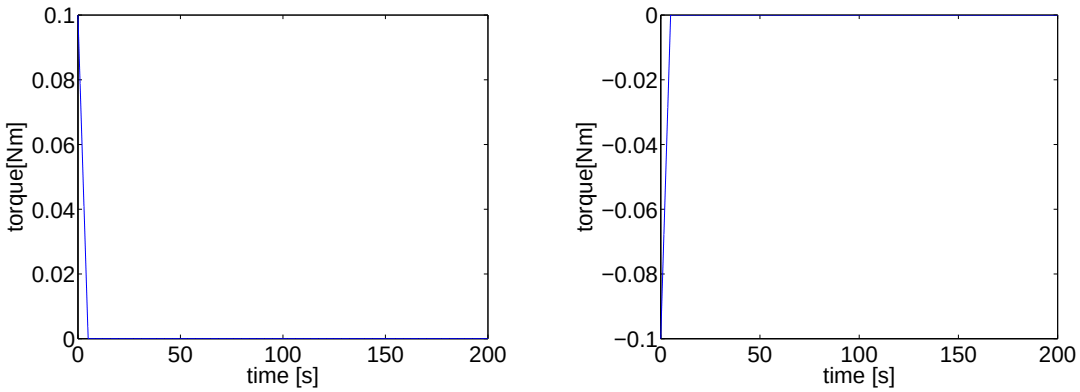

(a) t = 5s (b) t = 15s

Figure A.1: Applied torques at the actuated joints

Under the applied torques shown in Figure A.1, the results are plotted for a total time period of 200s. Figure A.2 shows the joint angles, velocities and accelerations for arm 1 on the left and arm 2 on the right.

Next we look at the motion of the platform. Plots on the top row of Figure A.3 are for the platform angle, angular velocity and angular acceleration. The bottom row plots of the same figure are the position, linear velocity and the linear acceleration of the platform.

Interaction forces and torques with the common load is presented in Figure A.4.

Figures A.5 through A.11 display the pictorial representation of the configuration of the system in 5 seconds intervals.

To contribute to the understanding of the numerical stability of the algorithm, the condition number of Jacobian which is defined as the ratio of the largest singular value of Jacobian matrix to the smallest one, is given in Figure A.12.

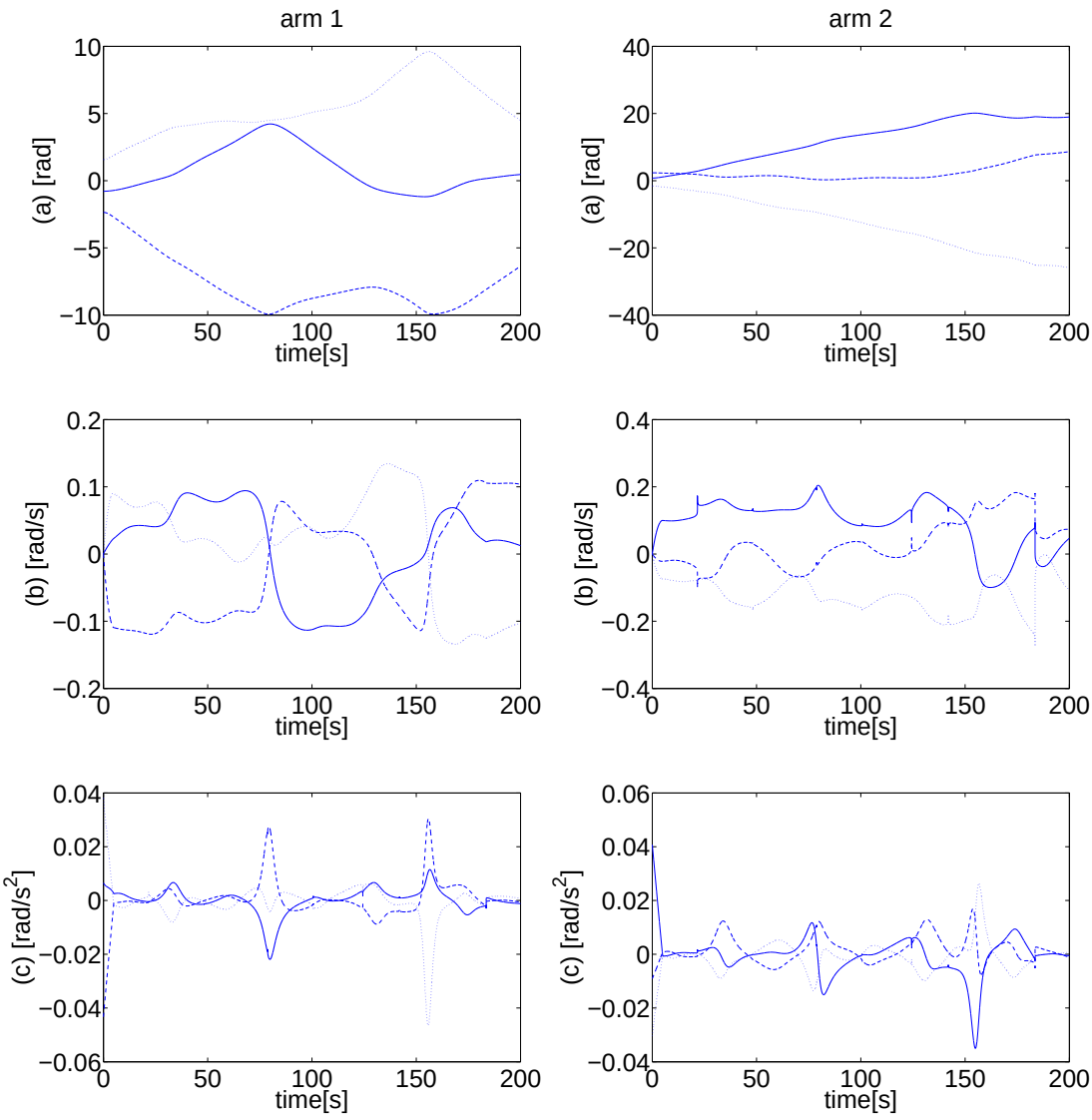

Figure A.2: Joint variables (the left column is for arm 1 and the right column is for arm 2): (a) joint angles, (b) joint velocities, (c) joint accelerations (solid lines are for x, dotted lines are for y and dashed lines are for z)

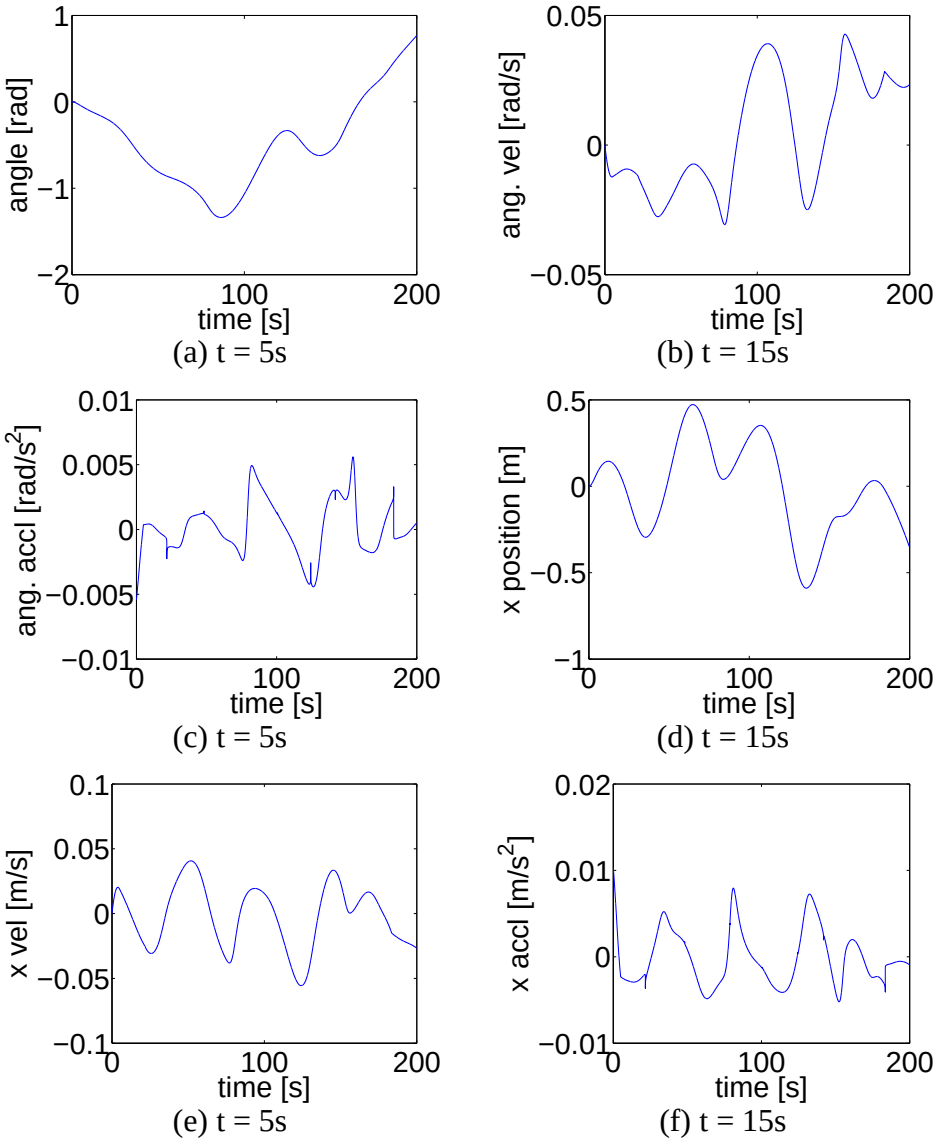

Figure A.3: Platform variables: (a) platform angle, (b)platform ang. vel, (c) platform ang. accl, (d) platform x position, (e) platform lin. x vel, (f) platform lin. x accl, (g) platform y position, (h) platform lin. y vel, (i) platform lin. y accl

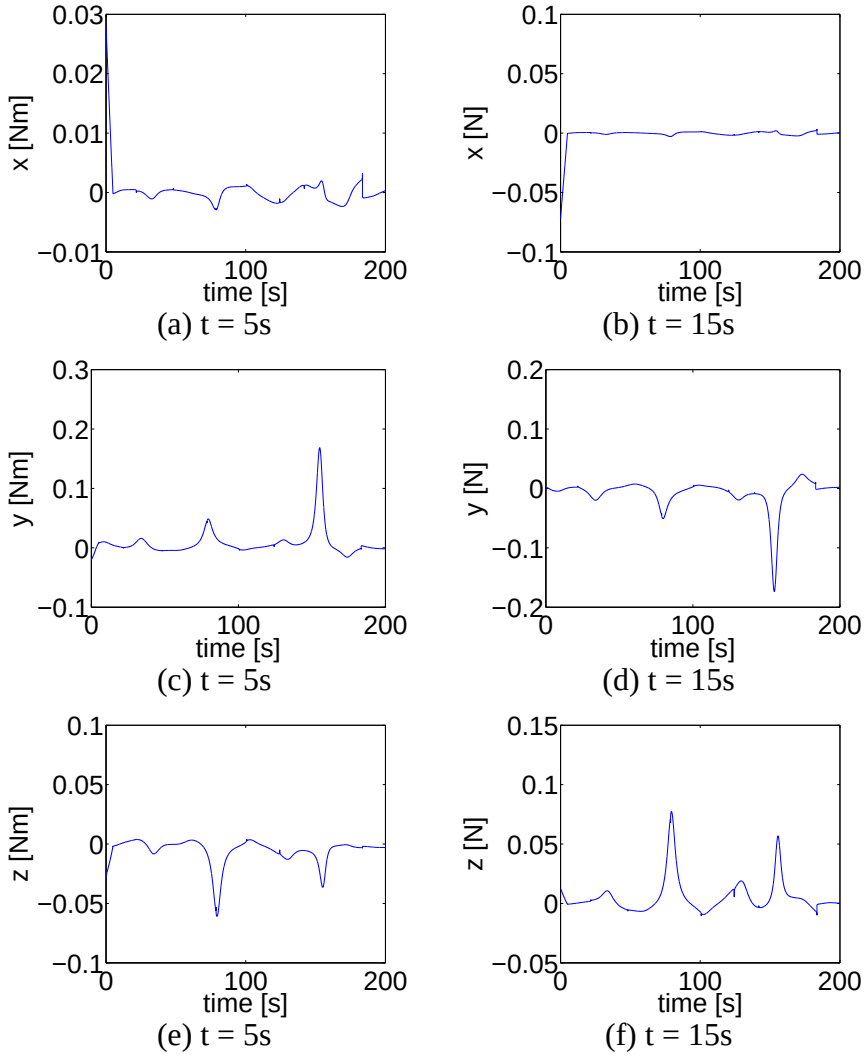

Figure A.4: Torques and forces on the common load

Figure A.5: Initial configuration

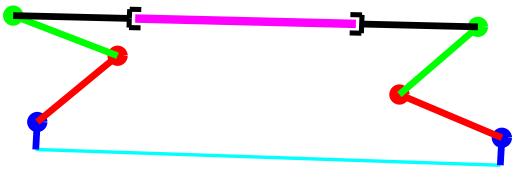

(a) t = 5s

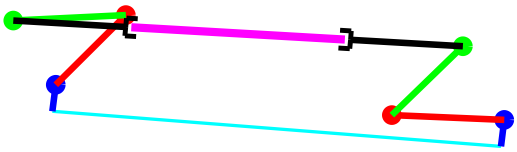

(b) t = 10s

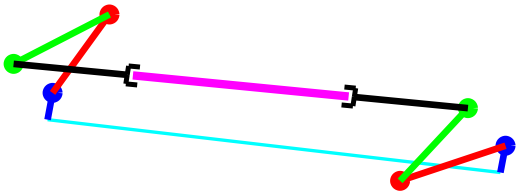

(c) t = 15s

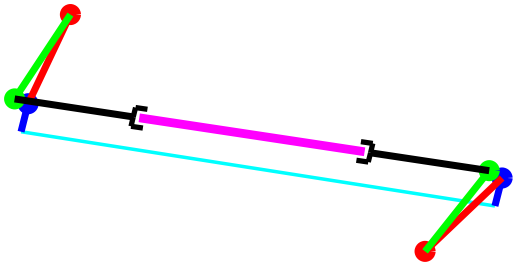

(d) t = 20s

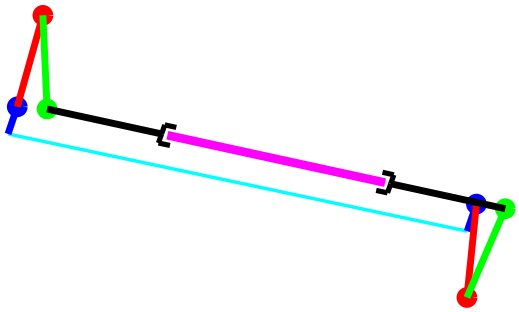

(e) t = 25s

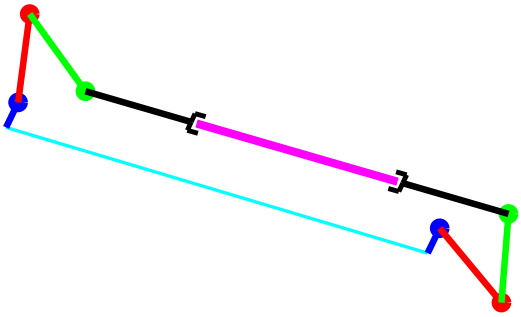

(f) t = 30s

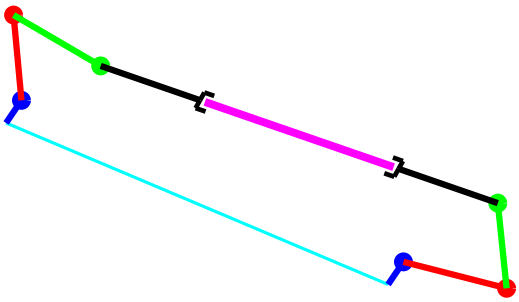

(g) t = 35s

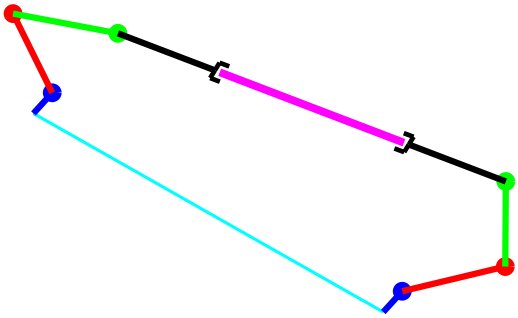

(h) t = 40s

Figure A.6: T = 5 - 40 s

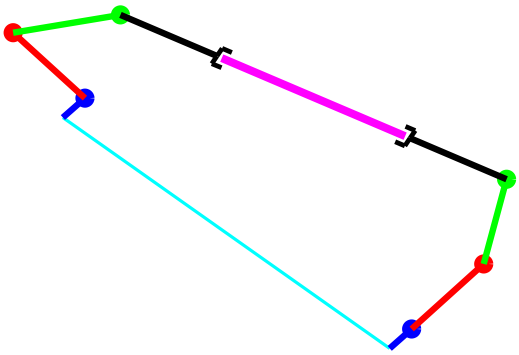

(a) t = 45s

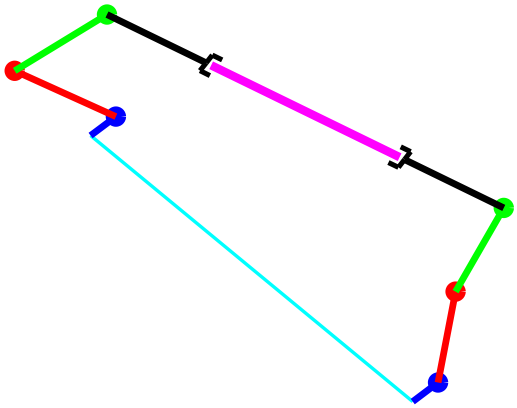

(b) t = 50s

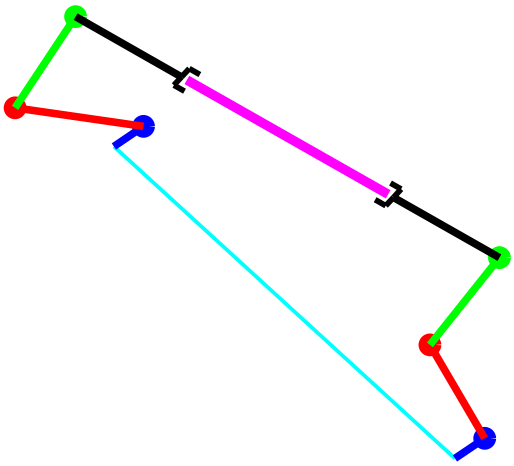

(c) t = 55s

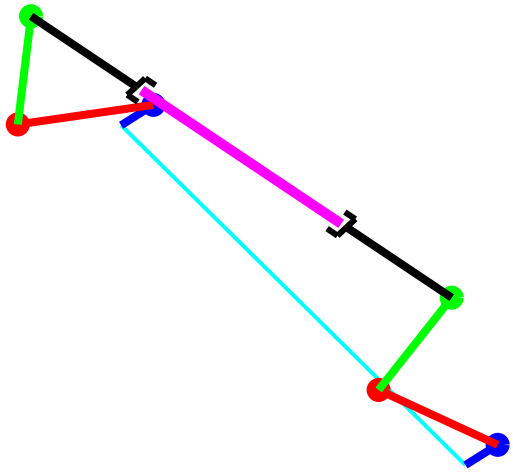

(d) t = 60s

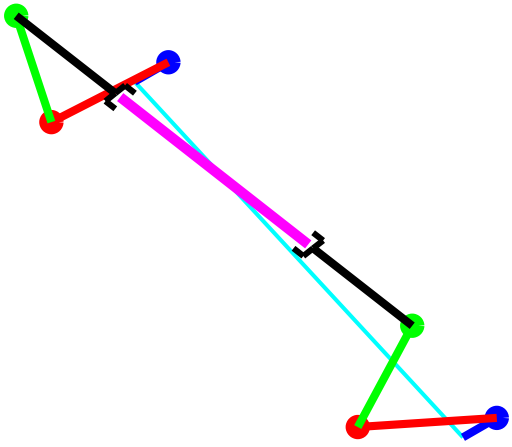

(e) t = 65s

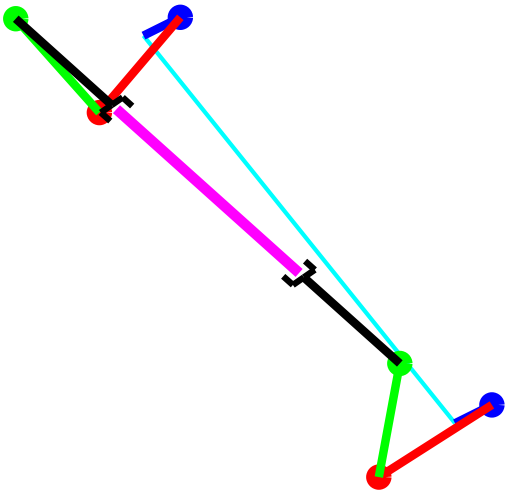

(f) t = 70s

Figure A.7: T = 45 - 70 s

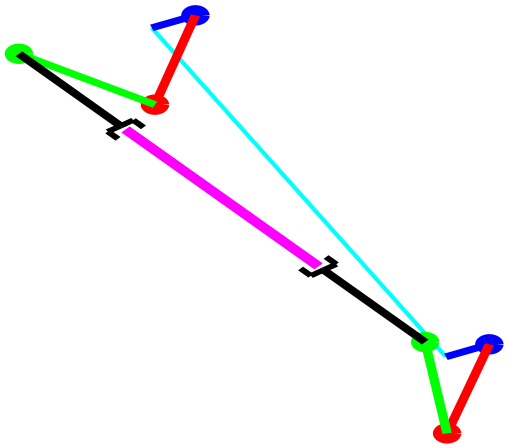

(a) t = 75s

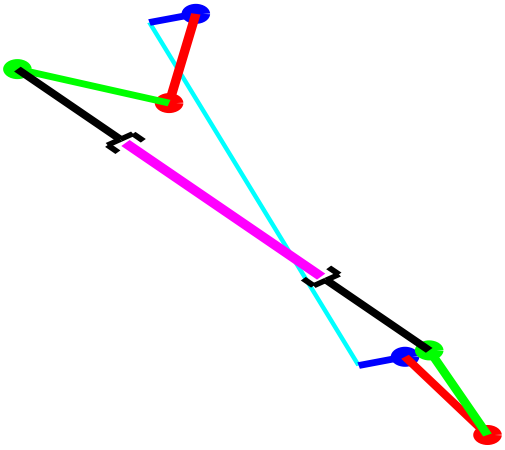

(b) t = 80s

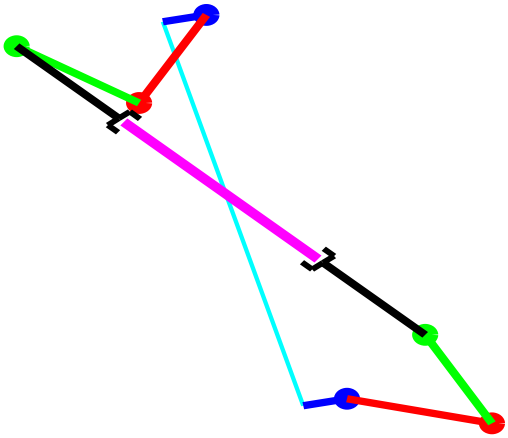

(c) t = 85s

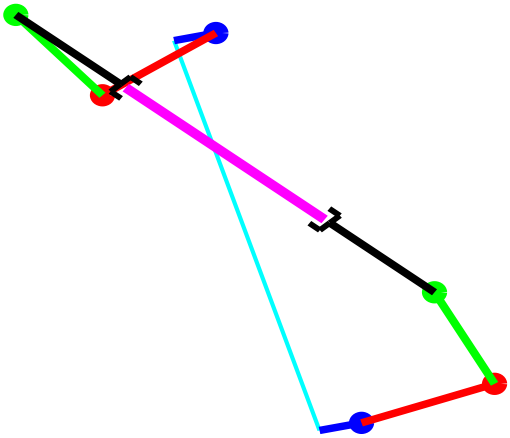

(d) t = 90s

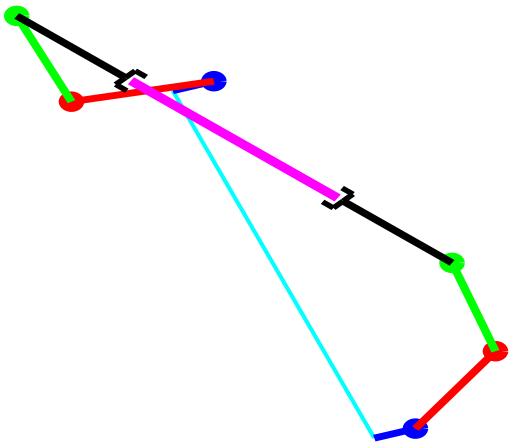

(e) t = 95s

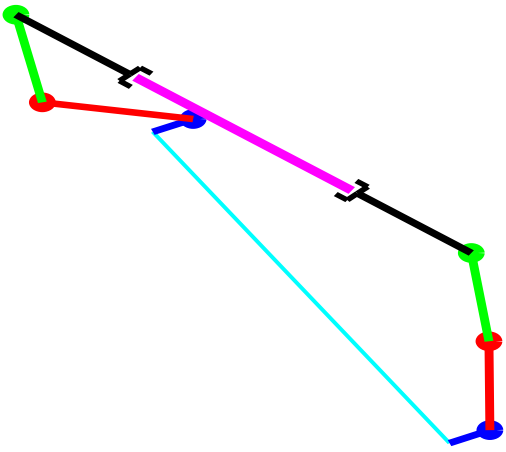

(f) t = 100s

Figure A.8: T = 75 - 100 s

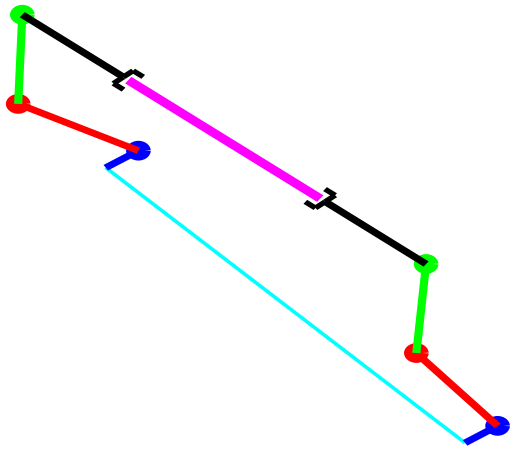

(a) t = 105s

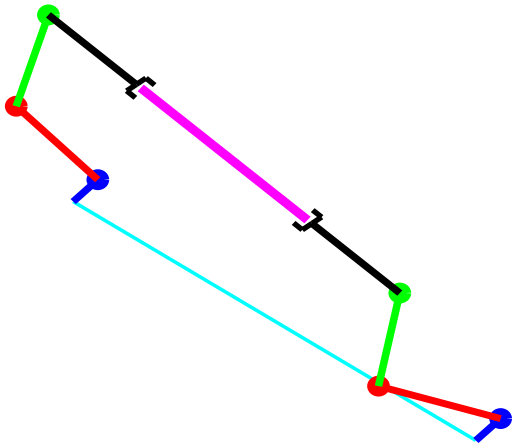

(b) t = 110s

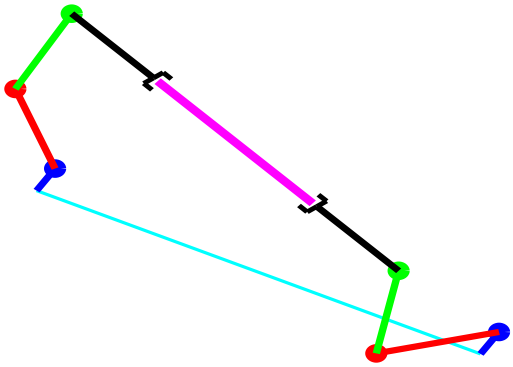

(c) t = 115s

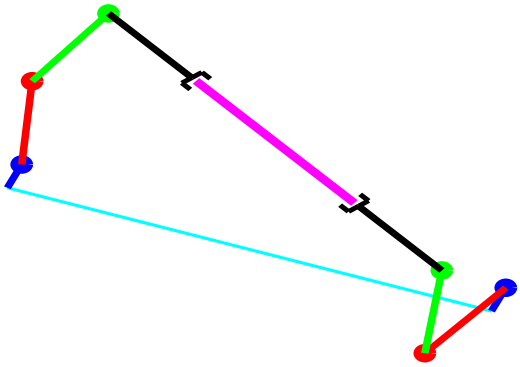

(d) t = 120s

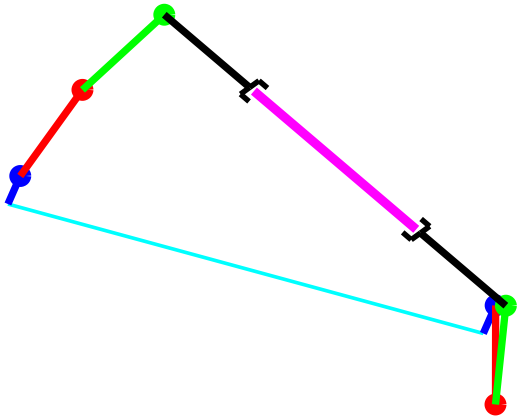

(e) t = 125s

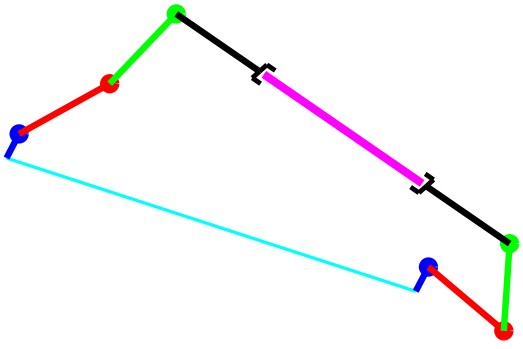

(f) t = 130s

Figure A.9: T = 105 - 130 s

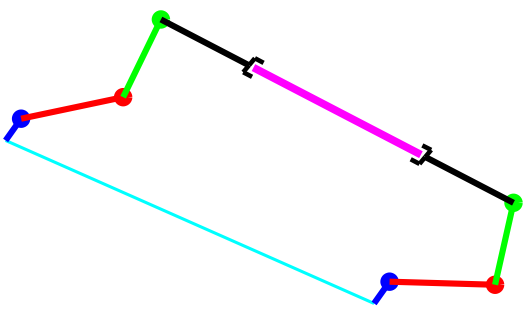

(a) t = 135s

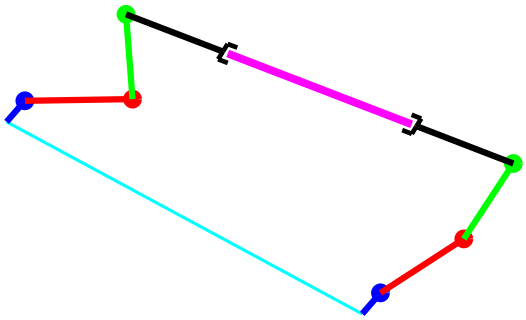

(b) t = 140s

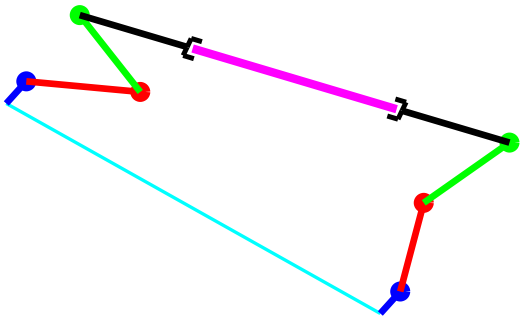

(c) t = 145s

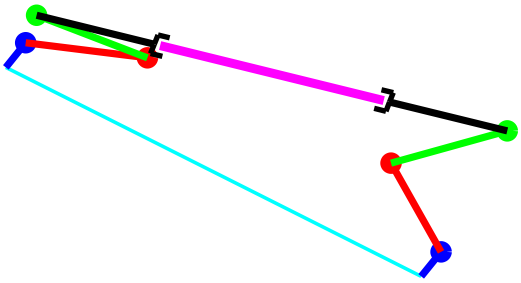

(d) t = 150s

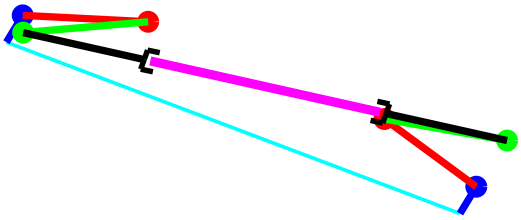

(e) t = 155s

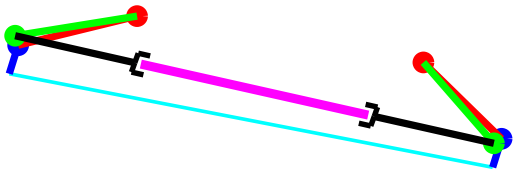

(f) t = 160s

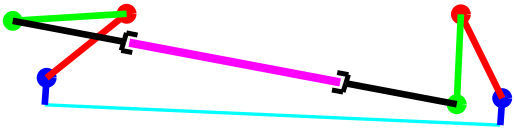

(g) t = 165s

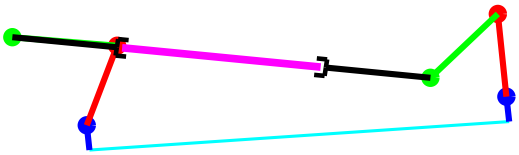

(h) t = 170s

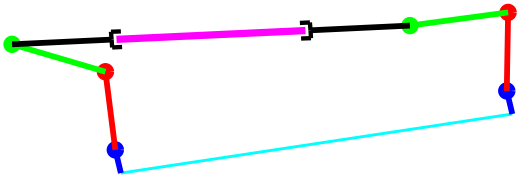

(g) t = 175s

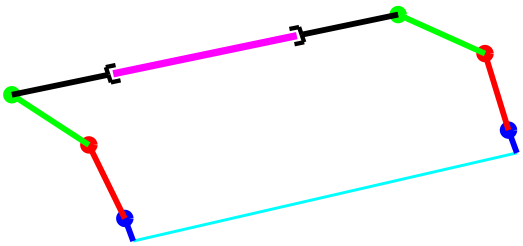

(h) t = 180s

Figure A.10: T = 135 - 180 s

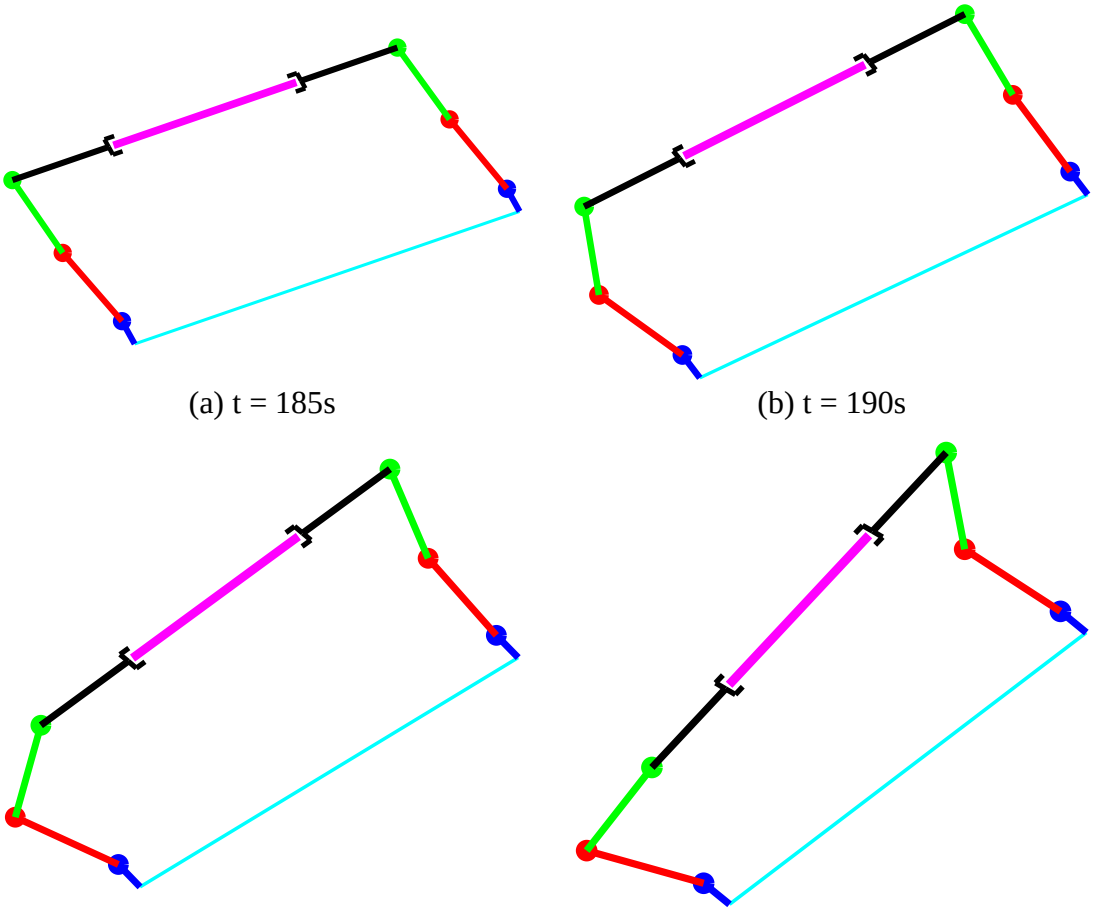

(a) t = 185s (b) t = 190s

(c) t = 195s (d) t = 200s

Figure A.11: T = 185 - 200 s

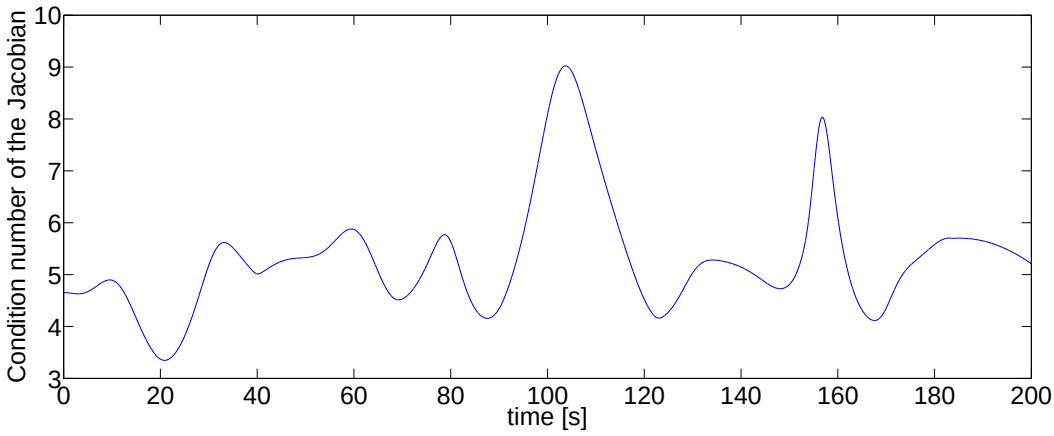

Figure A.12: The condition number of the $\mathcal{J}$

A.2 Conclusion

We have demonstrated the use of a dynamic algorithm for general underactuated cooperating manipulators. We utilized two planar arms each having 3 DOF. Only one joint is actuated at each arm. The results were displayed as both time charts and pictorial representation using MATLAB's visual environment.

B. SIMULATION RESULTS: TWO WHEELED CART

Using the methodology presented in Chapter 5.2, the system was simulated using MATLAB on a Pentium 4 computer. Although the simulation time can be made arbitrarily long, here we demonstrate 2 seconds of simulation time for the sake of simplicity in terms of the interprotation.

B.1 Results

Three cases were considered;

- going forward, where equal torques are applied to each wheel
- rotating around the center, where equal but opposite torques are applied
- rotating around off center, where different torques are applied

B.1.1 Going forward

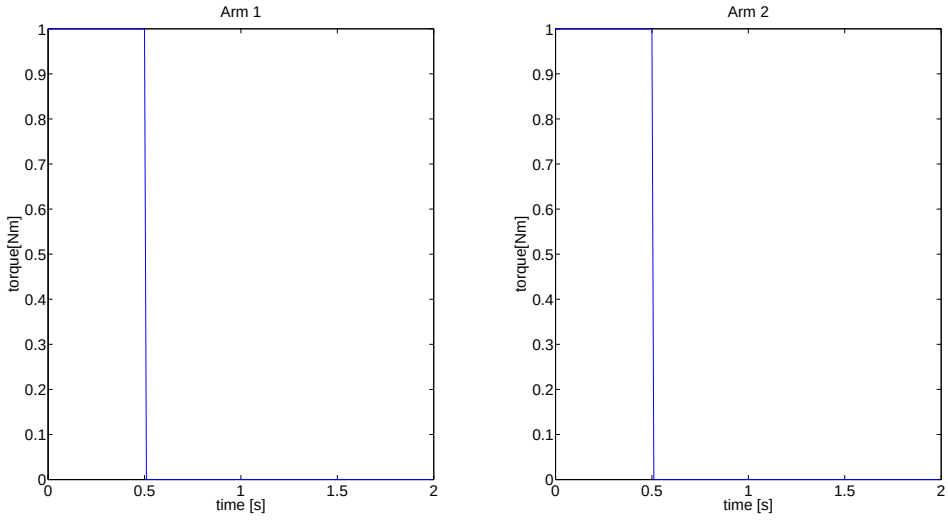

Figure B.1: Applied torques

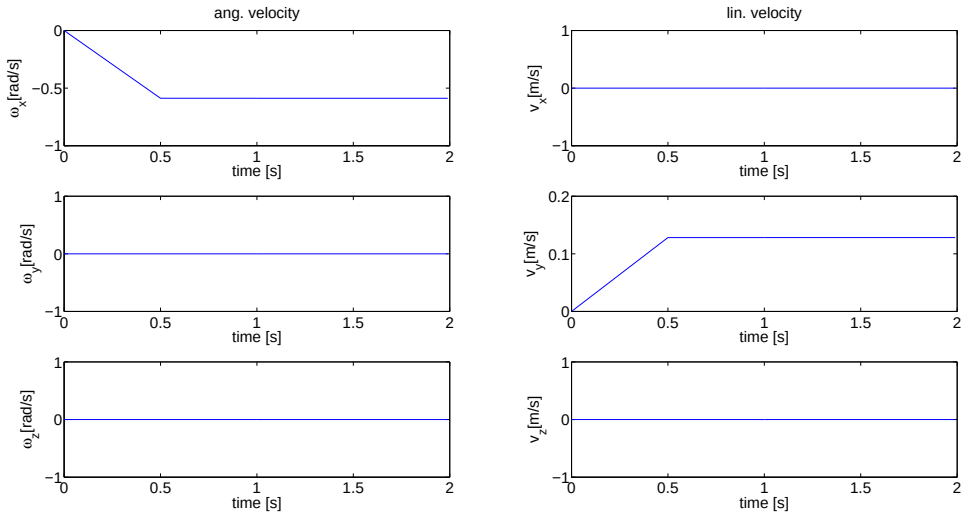

Figure B.2: Base velocities

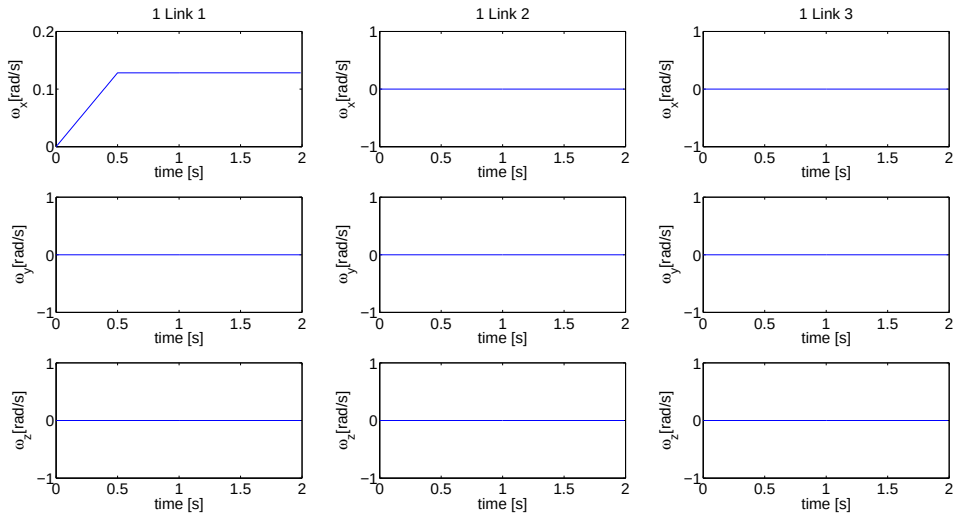

Figure B.3: Angular velocities of the links of Arm 1

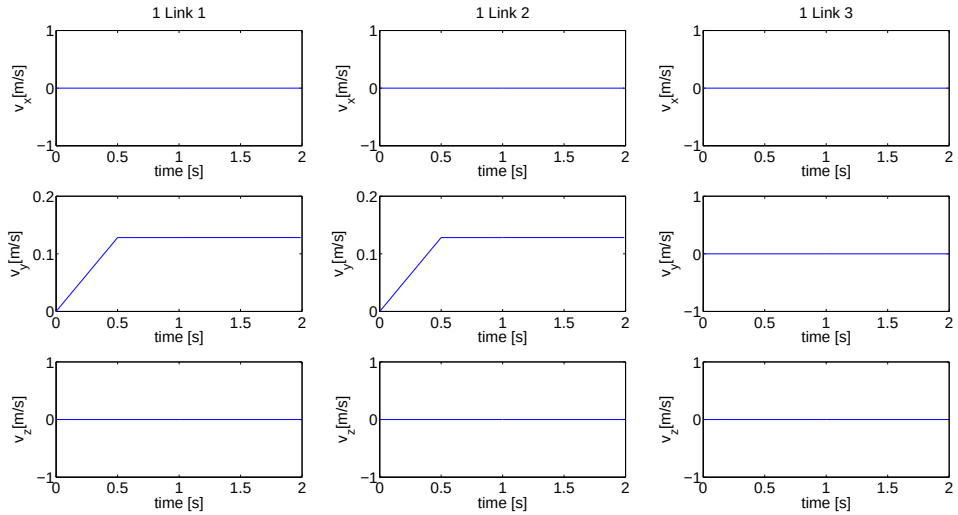

Figure B.4: Linear velocities of the links of Arm 1

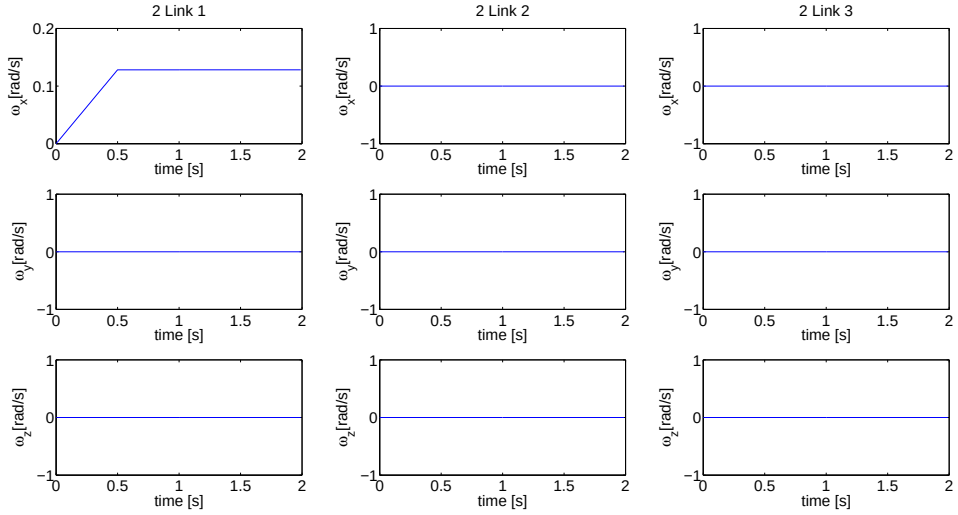

Figure B.5: Angular velocities of the links of Arm 2

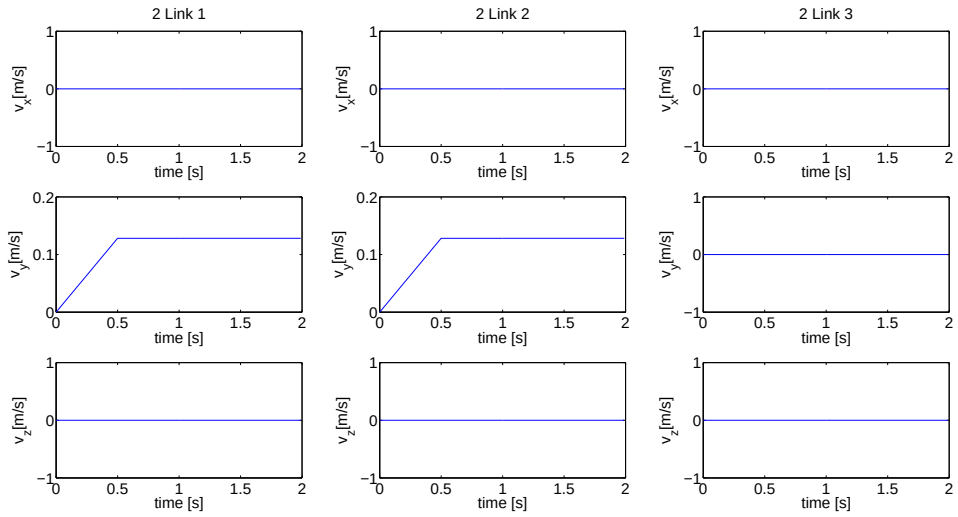

Figure B.6: Linear velocities of the links of Arm 2

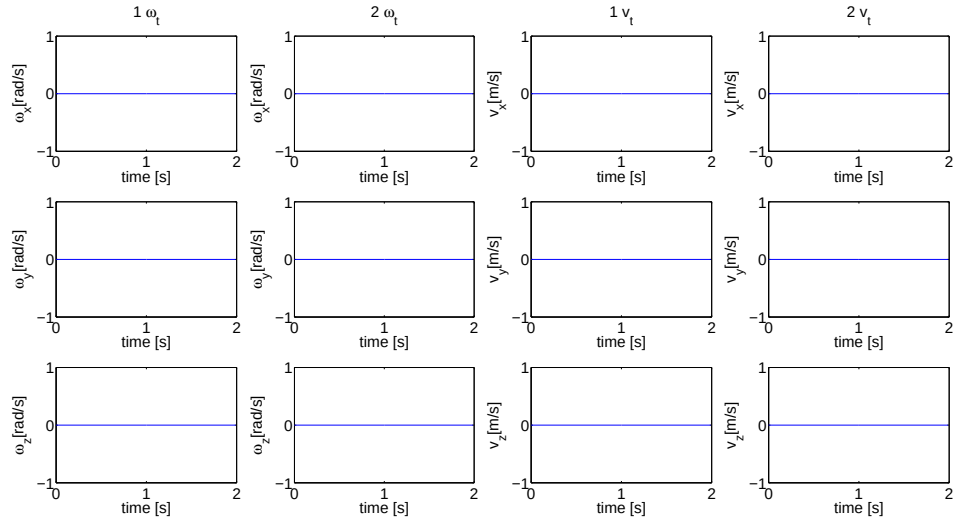

Figure B.7: Tip velocities

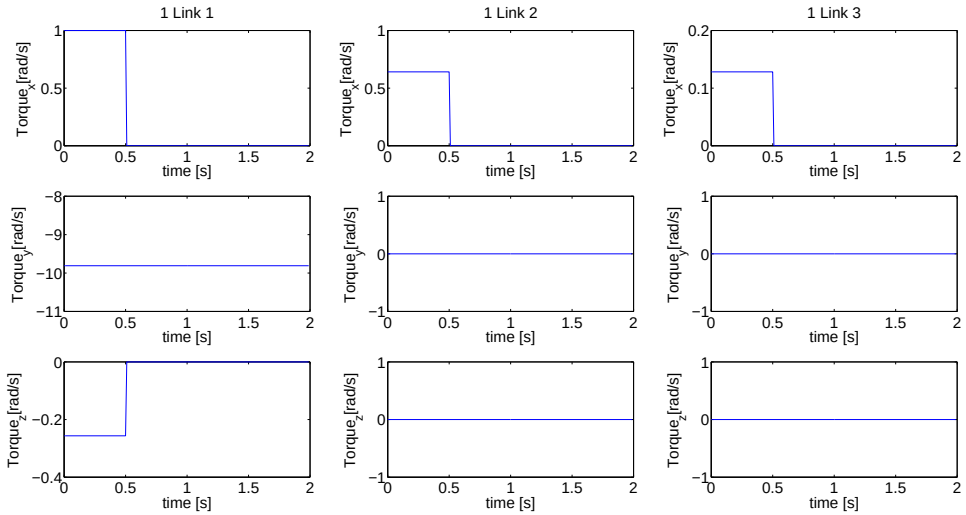

Figure B.8: Torques at the links of Arm 1

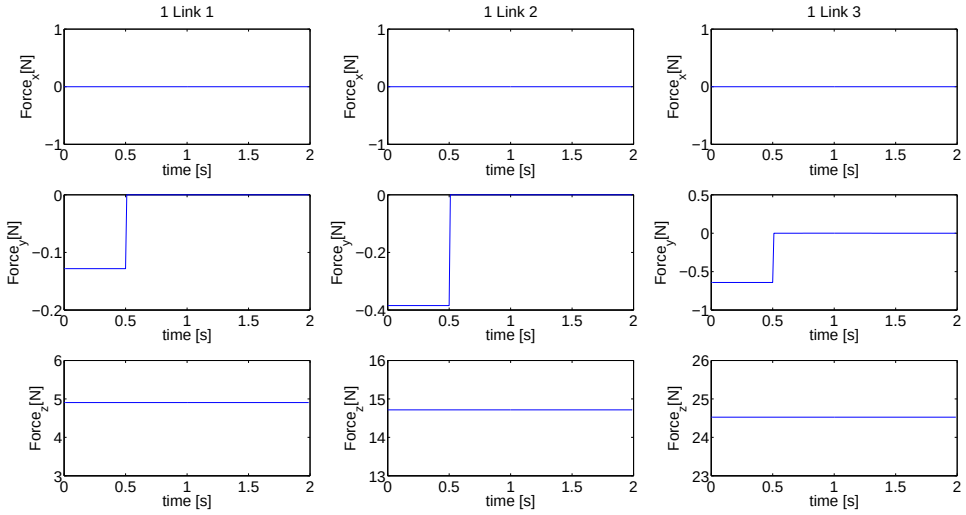

Figure B.9: Forces at the links of Arm 1

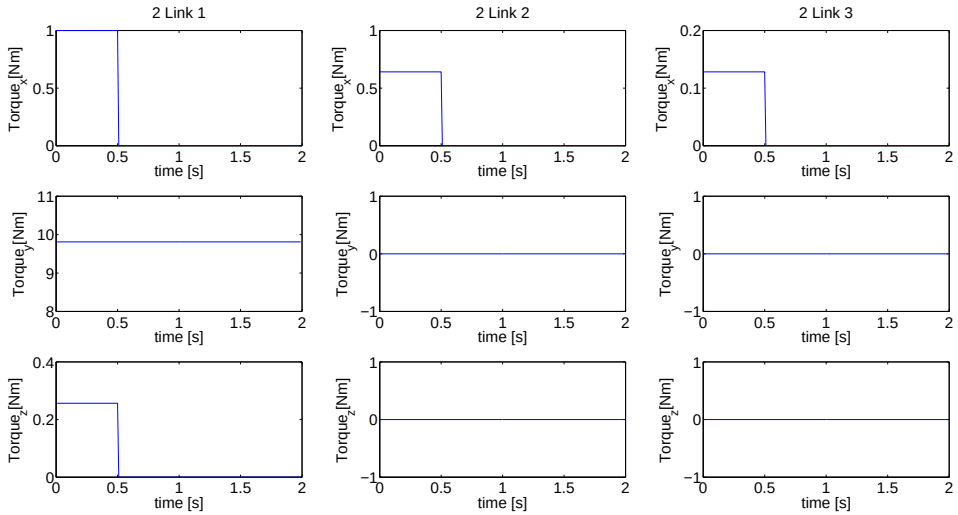

Figure B.10: Torques at the links of Arm 2

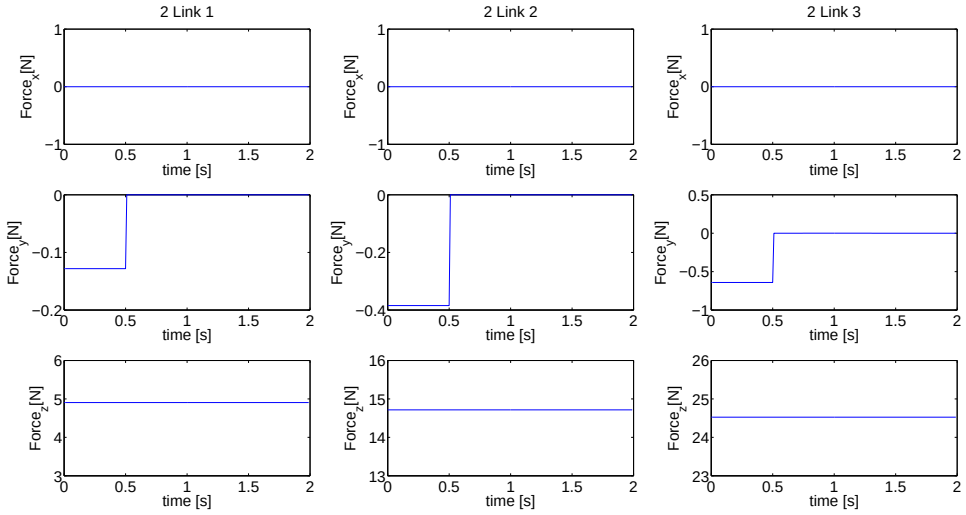

Figure B.11: Forces at the links of Arm 2

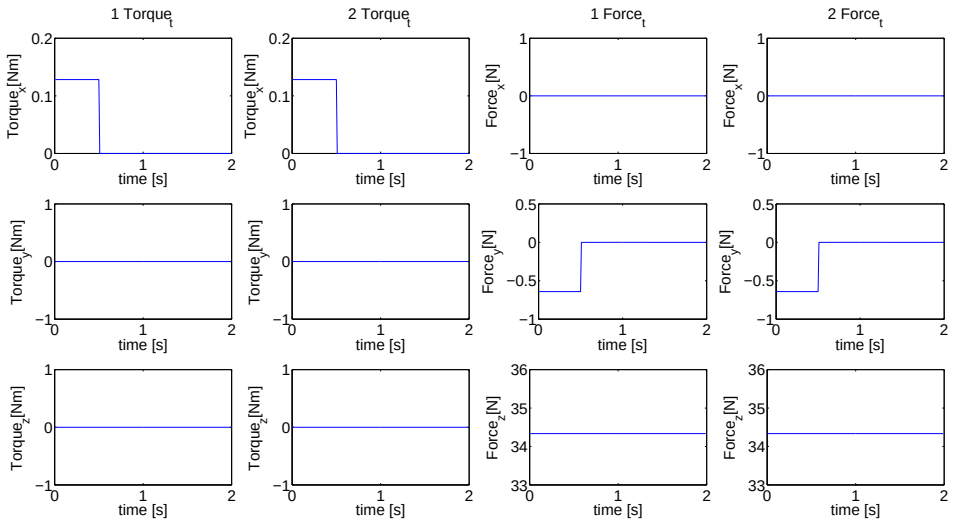

Figure B.12: Tip spatial forces

B.1.2 Rotating around the center

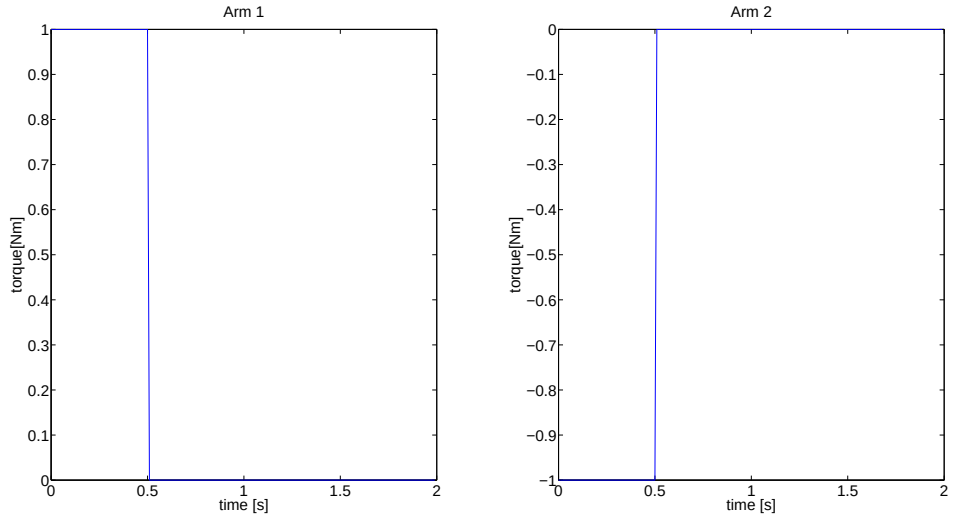

Figure B.13: Applied torques

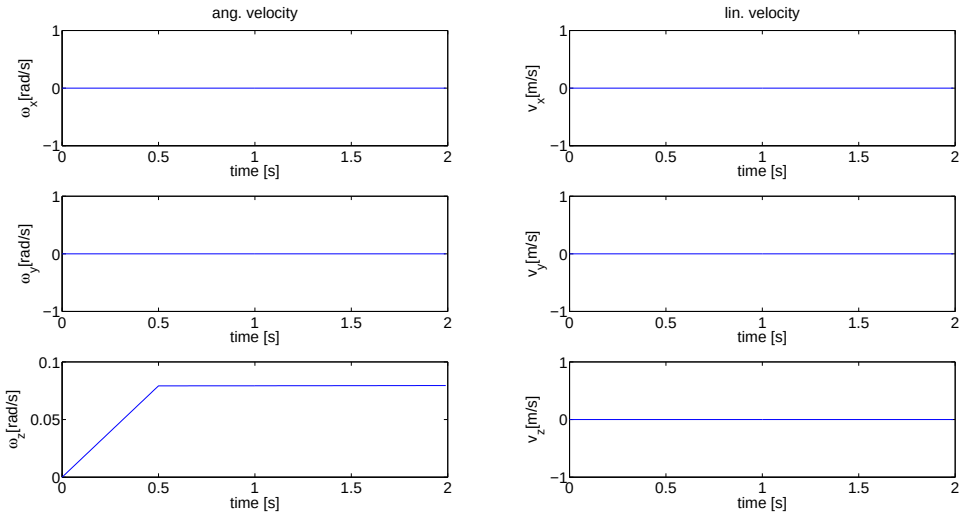

Figure B.14: Base velocities

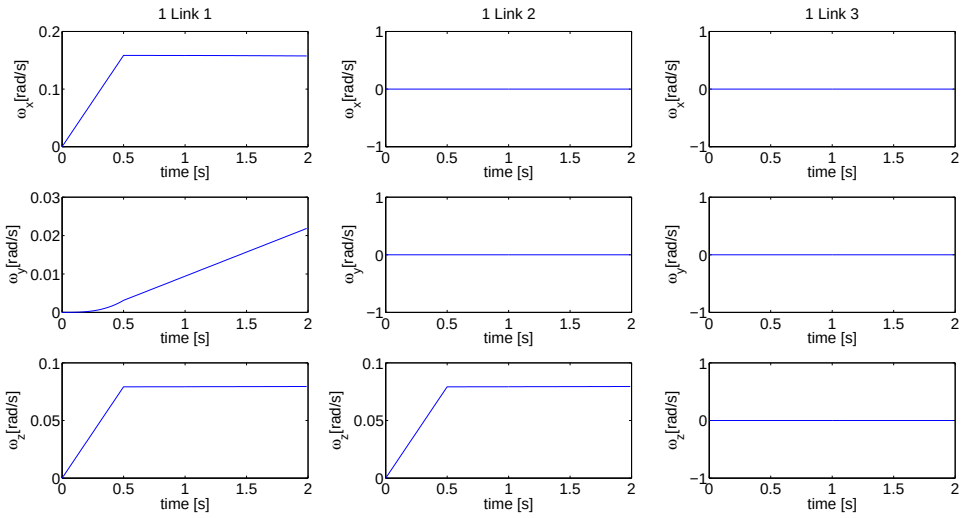

Figure B.15: Angular velocities of the links of Arm 1

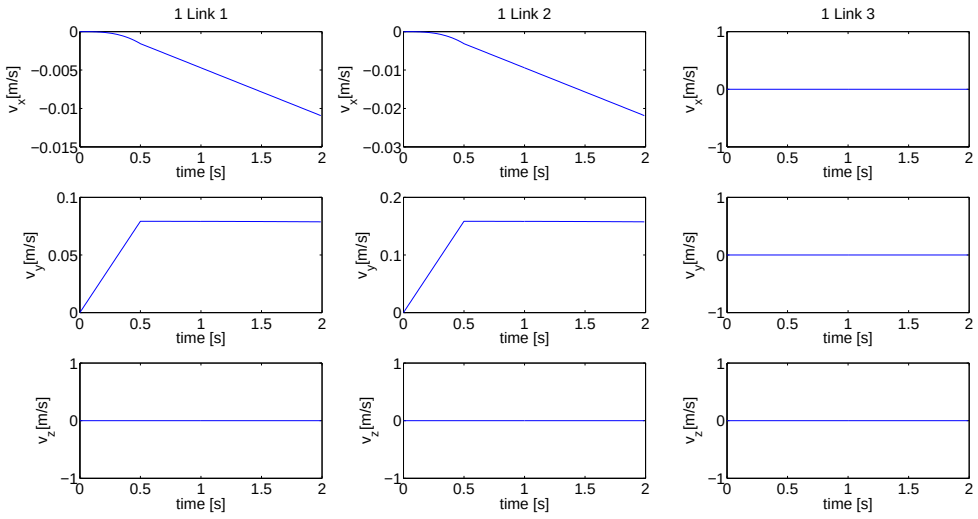

Figure B.16: Linear velocities of the links of Arm 1

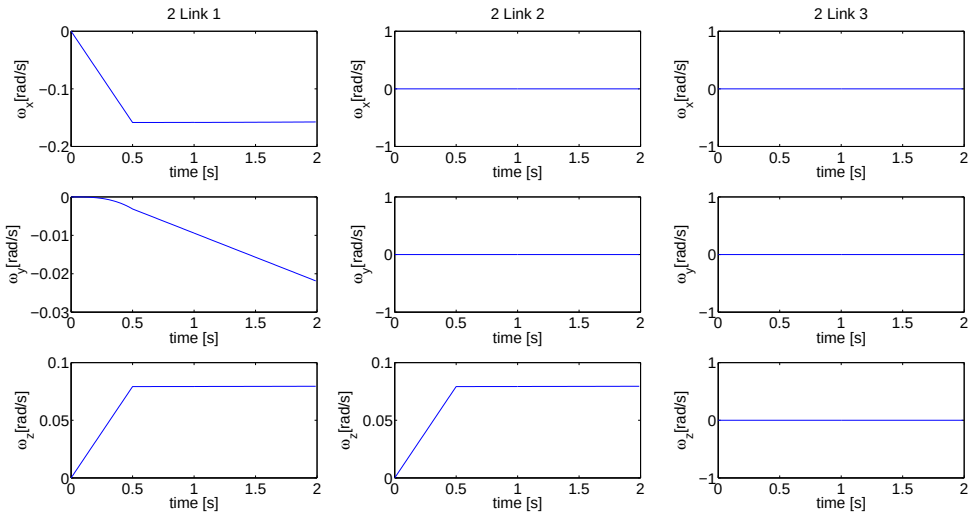

Figure B.17: Angular velocities of the links of Arm 2

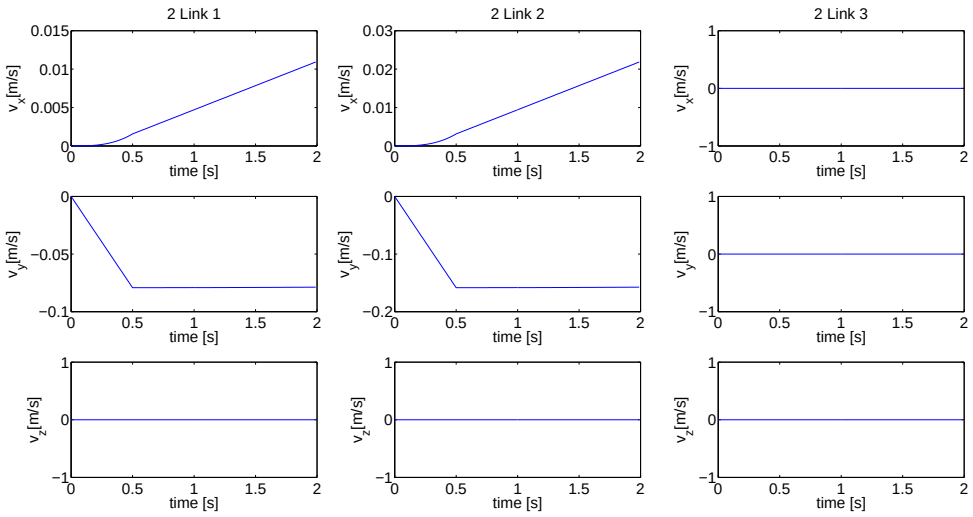

Figure B.18: Linear velocities of the links of Arm 2

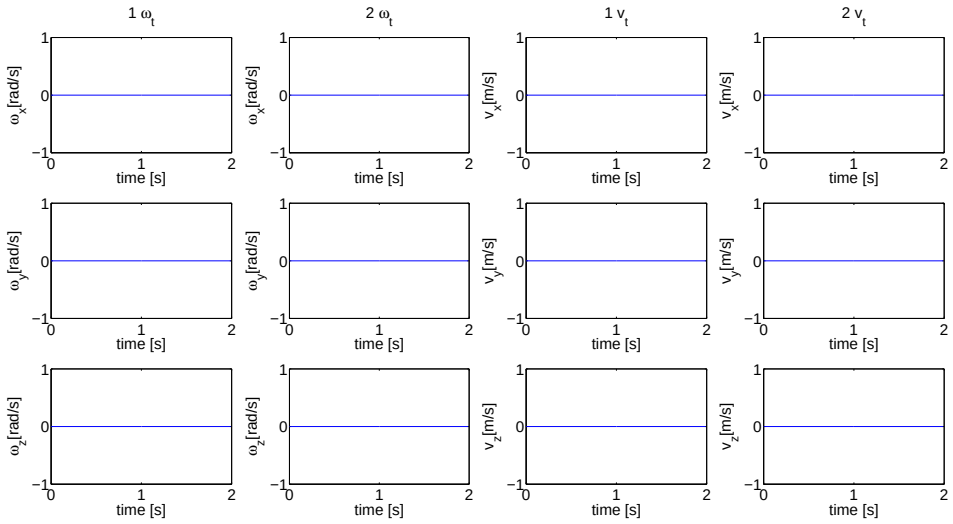

Figure B.19: Tip velocities

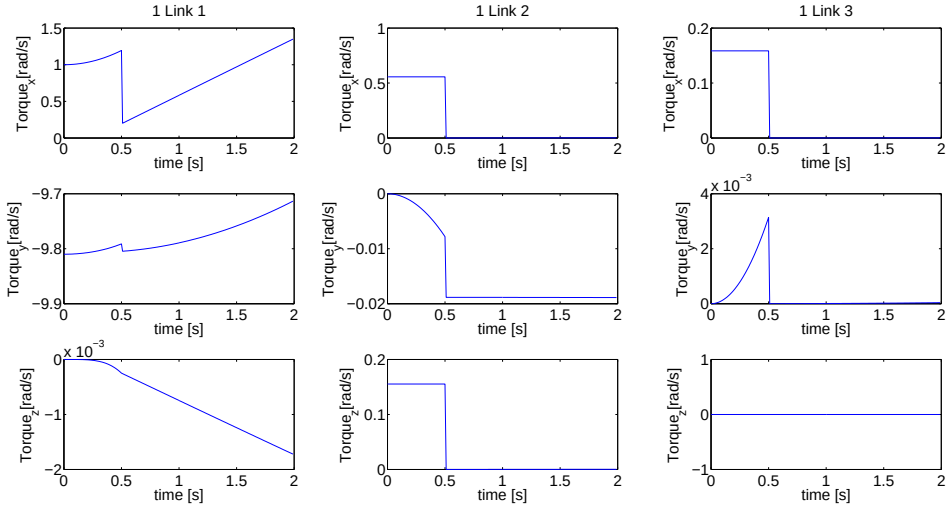

Figure B.20: Torques at the links of Arm 1

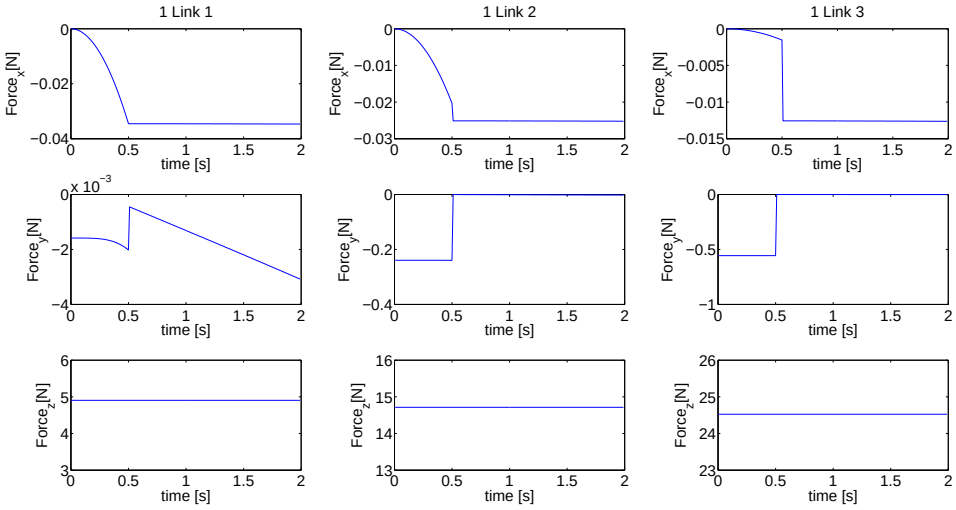

Figure B.21: Forces at the links of Arm 1

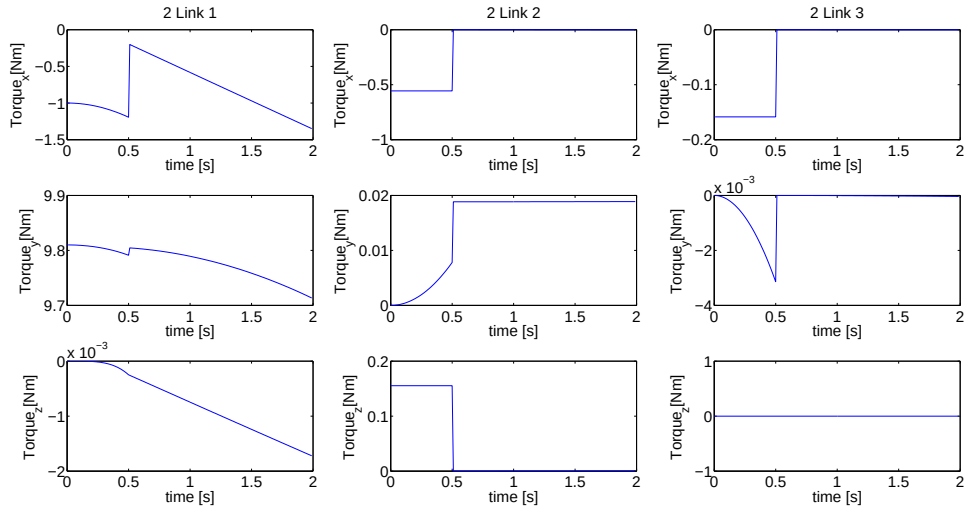

Figure B.22: Torques at the links of Arm 2

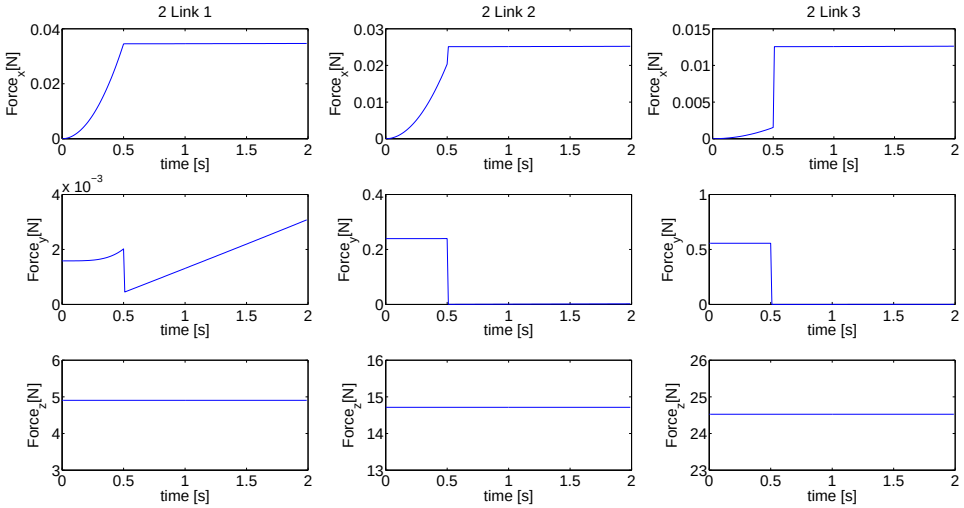

Figure B.23: Forces at the links of Arm 2

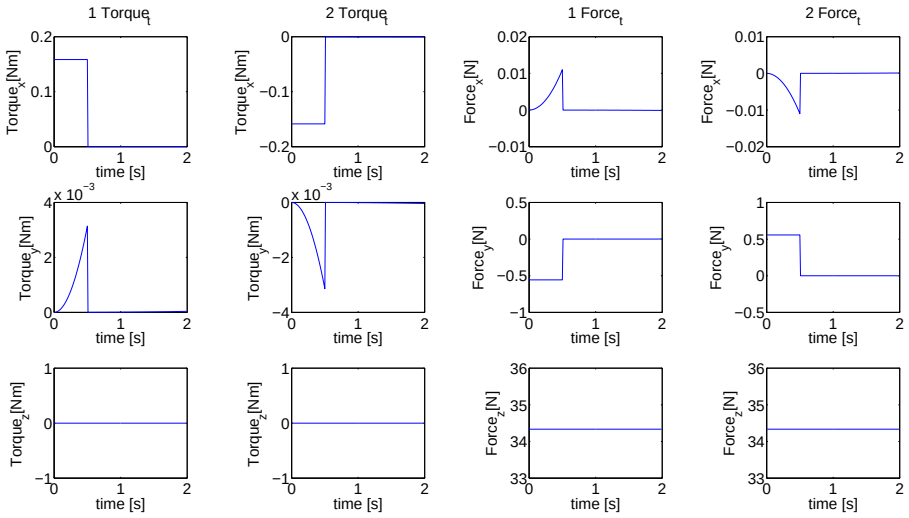

Figure B.24: Tip spatial forces

B.1.3 Rotating around off center

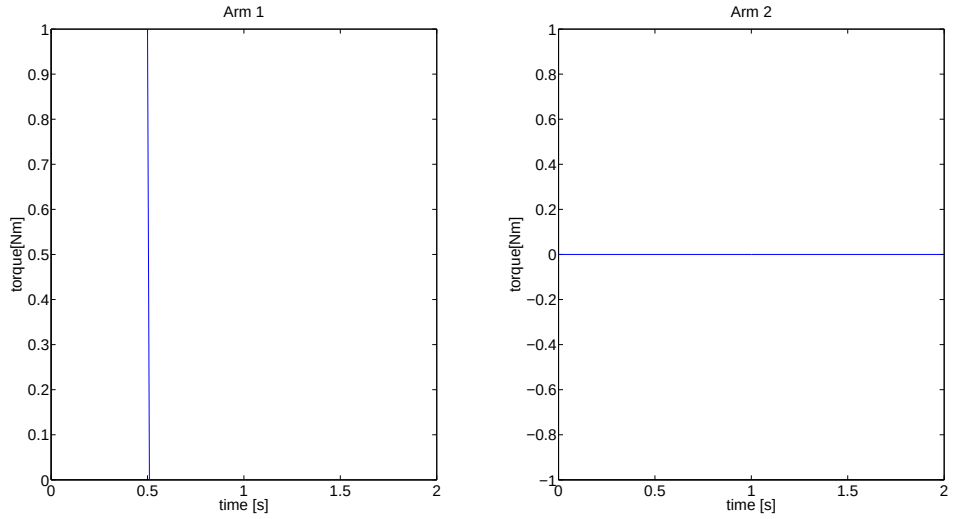

Figure B.25: Applied torques

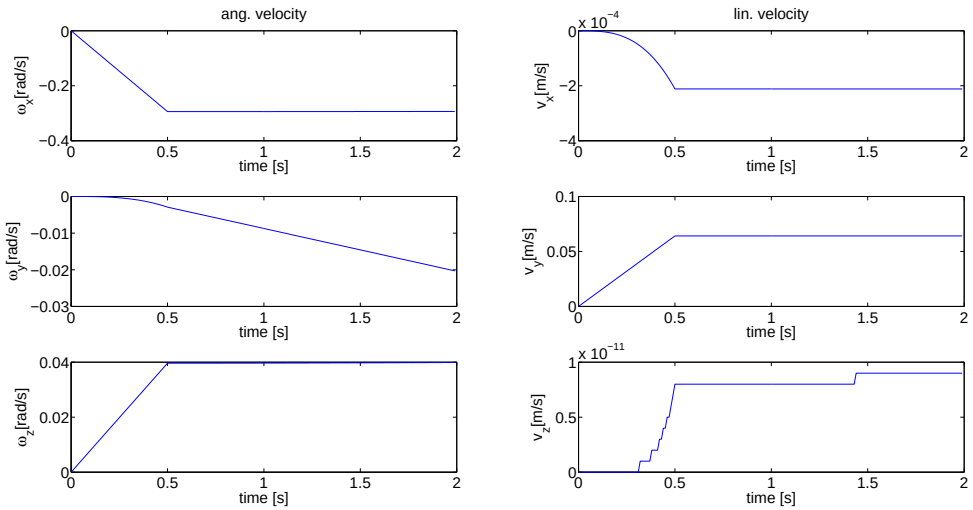

Figure B.26: Base velocities

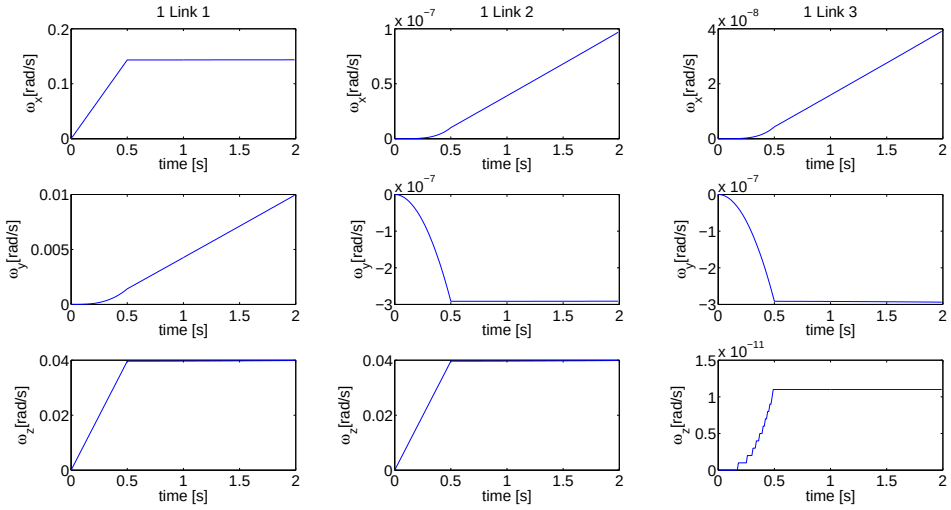

Figure B.27: Angular velocities of the links of Arm 1

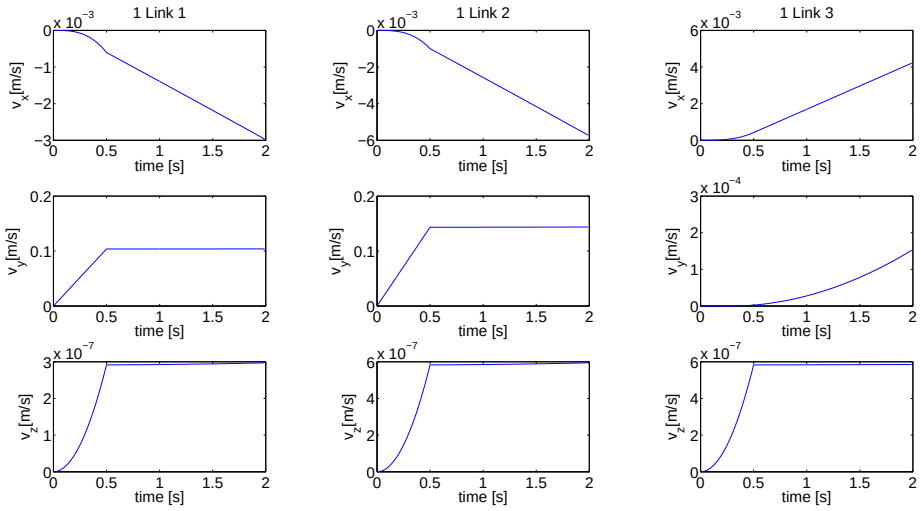

Figure B.28: Linear velocities of the links of Arm 1

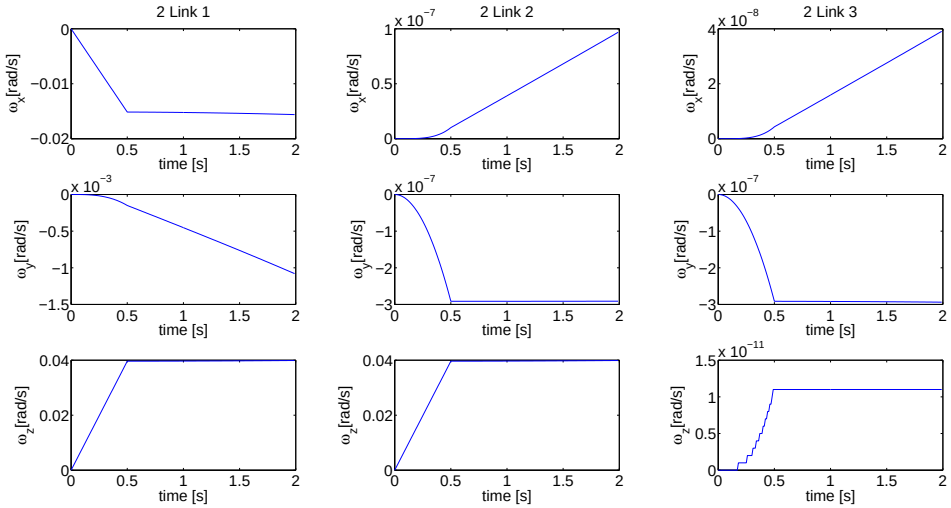

Figure B.29: Angular velocities of the links of Arm 2

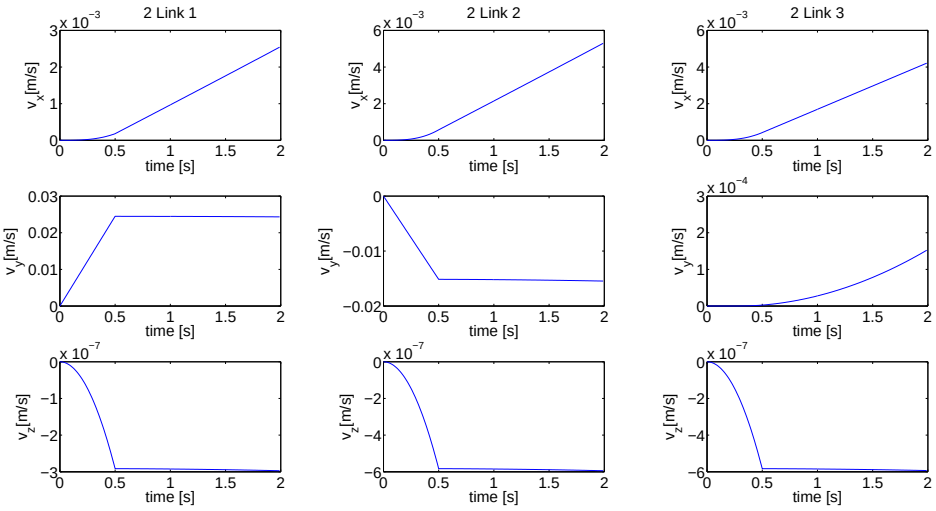

Figure B.30: Linear velocities of the links of Arm 2

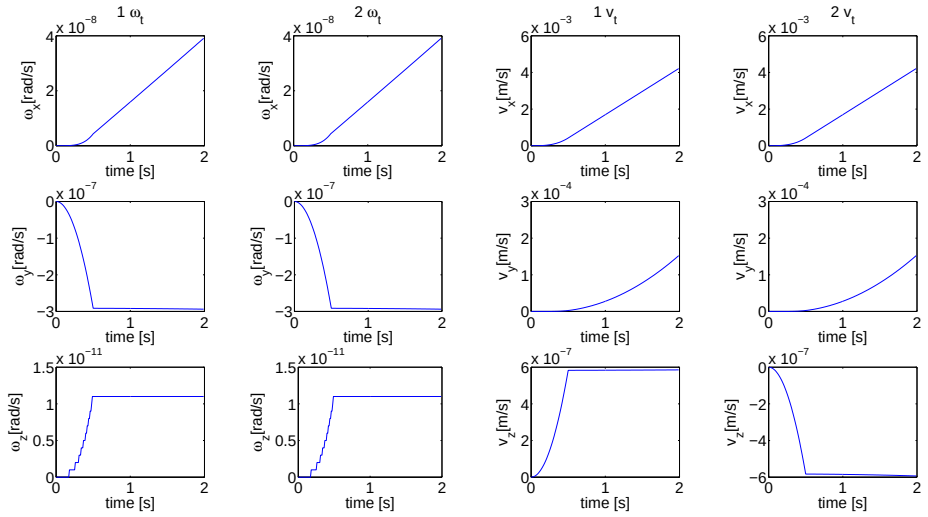

Figure B.31: Tip velocities

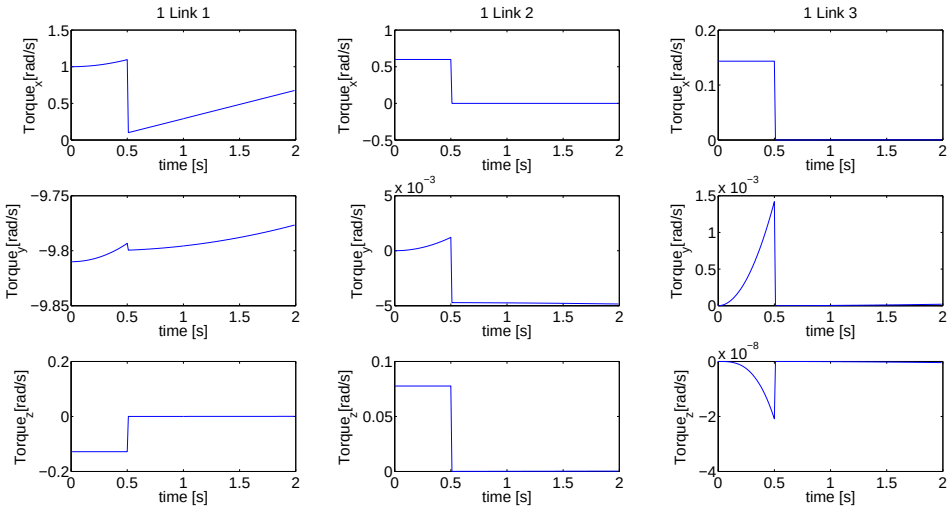

Figure B.32: Torques at the links of Arm 1

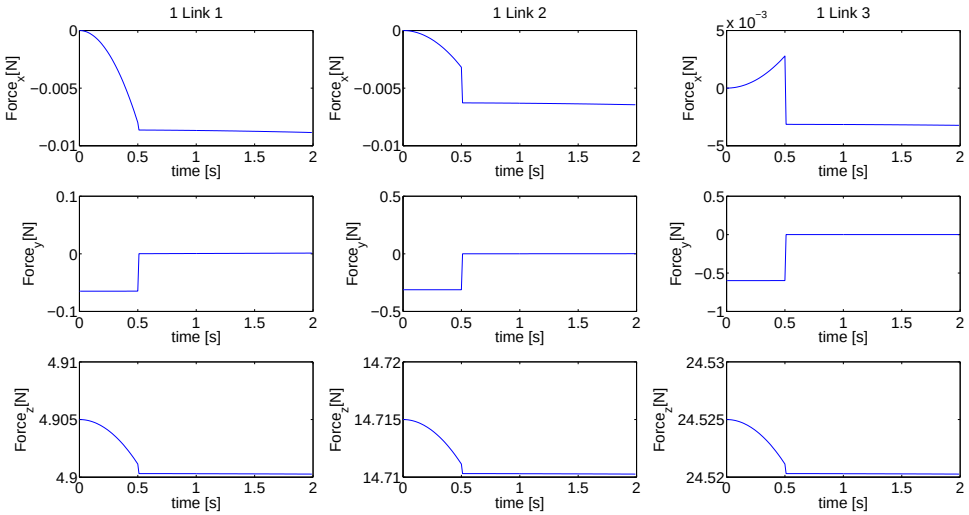

Figure B.33: Forces at the links of Arm 1

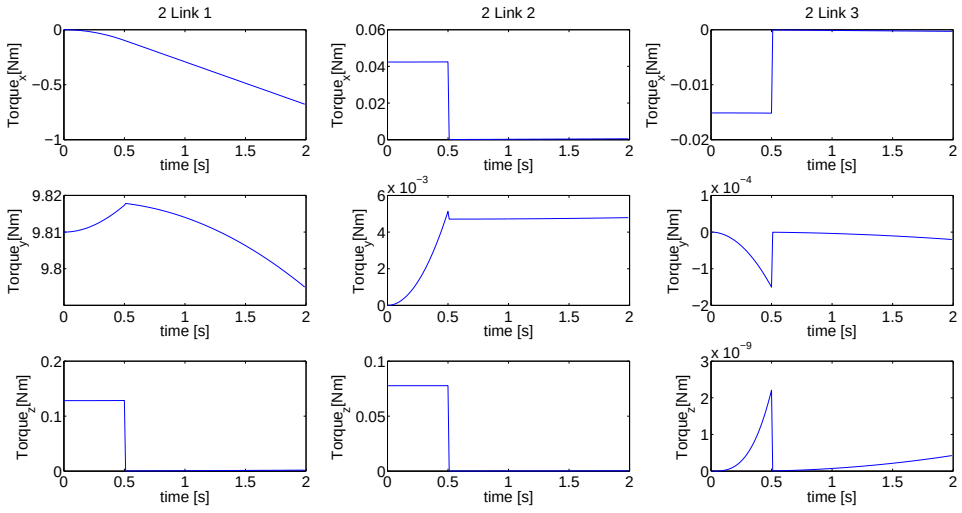

Figure B.34: Torques at the links of Arm 2

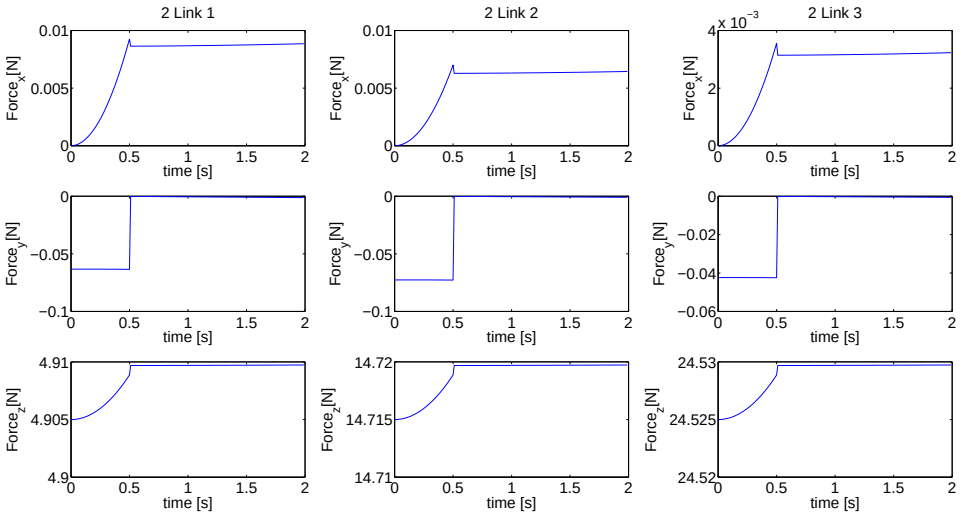

Figure B.35: Forces at the links of Arm 2

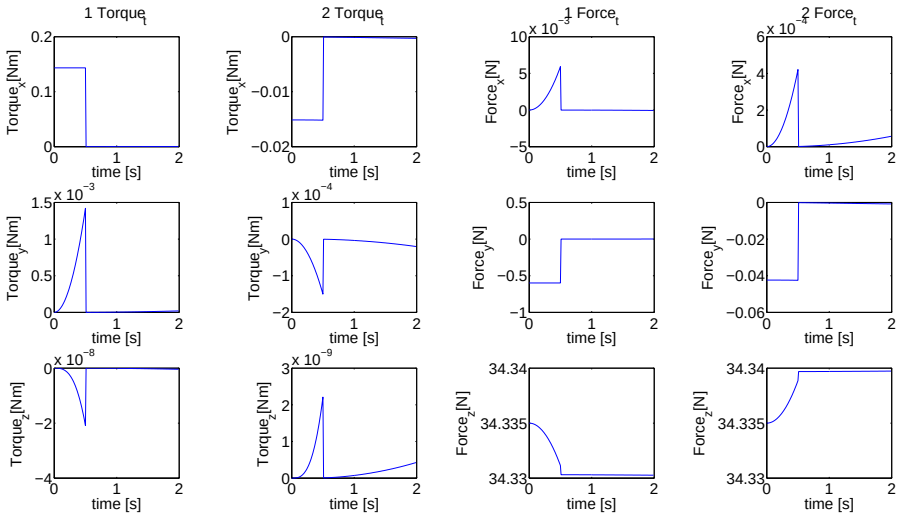

Figure B.36: Tip spatial forces

C. SIMULATION RESULTS: FOUR-WHEEL-DRIVE FOUR-WHEEL-STEER MOBILE MANIPULATOR

Using the methodology presented in Chapter 5.3, the system was simulated using MATLAB on a Pentium 4 computer.

C.1 RESULTS

Two cases were considered;

- drive only, where the driving torques are applied to each wheel
- steering only, where the steering torques are applied to each wheel

C.1.1 Steering

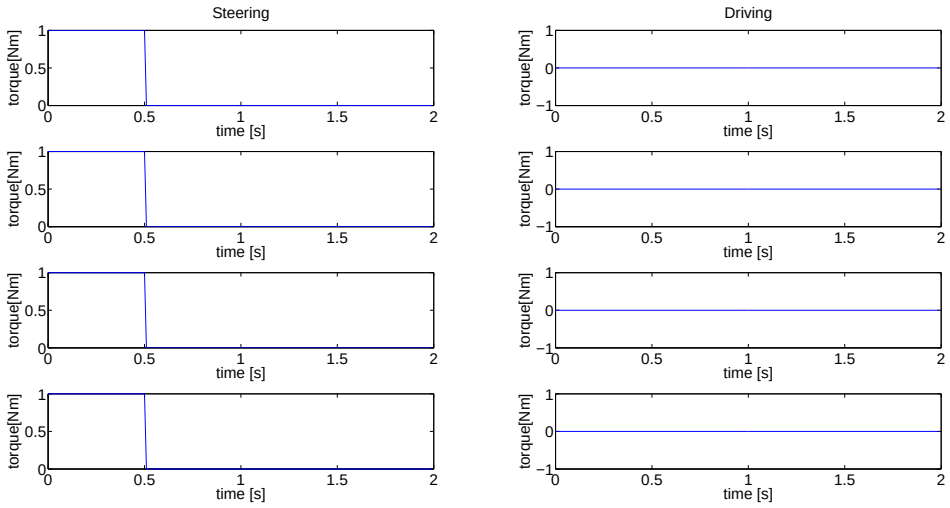

Figure C.1: Applied torques

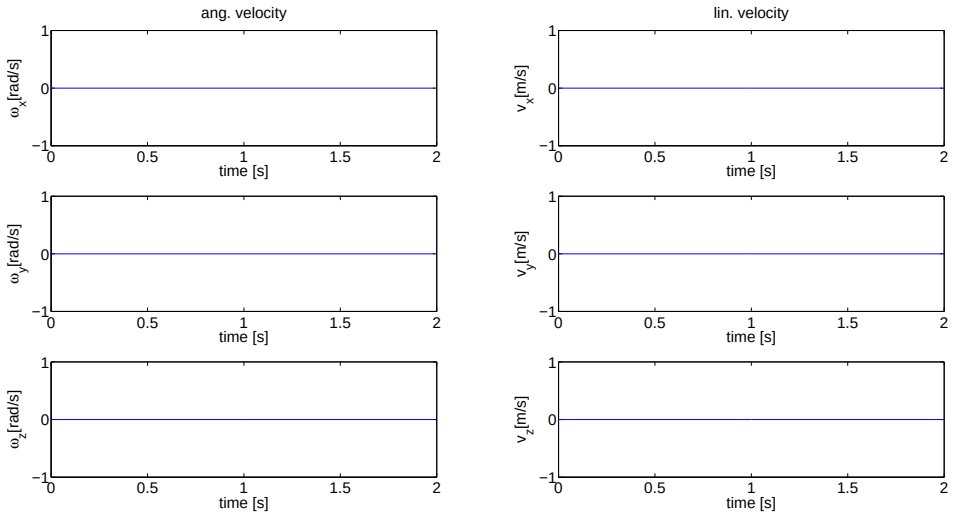

Figure C.2: Base velocities

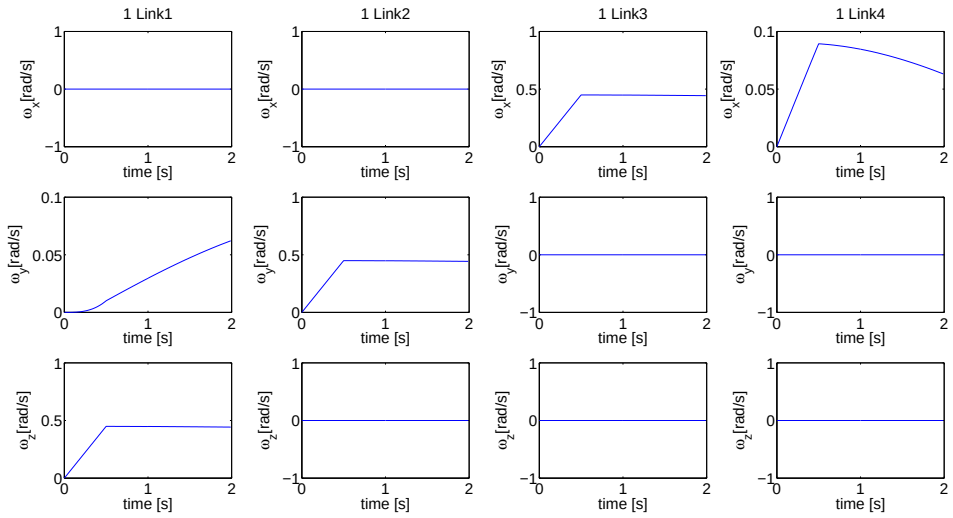

Figure C.3: Angular velocities of the links of Arm 1

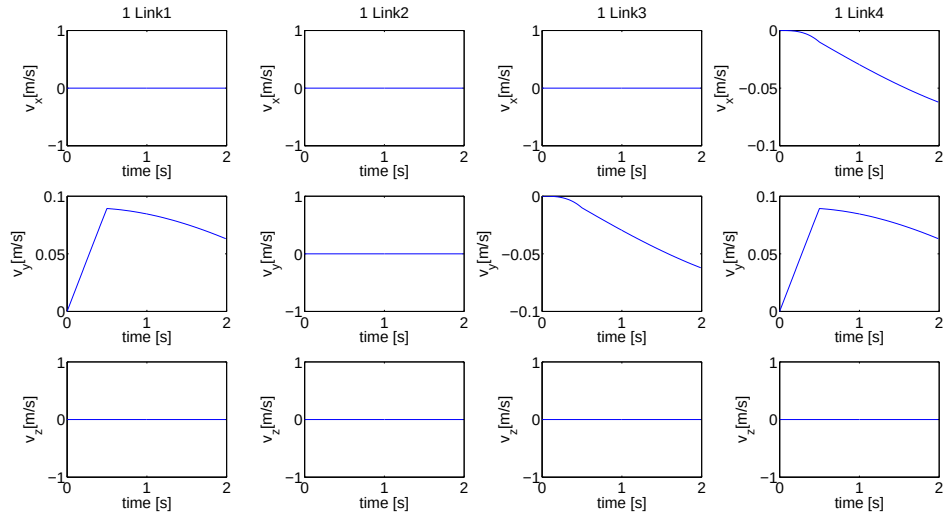

Figure C.4: Linear velocities of the links of Arm 1

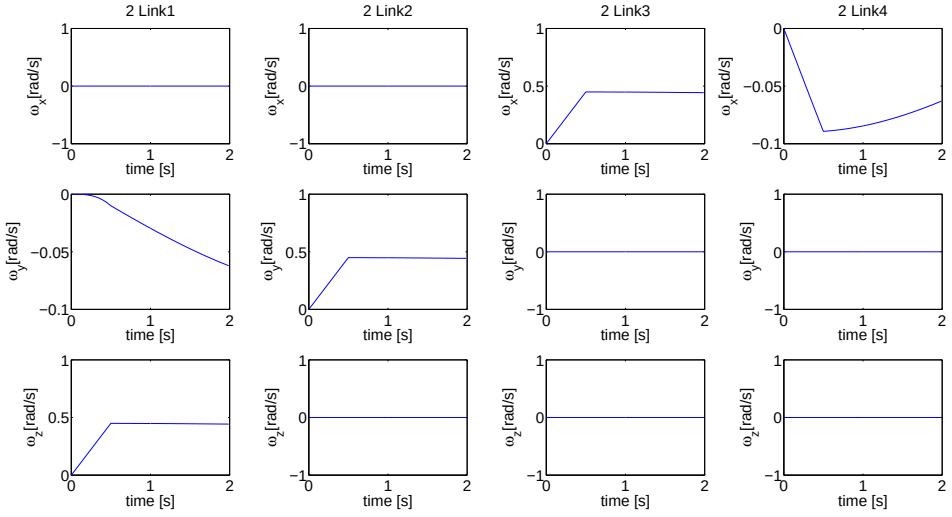

Figure C.5: Angular velocities of the links of Arm 2

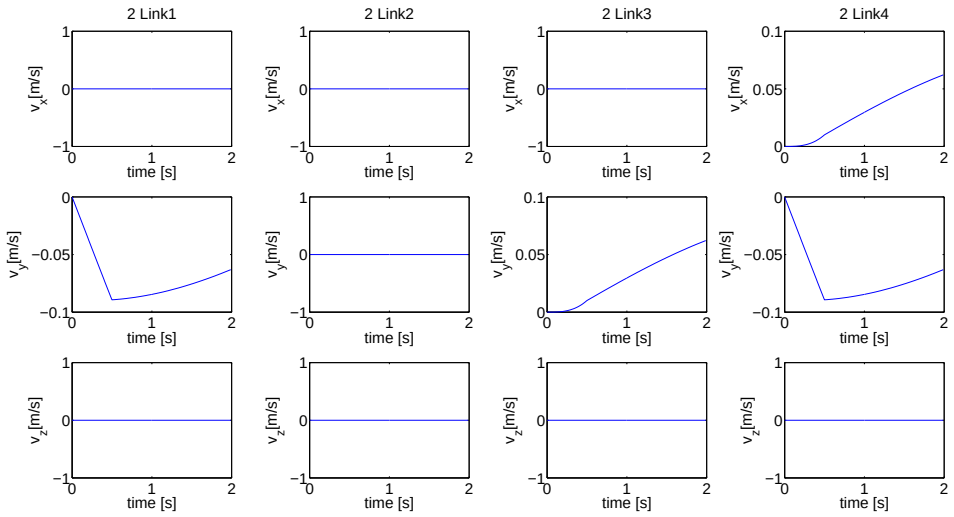

Figure C.6: Linear velocities of the links of Arm 2

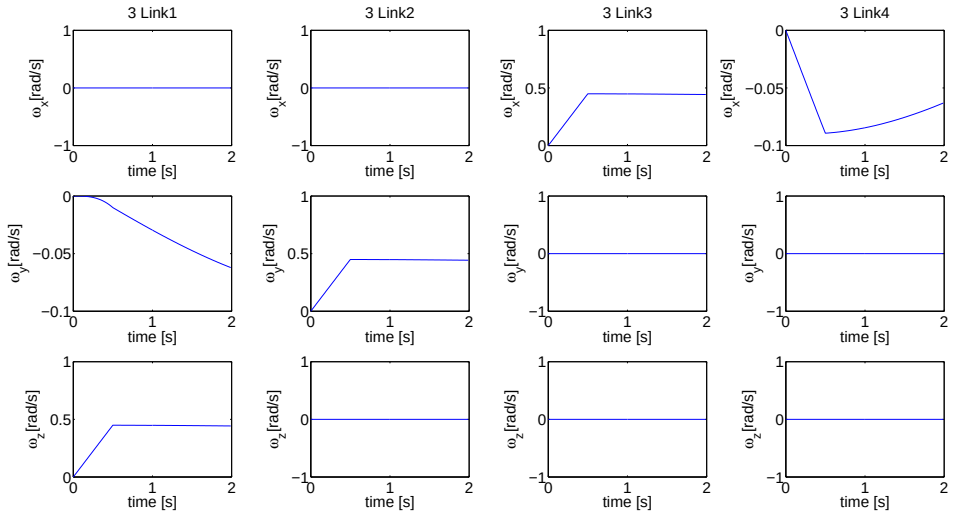

Figure C.7: Angular velocities of the links of Arm 3

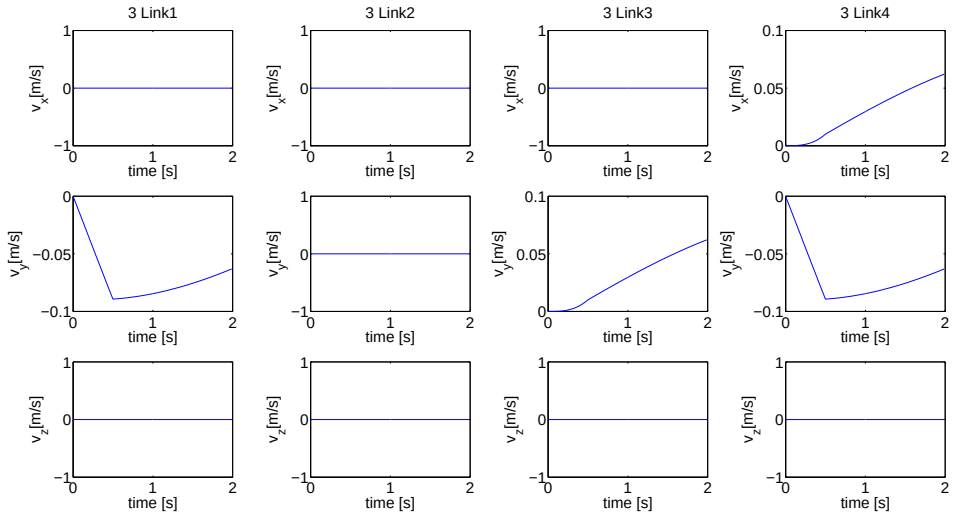

Figure C.8: Linear velocities of the links of Arm 3

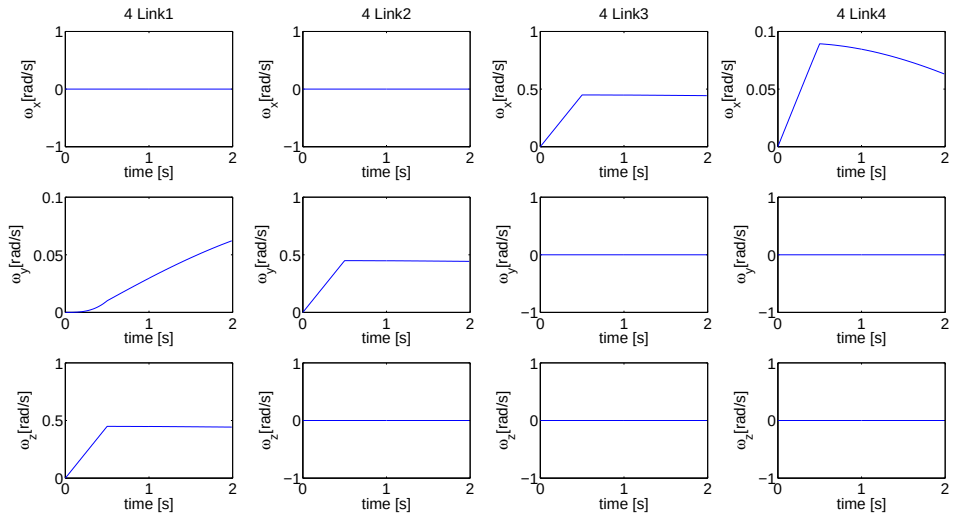

Figure C.9: Angular velocities of the links of Arm 4

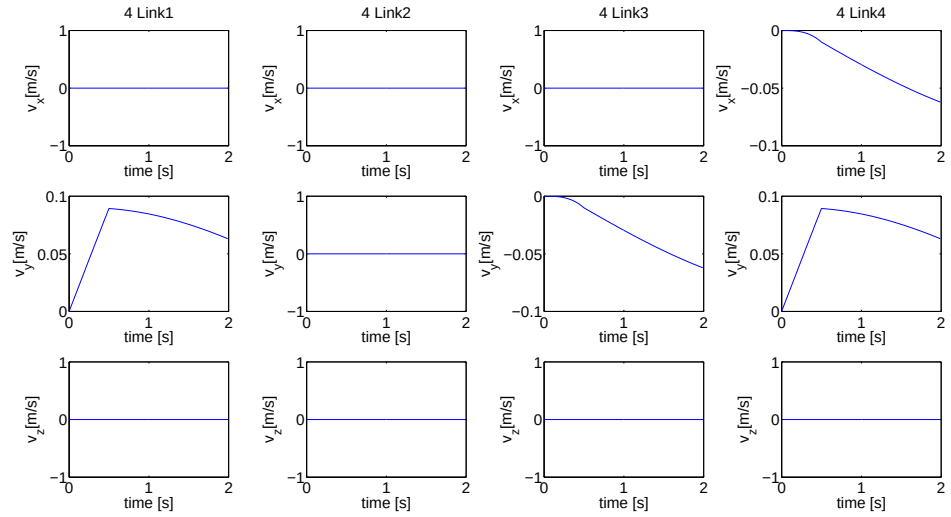

Figure C.10: Linear velocities of the links of Arm 4

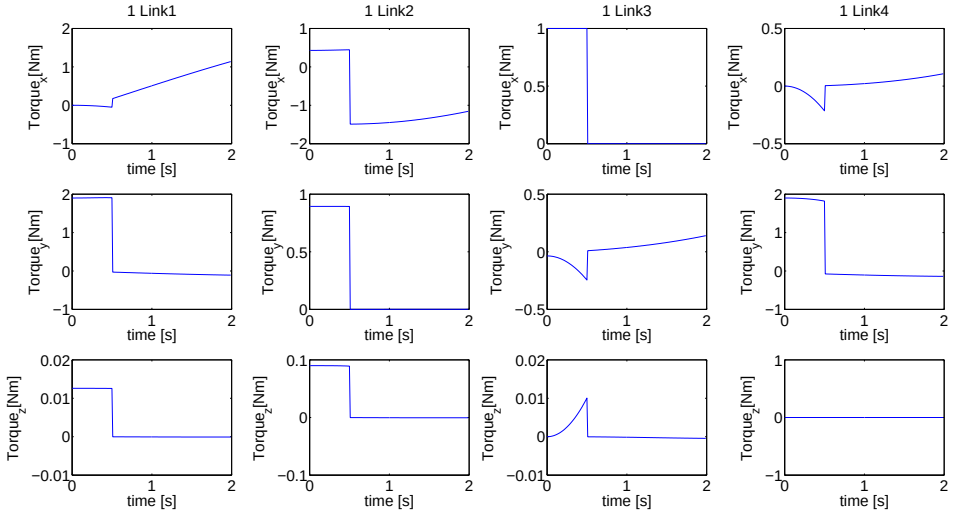

Figure C.11: Torques at the links of Arm 1

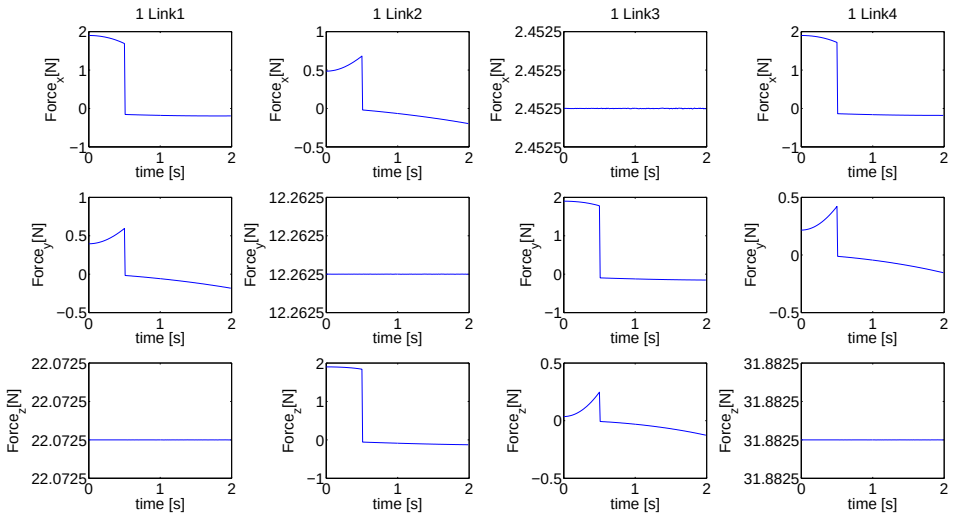

Figure C.12: Forces at the links of Arm 1

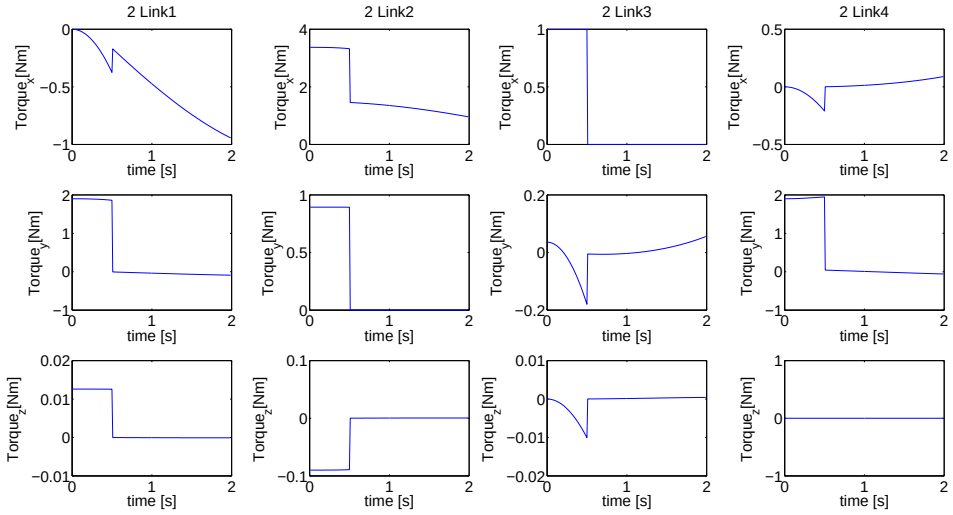

Figure C.13: Torques at the links of Arm 2

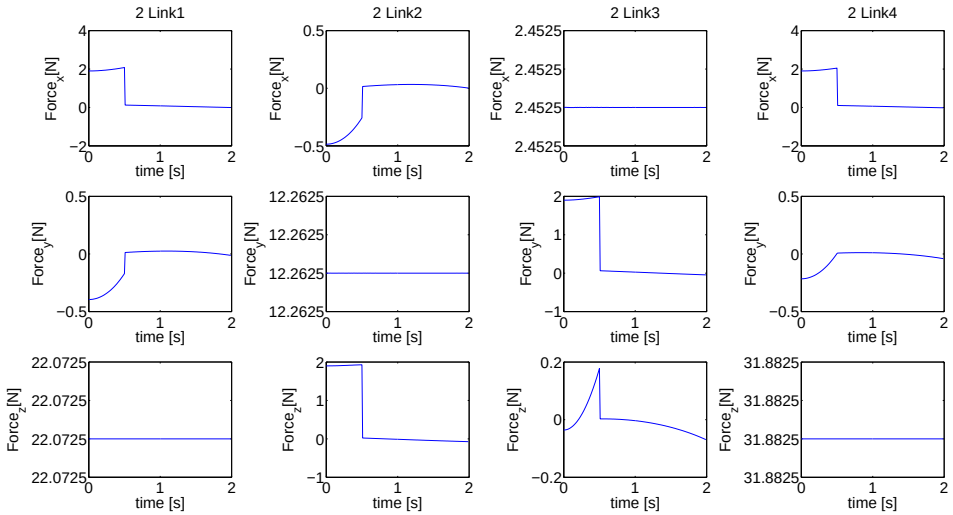

Figure C.14: Forces at the links of Arm 2

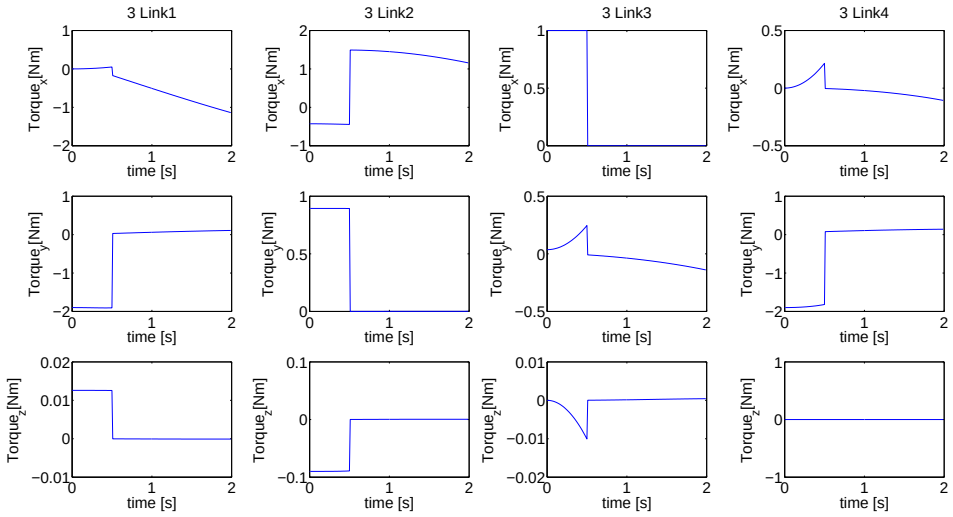

Figure C.15: Torques at the links of Arm 3

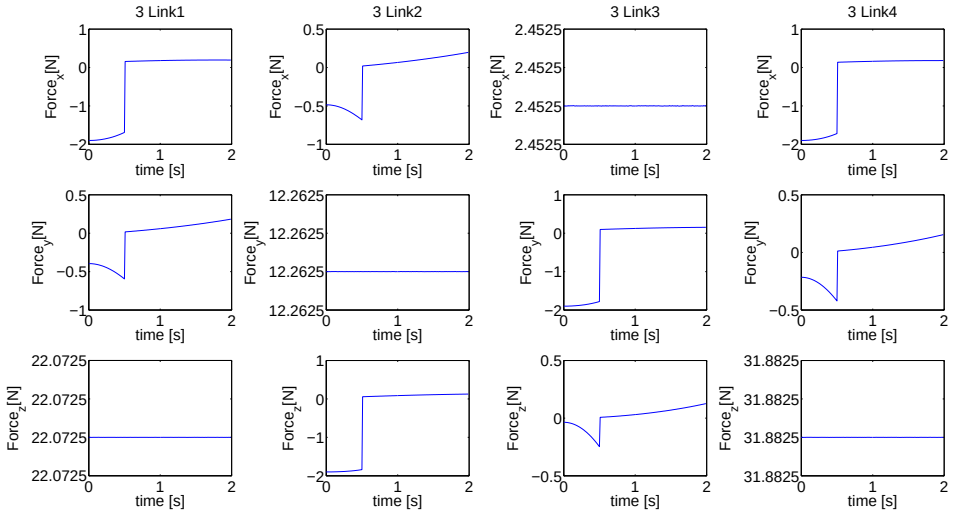

Figure C.16: Forces at the links of Arm 3

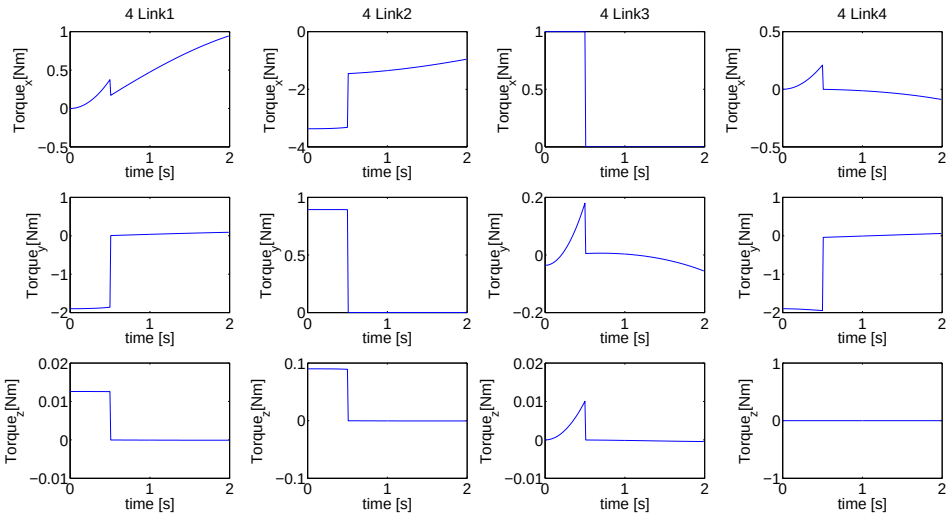

Figure C.17: Torques at the links of Arm 4

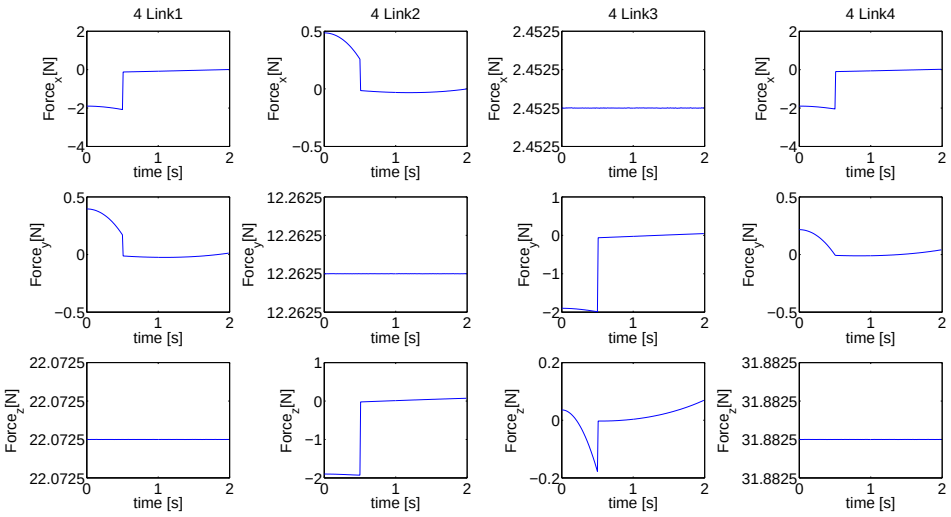

Figure C.18: Forces at the links of Arm 4

C.1.2 Driving

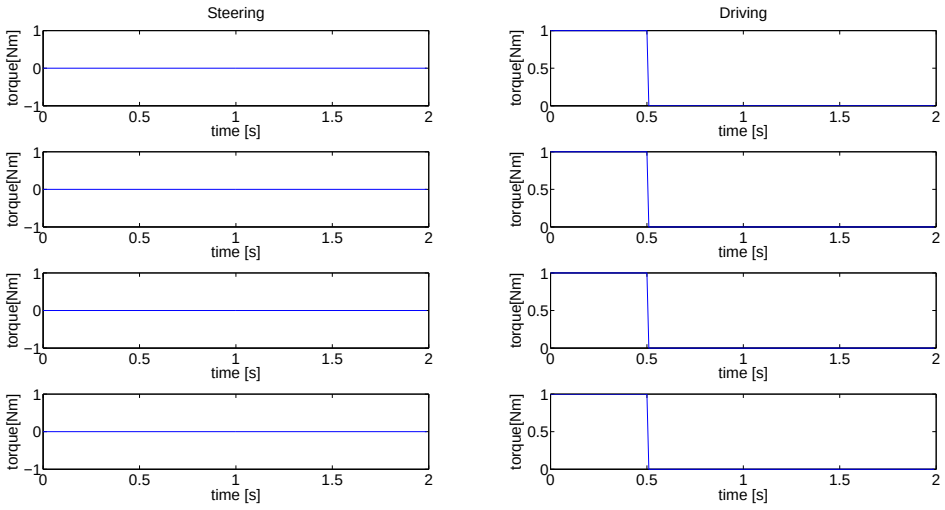

Figure C.19: Applied torques

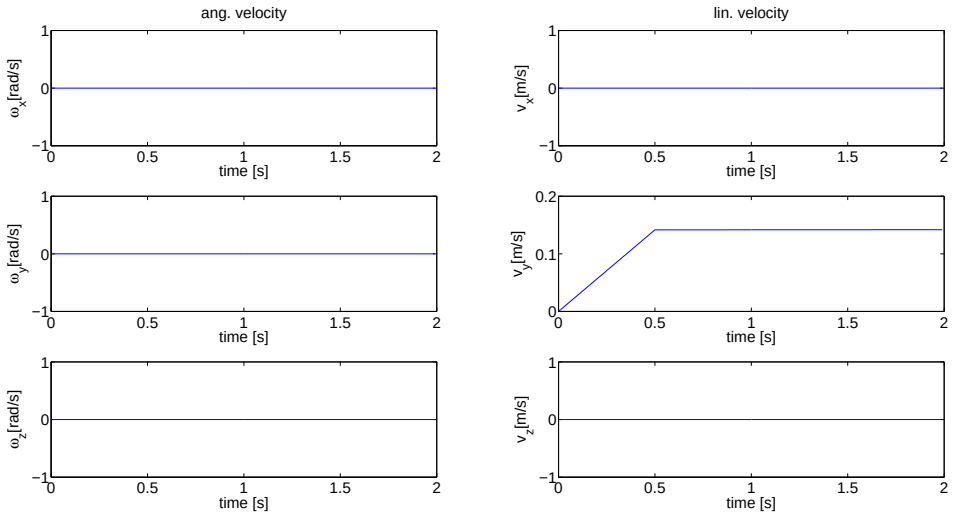

Figure C.20: Base velocities

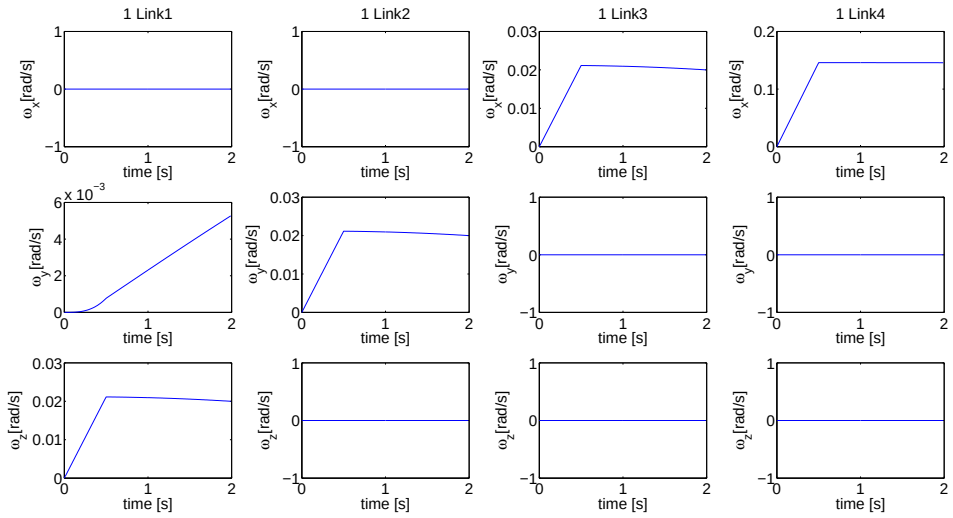

Figure C.21: Angular velocities of the links of Arm 1

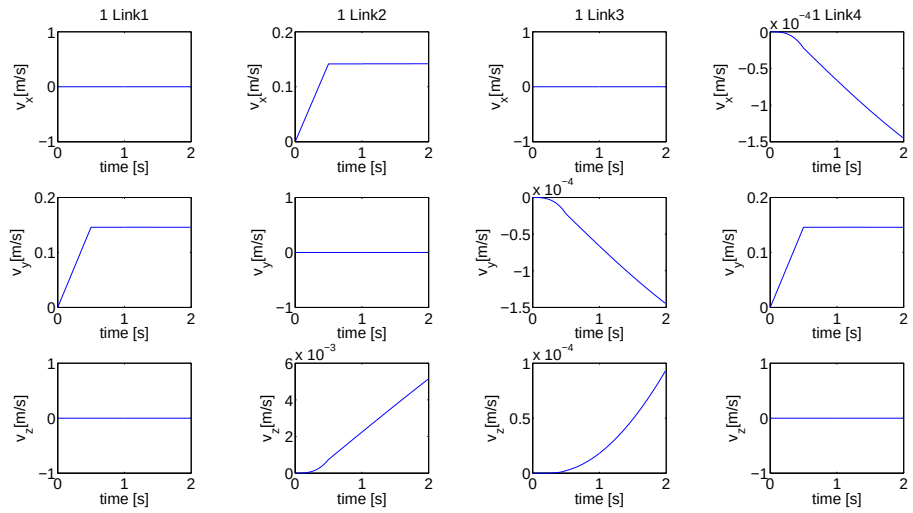

Figure C.22: Linear velocities of the links of Arm 1

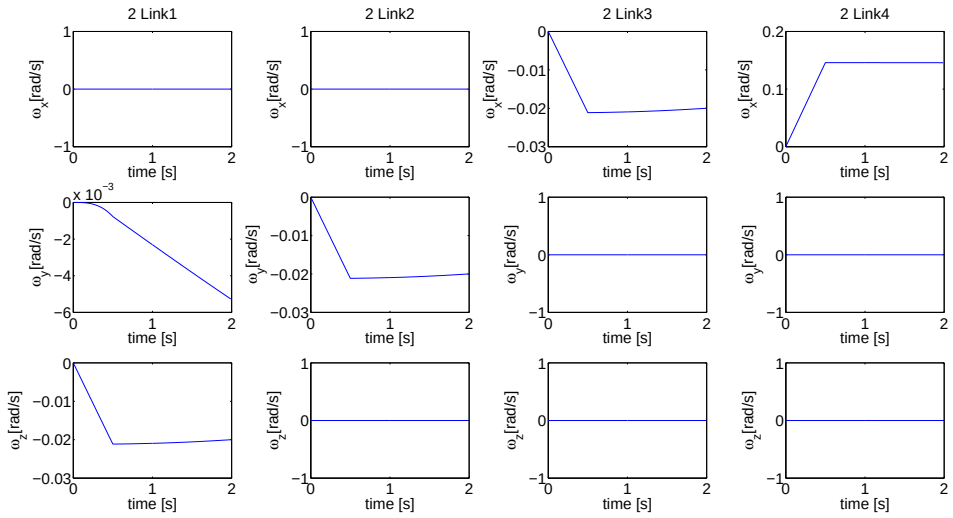

Figure C.23: Angular velocities of the links of Arm 2

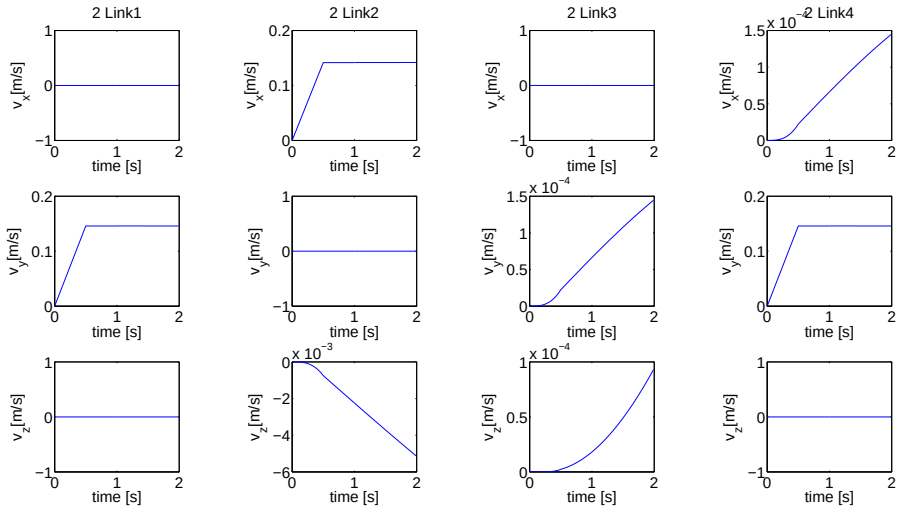

Figure C.24: Linear velocities of the links of Arm 2

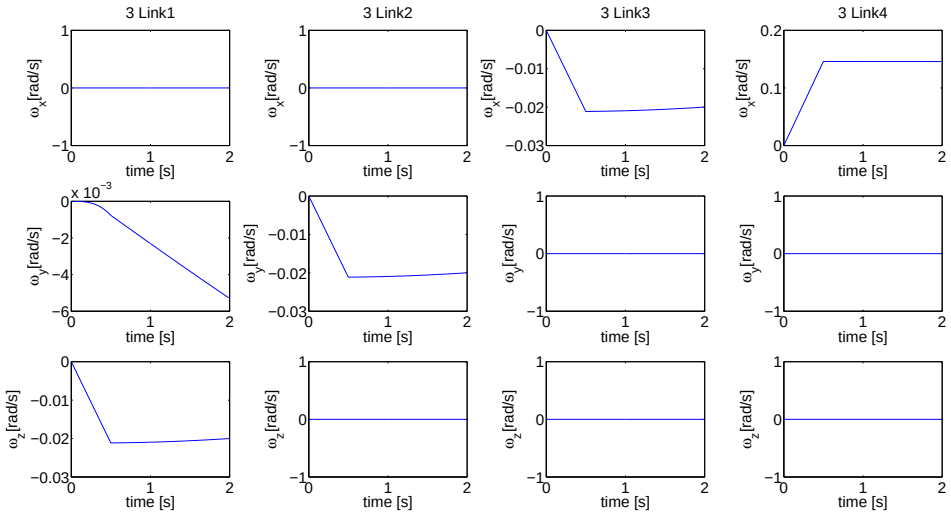

Figure C.25: Angular velocities of the links of Arm 3

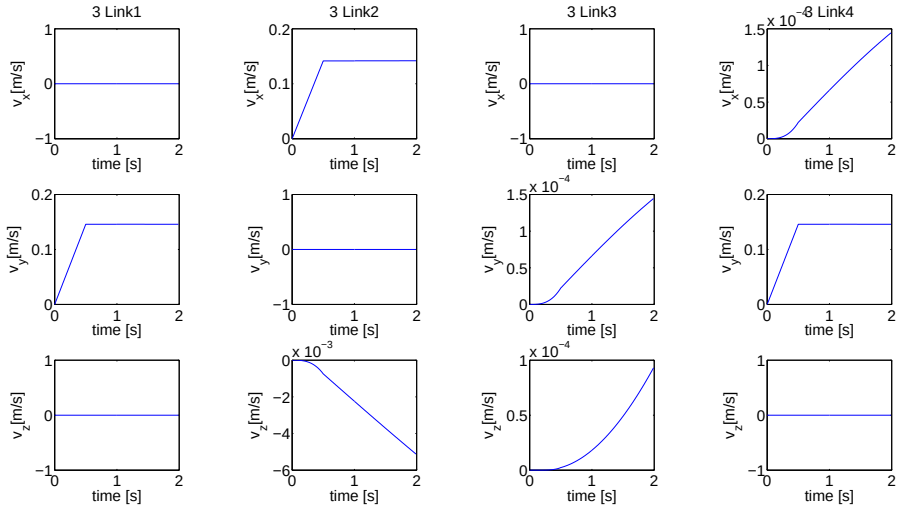

Figure C.26: Linear velocities of the links of Arm 3

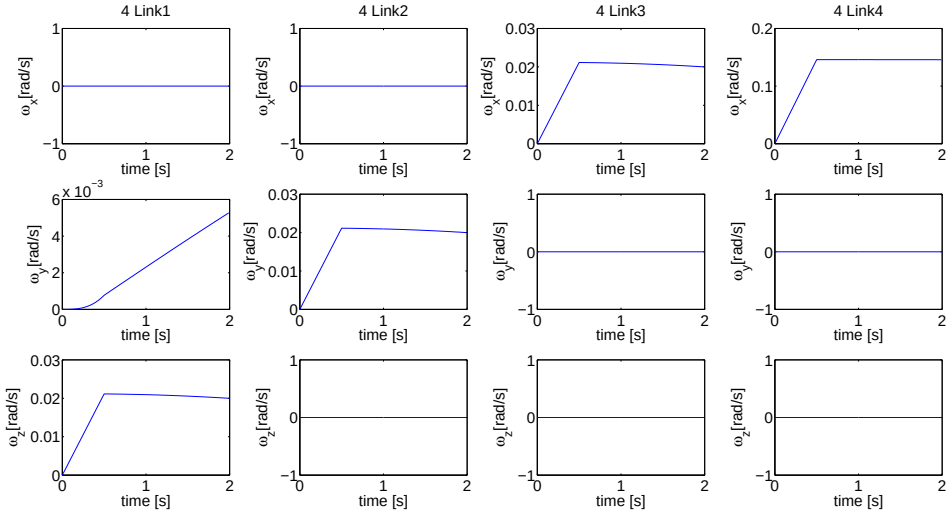

Figure C.27: Angular velocities of the links of Arm 4

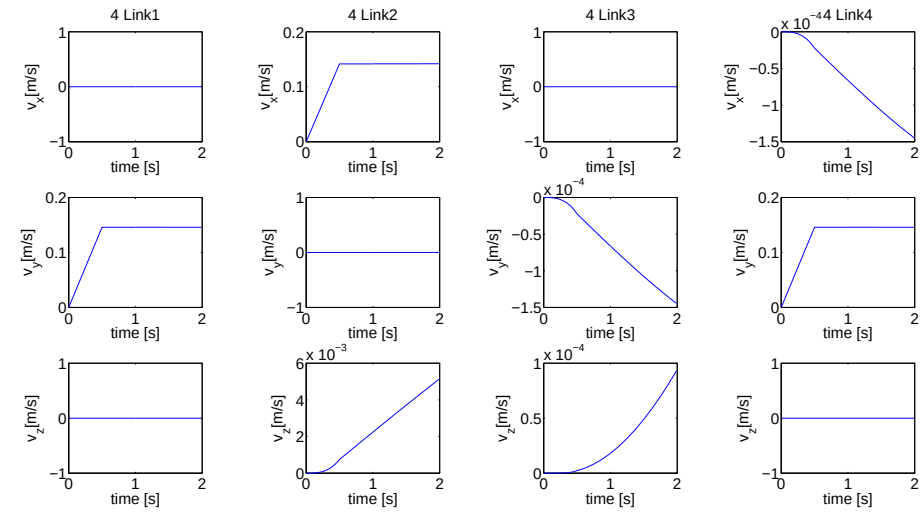

Figure C.28: Linear velocities of the links of Arm 4

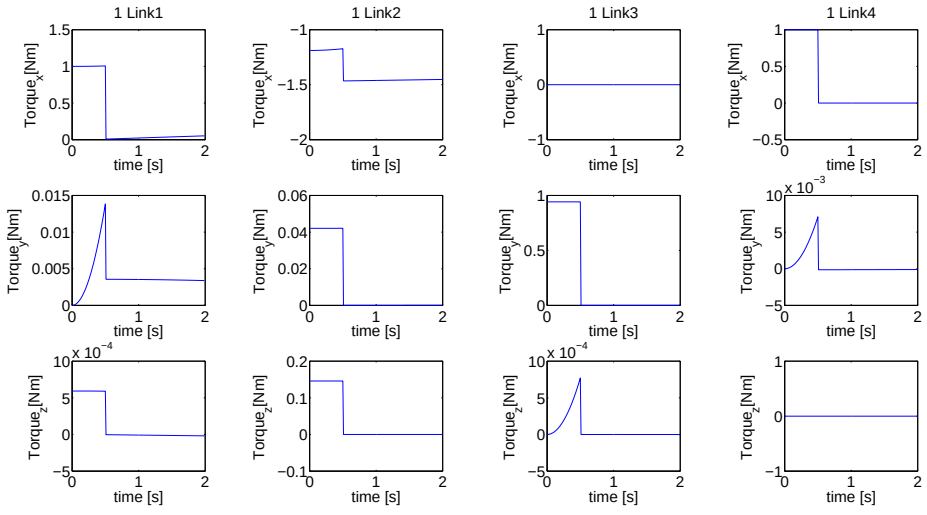

Figure C.29: Torques at the links of Arm 1

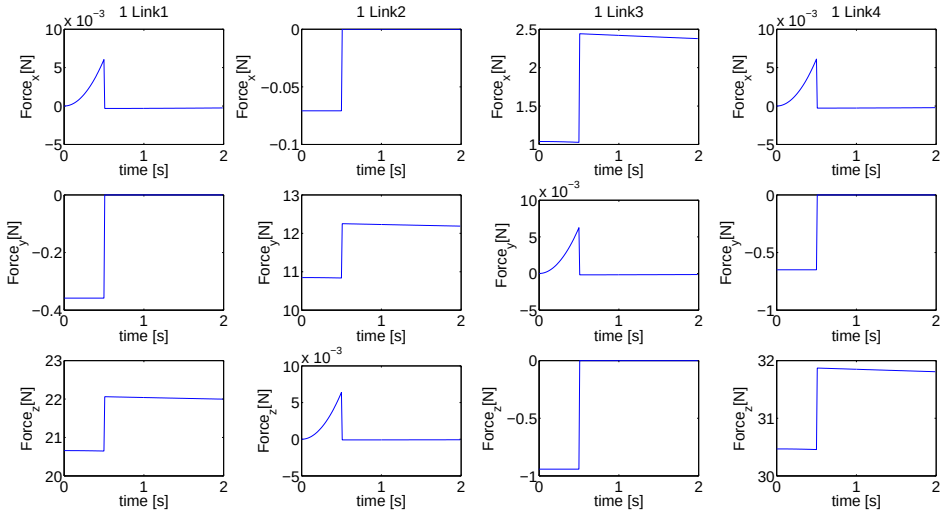

Figure C.30: Forces at the links of Arm 1

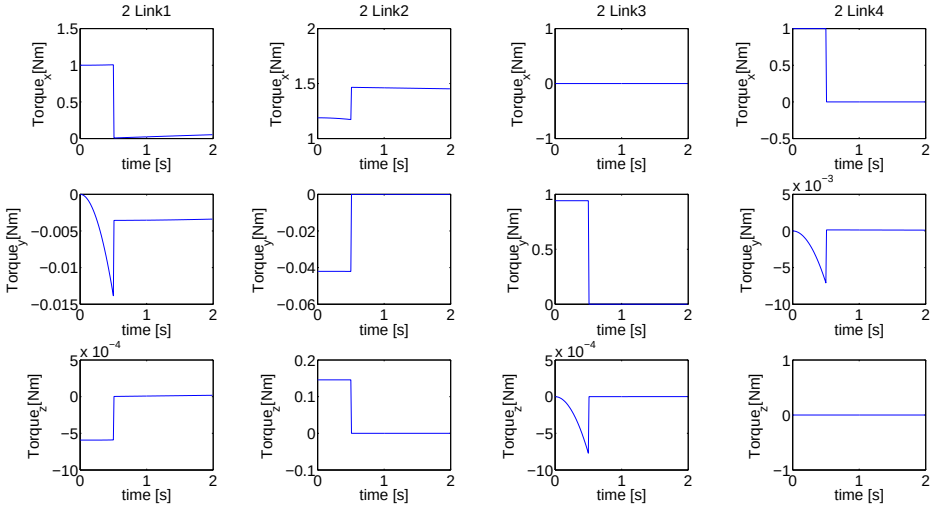

Figure C.31: Torques at the links of Arm 2

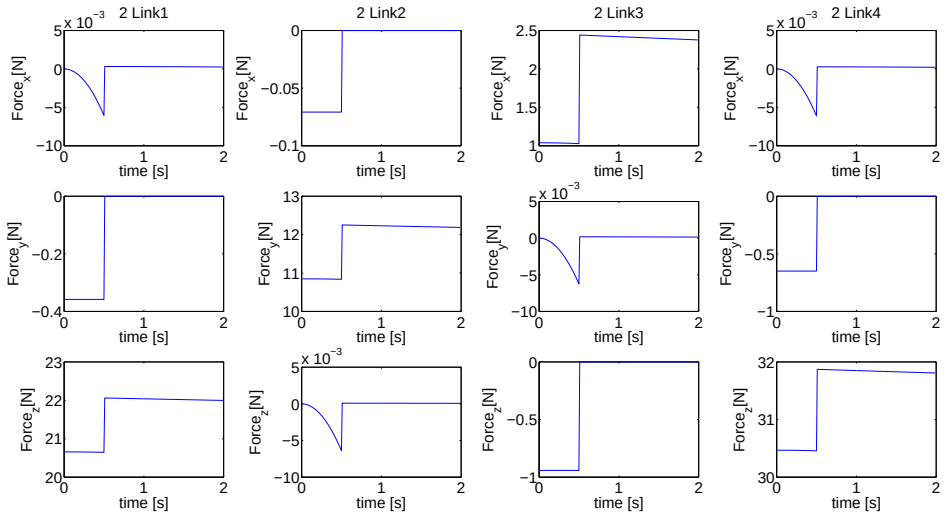

Figure C.32: Forces at the links of Arm 2

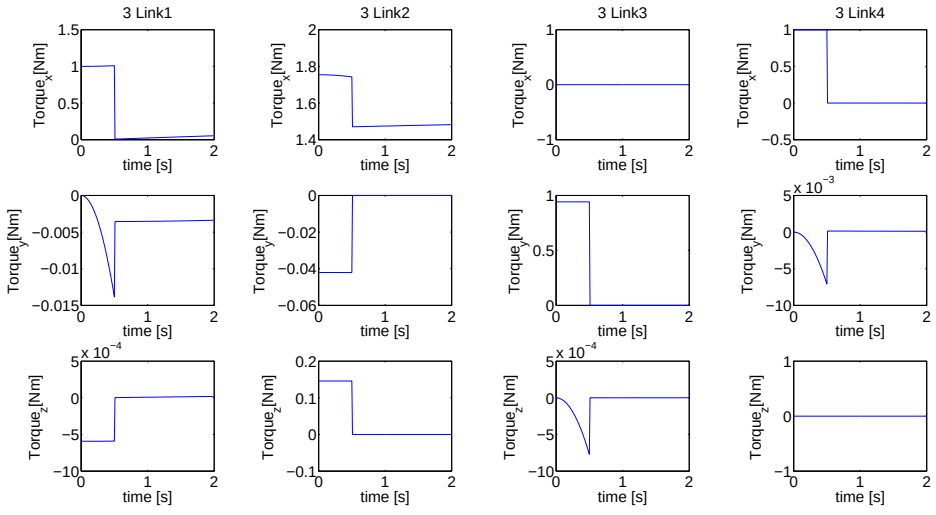

Figure C.33: Torques at the links of Arm 3

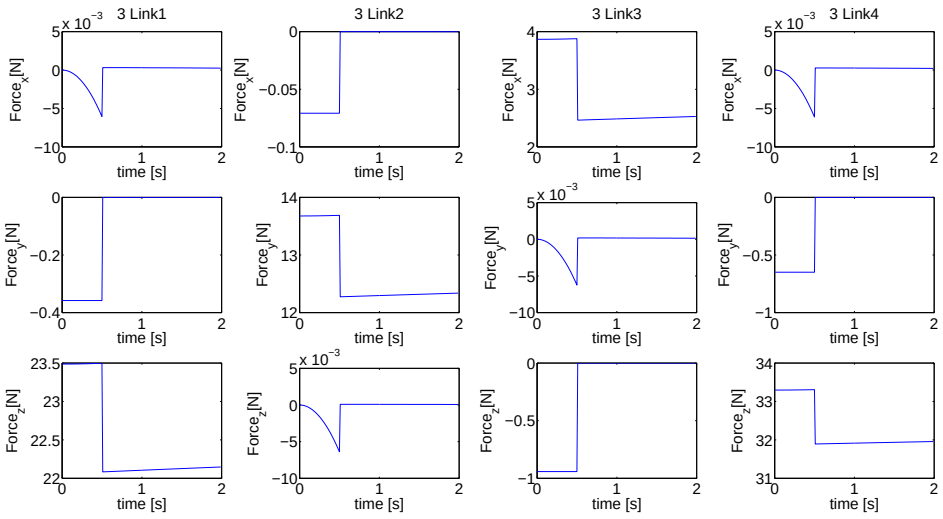

Figure C.34: Forces at the links of Arm 3

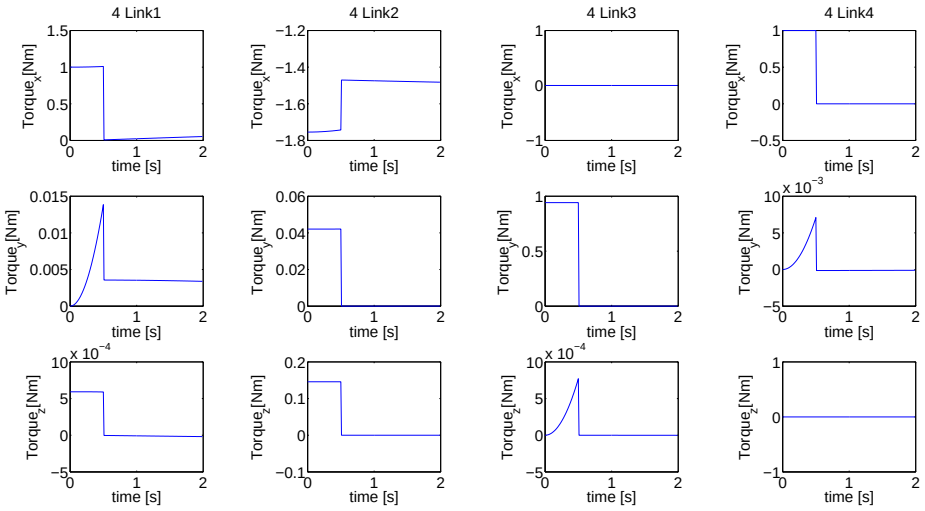

Figure C.35: Torques at the links of Arm 4

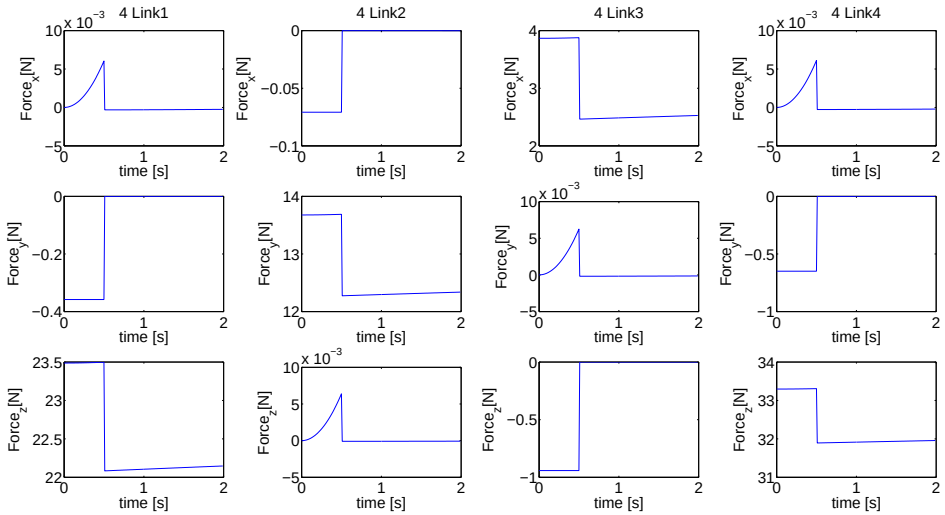

Figure C.36: Forces at the links of Arm 4

BIOGRAPHY

Sıddık Murat Yeşiloğlu received Control & Computer Engineering **B.Sc.** degree from Istanbul Technical University (ITU) with the second best GPA among the graduates of the same department in 1990. He then started working as a computer engineer at ESIT (Elektronik Sistem Imalat & Tasarim Corp.) developing communication software for heavy weight scales. The same year he ranked first at a nationwide exam for state sponsored full-scholarship of graduate education abroad organized by the Ministry of Education of Turkey. He completed the Intensive English Program at the University of Illinois Urbana-Champaign, USA in 1991. In 1993, he received **M.Sc.** degree in Electrical Engineering from Illinois Institute of Technology, Chicago IL, USA. He worked under the supervision of Prof.Dr. Mohammed Shahidehpour and his thesis was titled "Adaptive Control of Nonlinear Dynamical Systems by Artificial Neural Networks." He started his Ph.D. education in 1994 at the Electrical, Computer & Systems Engineering Department of Rensselaer Polytechnic Institute (RPI), Troy NY, USA. While at RPI, he worked as a research assistant at the Decision & Science Department designing Accident Prevention Techniques for Washington State Ferry Transportation in the Spring of 1998 and as a teaching assistant at the Physics Department in the Fall of 1998. He then joined to the General Electric Company, Power Systems (GEPS) in Schenectady NY, USA in 1999. He worked at the department of CASE (Control, Accessories and Systems Engineering) until 2002 with the title of Advanced Controls Engineer, responsible of the research & development of DLN (Dry Low Nox) and IGCC (Integrated Gasification Combined Cycle) gas turbine controls. While at GE, he designed, managed and implemented a $200K "Lean Blow Out" (LBO) project involving a test rig design to measure combustor minimal fuel-air ratio, including hardware design, integration of control algorithms and user interface software, and data analysis. He also developed a method for data collection from Mark V controlled gas turbines and implemented it which is now an indispensable tool for GEPS field engineers worldwide. Some of the other projects whom he was the owner include development of a mathematical model for Annubar flow meters used on Mark VI controllers and the implementation of combustion mode reference dynamic bar graph which required new coding methodology on Mark V controllers. He was certified as a green belt engineer and completed numerous courses as a part of the six-sigma quality management program. He was the host of The Turkish Rainbow Radio Program on WRPI - Troy, NY, USA from 1996 to 2003 and the General Secretary of the Turkish American Society of Capital District of NY, USA from 2000 to 2003. In 2003, he worked as a lecturer at the Computer Engineering Department of Girne American University in Turkish Republic of Northern Cyprus where he taught Microprocessors, Operating Systems, Signals & Systems, and General Physics. He served in the Turkish Military during the month of April 2004 in Burdur, Turkey and then joined to ITU as a research assistant.